

# TECHNISCHE UNIVERSITÄT MÜNCHEN

Fakultät für Medizin

Mapping Division Speed During the Early Differentiation Phase  
of CD8 T Cells

Marten Matthias Plambeck

Vollständiger Abdruck der von der Fakultät für Medizin der Technischen Universität München zur Erlangung eines Doktors der Naturwissenschaften genehmigten Dissertation.

Vorsitz: Prof. Carsten Schmidt-Weber

Prüfer\*innen der Dissertation:

1. Prof. Dr. Dirk H. Busch
2. Prof. Dr. Gabriele Multhoff

Die Dissertation wurde am 07.02.2022 bei der Technischen Universität München eingereicht und durch die Fakultät für Medizin am 08.11.2022 angenommen.

# Content

Table of Figures .....	iv
Abbreviations.....	vii
1 Introduction .....	1
1.1 Innate and adaptive immunity .....	1
1.1.1 Pathogen recognition in the innate immune system .....	1
1.1.2 Crosstalk between innate and adaptive immunity.....	2
1.2 Cytotoxic T lymphocytes .....	4
1.2.1 Activation of epitope-specific CTLs (CD8 T cells).....	4
1.3 The adaptive immune system can protect against reinfection.....	6
1.3.1 CD8 T cell memory is provided by specialized subsets.....	7
1.4 The pathway of differentiation .....	10
1.4.1 Effector and memory cells arise in parallel .....	11
1.4.2 MPs emerge from SLECs .....	13
1.4.3 SLECs emerge from MPs .....	14
1.5 How are fate decisions made?.....	15
1.6 Call for new methods.....	17
1.6.1 The gold standard in immunology.....	17
1.6.2 Live-cell imaging .....	18
2 Aim of this thesis .....	19
3 Material and Methods.....	21
3.1 Materials.....	21
3.1.1 Chemicals and Reagents.....	21
3.1.2 Antibodies (anti-murine).....	23

---

3.1.3	Buffers .....	26
3.1.4	Equipment .....	26
3.1.5	Software .....	28
3.2	Methods .....	29
3.2.1	Transfer of T cells .....	29
3.2.2	Infection with <i>Listeria monocytogenes</i> .....	29
3.2.3	Single-cell suspension from spleen or lymph nodes.....	30
3.2.3	Single-cell suspension from blood .....	31
3.2.4	Staining for flow cytometry.....	31
3.2.5	CTV staining .....	33
3.2.6	Single-cell expansion (continuous stimulation) .....	34
3.2.7	Single-cell expansion (discontinuous stimulation).....	34
3.2.8	Single-cell expansion (splenocyte cultures).....	35
3.2.9	Enzyme-linked immunosorbent assay (ELISA).....	36
4	Results .....	37
4.1	Establishment of a feeder-cell free single-cell culture .....	37
4.2	Functionality .....	44
4.3	Establishment of a feeder-cell free single-cell culture without continuous stimulation .....	45
4.4	Investigation of inter-division times within and between T-cell families under continuous stimulation .....	53
4.5	Investigation of inter-division times with short stimulation in the presence or absence of IL-12 .....	56
4.6	CD25 expression in fast and slow dividing cells.....	59
4.7	Development of inter-division times over time.....	64
4.8	Expression of the memory-related marker CD62L in fast vs. slow dividing cells .....	71

---

5	Discussion.....	76
5.1	Distribution of Cell-cycle speed and phenotype during the early phase of the immune response.....	77
5.1.1	Contribution of distinct division speeds to the variable expansion of single T cell-derived clones.....	77
5.1.2	How division speed is influenced by antigenic and cytokine-based stimuli beyond priming.....	80
5.1.3	Development and maintenance of division speeds in separate subpopulations of the same clone.....	81
5.1.4	Correlation between SLEC and MP phenotypes and division speed	82
5.2	Implications for our understanding of T cell differentiation .....	84
5.2.1	Order of differentiation .....	84
5.2.2	Signal integration.....	85
5.2.3	Diversification under homogenous conditions .....	86
6	Summary.....	92
	Bibliography.....	94
	Acknowledgement.....	106

# Table of Figures

Fig. 1: Subsets of CD8 T cells .....	9
Fig. 2: Possible pathways of differentiation .....	11
Fig. 3: 'One cell one fate' or 'One cell multiple fates' .....	12
Fig. 4: Asymmetric cell division .....	12
Fig. 5: The phases of a CD8 T cell response are dominated by different phenotypes .....	13
Fig. 6: Decreasing Potential hypothesis .....	14
Fig. 7: Stochastic model of progressive differentiation .....	15
Fig. 8: Differentiation-linked division vs. Division-linked differentiation .....	16
Fig. 9: Expansion of cells <i>in vitro</i> leads to similar phenotypes as <i>in vivo</i> ..	38
Fig. 10: Expansion of single OT-I cells <i>in vitro</i> is extremely variable .....	39
Fig. 11: Single CD8 T cells can be expanded for at least 5 days <i>in vitro</i> ..	40
Fig. 12: The outcomes of single cell-derived progenies are very variable – even under well-defined <i>in vitro</i> conditions .....	41
Fig. 13: Single cell-derived progenies can expand with different proliferation rates .....	42
Fig. 14: The first cell division needs more time than the subsequent divisions .....	43
Fig. 15: Under continuous stimulation, <i>in vitro</i> differentiated T cells do not show subset-associated survival and expansion upon transfer <i>in vivo</i> .....	45
Fig. 16: Abrogation of stimulation via $\alpha$ CD3 results in reduced cell numbers. ....	46
Fig. 17: IL-7, 12 and 15 cannot enhance proliferation in the absence of IL-2, and IL-12 upregulates the expression of CD25 .....	49
Fig. 18: Levels of IL-2 in the medium are stable .....	50
Fig. 19: CD90.1 and CD90.2 cells show reduced proliferation when the respective antibody is bound to the culture plate .....	51
Fig. 20: High concentrations of $\alpha$ CD25 in culture can interfere with T cell proliferation .....	52
Fig. 21: Schematic family tree of a single T cell	

Fig. 22: Under continuous stimulation, there is huge intra- and inter-clonal variability .....	54
Fig. 23: Inter-division times of sibling cells are more closely correlated than between mother and daughter cells .....	55
Fig. 24: Intra- and inter-clonal variability of inter-division times contribute similarly to total variability.....	55
Fig. 25: Live-cell imaging under short stimulation conditions .....	56
Fig. 26: Representative trees from continuous stimulation, short (24 h) stimulation without IL-12 and short stimulation with subsequent cultivation in 10 ng/mL IL-12. ....	57
Fig. 27: Continuously-stimulated cells have the shortest inter-division times, followed by short stimulation + IL-12 and short stimulation without IL-12.	58
Fig. 28: Small differences in mean inter-division time can amplify into substantial differences in the size of a single cell-derived progeny .....	58
Fig. 29: CD25 is preferentially expressed by fast-dividing cells.....	59
Fig. 30: Intra-clonal distribution of CD25 weakly correlates with cell-cycle speed .....	61
Fig. 31: Correlation between inter-division time and expression of CD25 is strongest in the shortly-stimulated setting and weakest when IL-12 was added .....	61
Fig. 32: Inter-division times and CD25 expression of continuously, shortly and shortly + IL-12 stimulated cells .....	62
Fig. 33: Correlation between CD25 and inter-division time depends on the generation and the stimulation conditions .....	63
Fig. 34: With short stimulation, the cells slow down with each generation, and the variability of inter-division times increases.....	65
Fig. 35: Standard deviations of inter-division time within individual trees increases during the first few cell divisions.....	66
Fig. 36: Variability of inter-division time within individual tree increases after a few cell divisions.....	66
Fig. 37: More than 30 % of the trees contain subtrees that divide significantly slower or faster than the other subtrees in that tree .....	67
Fig. 38: Schematic illustration of ranges.....	67

---

Fig. 39: Ranges are very small during the first 72 h but diverge in later generations.....	68
Fig. 40: Ranges diverge faster when cells divide fast, but they diverge similarly when the ranges are plotted in relation to the mean generation of the tree	
Fig. 41: CD62L low cells divide within the same time more often than CD62L high cells .....	72
Fig. 42: Downregulation of CD62L is correlated with the number of cell divisions within the same single cell-derived progeny .....	72
Fig. 43: Overlay of 30 single-cell CTV-plots. ....	73
Fig. 44: Slow-dividing cells are CD62L high .....	74
Fig. 45: Also within the same single-cell tree CD62L high cells divide slower than CD62L low cells.....	75
Fig. 46: CD62L high cells are more affected by slowing down of cell-cycle over time and IL-12 reduces the difference in inter-division times of CD62L high and low cells .....	75
Fig. 47: Differentiation-linked division.....	85
Fig. 48: Generation of Variability .....	88
Fig. 49: Model for CD25-driven diversification.....	91

# Abbreviations

ACT	ammonium chloride / Tris
AP-1	activator protein 1
APC	allophycocyanin
APC	antigen presenting cell
BCR	B cell receptor
BHI	brain heart infusion
BSA	bovine serum albumin
CD	cluster of differentiation
cfu	colony forming units
CTL	cytotoxic T lymphocyte
CV	coefficient of variation
DC	dendritic cell
DNA	deoxyribonucleic acid
EDTA	ethylenediaminetetraacetic acid
eF	eFluor
e.g.	example given
ELISA	enzyme-linked immunosorbent assay
EMA	ethidium-monoazied-bromide
Fc	fragment crystallizable (of an antibody)
FCS	fetal calf serum
FITC	fluoresceinisothiocyanat
Gads	GRB2-related adaptor downstream of Shc
h	hour
HEV	high endothelial venule
idt	inter-division time
IL	interleukin
i.p.	intraperitoneal
ITAM	immuno-receptor tyrosine-based activation motif
Itk	interleukin-2-inducible T-cell kinase
i.v.	intravenously

---

kDa	kilo Dalton
KLRG1	killer cell lectin-like receptor subfamily G member 1
<i>L.m.</i>	<i>Listeria monocytogenes</i>
Lck	lymphocyte-specific tyrosine kinase
LAT	linker for activation of T cells
LPS	lipopolysaccharides
MHC	major histocompatibility complex
min	minute
mL	milliliter
MP	memory precursor cell
MPEC	memory precursor effector cell
NF- $\kappa$ B	nuclear factor kappa-light-chain-enhancer of activated B-cells
NFAT	nuclear factor of activated T cells
ng	nanogram
OD	optical density
Ova	chicken ovalbumin
PAMP	pathogen-associated molecular pattern
PBS	phosphate buffered saline
PE	phycoerythrin
PFA	paraformaldehyde
PI	propidium iodide
PLC- $\gamma$	phospholipase C- $\gamma$
PI3K	phosphoinositide 3-kinase
PIP <sub>2</sub>	phosphatidylinositol bisphosphate
PIP <sub>3</sub>	phosphatidylinositol trisphosphate
PMA	phorbol-myristate-acetate
pMHC	peptide-loaded major histocompatibility complex
PRR	pattern recognition receptor
RNA	ribonucleic acid
rpm	revolutions per minute
RT	room temperature

---

SC	single color
SD	standard deviation
secs	seconds
SEM	standard error of the mean
SLEC	short-lived effector T cell
SLP-76	SH2 domain-containing leukocyte phosphoprotein of 76 kDa
Src	sarcoma
T <sub>CM</sub>	central memory T cell
TCM <sub>p</sub>	central memory precursor cell
TCR	T cell receptor
T <sub>EM</sub>	effector memory T cell
TEM <sub>p</sub>	effector memory precursor cell
Th	helper T cell
T <sub>RM</sub>	tissue resident memory T cell
U	units
μl	microliter
μm	micrometer
US	unstained
wt	wild type
ZAP-70	Zeta-chain-associated protein kinase 70

# 1 Introduction

## 1.1 Innate and adaptive immunity

Although people and animals are under constant attack from different kinds of bacteria, viruses, and parasites during their life, most people get sick just occasionally. In addition to physical barriers like skin and epithelium that hinder pathogens from entering the body, it is our immune system that defeats most of the potentially harmful invaders before we even recognize them. Most infections that are cleared before we become conscious of them are defeated by the innate immune system, which recognizes conserved structures that are shared among many pathogens. In contrast, the adaptive immune system evolved a machinery to generate receptors against any structure. Thus, it is able to attack pathogens that hide from detection by the innate immune system [1, 2].

### 1.1.1 Pathogen recognition in the innate immune system

Cells of the innate immune system, especially macrophages, patrol through the tissues of the body to search for pathogens. To be able to discriminate between pathogens and structures of the body, they are outfitted with so-called pattern recognition receptors (PRRs). Most pathogens have common structures on their surface or intracellularly that make them distinguishable from eukaryotic cells. These structures are called pathogen-associated molecular patterns (PAMPs) and can be recognized by PRRs. Examples for PAMPs are lipopolysaccharides (LPS) in the outer membrane of gram-negative bacteria, lipoteichoic acids in the cell walls of gram-positive bacteria, mannose-rich oligosaccharides, peptidoglycans, flagellin, unmethylated CpG DNA, double-stranded or long single-stranded RNA, associated to viruses, and zymosan, present in fungi.[1-5] If a PRR on the surface of a macrophage binds to such a PAMP, the target is usually phagocytized, meaning that it is engulfed by the cell membrane of the

macrophage, thus being captured in a vesicle (phagosome) [5, 6]. These intracellular vesicles fuse with lysosomes that are highly acidified and contain toxic molecules and enzymes to digest the pathogen [6, 7]. In addition, the macrophage releases chemokines that attract further immune cells (e.g., neutrophil granulocytes) and secrete cytokines that initiate inflammation in the infected tissue [8-10]. The inflammation activates the endothelial cells of local small blood vessels, thereby enabling large numbers of immune cells to invade the infected tissue from the blood stream [11, 12].

The efficient killing of pathogens by attracted neutrophil granulocytes can only work if the PRRs recognize structures on the surface of the pathogen. Unfortunately, a lot of pathogens try to hide themselves from the immune system, e.g., by downregulation of PAMPs, by hiding them under a layer of mucus, or by living inside the cells of the host [1]. Pathogens that hide their surface from the innate immune system can still be recognized as being non-self because after degradation in the phagolysosomes, internal PAMPs (e.g., unmethylated CpG DNA, double-stranded RNA) can be detected by intracellular PRRs [2, 4, 8]. Nevertheless, help by the adaptive immune system is often needed to keep the pathogen in check.

### **1.1.2 Crosstalk between innate and adaptive immunity**

Besides macrophages and B cells, dendritic cells (DCs) belong to the group of antigen-presenting cells [1, 13]. DCs are the most potent link between the innate and the adaptive immune system. Like macrophages, they express PRRs and patrol through tissues, where they take up antigens. In addition to phagocytosis, they take up antigens via receptor-independent macropinocytosis [14]. If the DC is activated (e.g., because it detected pathogens by intra- or extracellular PRRs), it migrates through the lymphatic system to local lymph nodes and undergoes a process termed 'maturation' [15]. Mature DCs are able to activate T cells of the adaptive immune response. Mature DCs reduce their ability to take up new antigen and instead upregulate the expression of costimulatory molecules and stably maintain expression of major histocompatibility complexes (MHCs), loaded with antigen.[16, 17]

### **1.1.2.1 Peptide presentation on MHCs**

Two MHC molecules are of great importance for the adaptive immune system: MHC-I and MHC-II. Antigens that were taken up from the extracellular space are cut into small peptides and loaded on MHC-II molecules. Together with costimulatory molecules, the peptide-loaded MHC-II molecules are presented to naïve CD4 T cells on the surface of the antigen presenting cell (APC) [18]. Intracellular antigens are also cut into small peptides but presented on MHC-I molecules to CD8 T cells [17]. During their development, T cells are equipped with a unique T cell receptor (TCR) of defined specificity via somatic recombination of the TCR gene locus [19, 20]. In the rare case that a naïve T cell recognizes the combination of MHC-II and cognate foreign peptide that is presented on the surface of a mature DC, it becomes activated, starts to proliferate, and differentiates into diverse subsets [1]. TCRs that would be autoreactive or would not be able to bind to peptide-MHC complexes with sufficient affinity have already been taken out of the naïve repertoire during positive and negative selection in the thymus [21, 22]. Most of the CD4 T cell subsets help the body to cope with extracellular or intra-phagosomal pathogens. For example, T helper 1 (Th1) cells can further activate macrophages to generate reactive oxygen species that enhance killing of phagocytized bacteria, while Th2 cells help B cells and recruit eosinophil granulocytes to fight extracellular parasites [23].

### **1.1.2.2 Adaptive immunity helping innate immunity**

B cells are also a member of the adaptive immune system. Their antigen receptors are called B cell receptors (BCRs), which, similar to TCRs, are also generated through somatic recombination of the respective gene locus [24]. If a cognate antigen binds to the BCR, it is internalized, processed, and its peptide fragments are presented on MHC-II. An activated Th cell that recognizes the peptide-MHC-II complex can activate the B cell which in turn produces large amounts of soluble BCRs — i.e., antibodies [25, 26]. The antibodies bind to their targets, thereby marking the pathogen as being dangerous, and they provide targets for the innate immune system like phagocytes that express antibody-receptors or for the soluble complement system, which can lyse certain bacteria [27]. As opposed to the TCR, BCRs

and antibodies recognize not only peptide fragments, but three-dimensional protein structures.

## 1.2 Cytotoxic T lymphocytes

A challenge for the immune system is to detect and fight pathogens that replicate in the cytoplasm of infected cells, e.g., viruses or certain bacteria like *Listeria monocytogenes*. These pathogens are not accessible to antibodies, the complement system, or to phagocytes. To contain intracellular pathogens, the host cell has to be killed. Therefore, immune responses against intracellular pathogens have to be tightly regulated. Not just in DCs, but in all nucleated cells, the proteasome constantly degrades proteins from the cytoplasm to oligopeptides [28]. These peptides are loaded onto MHC-I molecules which are presented on the surface of the cell [17]. In essence, the cells show, via MHC-I-loaded peptides, which proteins are present inside their cytoplasm. If a foreign antigen on MHC-I is detected by an activated CD8 T cell with the respective TCR specificity, the CD8 T cell induces cell death in the peptide-presenting cell [29, 30]. Therefore, CD8 T cells are also named cytotoxic T lymphocytes (CTLs).

### 1.2.1 Activation of epitope-specific CTLs (CD8 T cells)

The activation process of CD8 T cells is similar to that of CD4 T cells. DCs are very susceptible to infections with many viruses [16]. Virus infection can e.g. be sensed via recognition of double-stranded RNA inside the DC. After virus sensing, it migrates to the local lymph node and presents viral peptides, which have been processed by the proteasome, on MHC-I molecules to naïve CD8 T cells [8, 15, 16]. Antigens derived from pathogens that do not directly infect DCs, can also be presented on MHC-I via a mechanism called 'cross-presentation'[31], by which intra-phagosomal peptides are diverted from presentation on MHC-II to MHC-I. Naïve CD8 T cells in the lymph nodes scan peptide-MHC-I (pMHC-I) complexes on the surface of activated APCs with their TCRs and bind, if the specificity of the T cell's TCR fits to the peptide that is presented [32, 33].

### **1.2.1.1 Transduction of the activation signal**

The TCR complex is composed of different proteins. The  $\alpha$  and the  $\beta$  chain of the TCR itself associate with membrane-anchored intracellular  $\zeta$  chains and the four chains of the CD3 complex [34, 35]. The intracellular parts of these accessory chains contain immuno-receptor tyrosine-based activation motifs (ITAMs). When the TCR binds to the pMHC-I complex, the CD8 coreceptor is recruited to the TCR complex, binds to the MHC-I molecule and further stabilizes the binding between pMHC-I and TCR [36]. With its intracellular tail, CD8 recruits the sarcoma (Src) family kinase 'lymphocyte-specific tyrosine kinase' (Lck) to the TCR-complex. Lck phosphorylates tyrosine residues in the ITAMs of CD3 and the  $\zeta$  chains [37, 38]. The kinase 'Zeta-chain-associated protein kinase 70' (ZAP-70) then binds via its SH2 domains to the phosphorylated ITAMs and is also phosphorylated and activated by Lck [38, 39]. Activated ZAP-70 recruits and phosphorylates the scaffold proteins 'SH2 domain-containing leukocyte phosphoprotein of 76 kDa' (SLP-76) and 'linker for activation of T cells' (LAT) which will then be connected by the adaptor protein 'GRB2-related adaptor downstream of Shc' (Gads) [40]. The resulting complex can bind phospholipase C- $\gamma$  (PLC- $\gamma$ ), which in turn can be activated by the Tec-family kinase 'interleukin-2-inducible T-cell kinase' (Itk) [41]. PLC- $\gamma$  activates several signaling cascades, which finally result in the activation of the transcription factors 'nuclear factor kappa-light-chain-enhancer of activated B-cells' (NF- $\kappa$ B), 'nuclear factor of activated T cells' (NFAT), and 'activator protein 1' (AP-1), and thus in T cell activation and proliferation [42-44].

### **1.2.1.2 Costimulation**

However, to be efficiently recruited to the membrane, PLC- $\gamma$  and Itk need to bind to the membrane-anchored molecule phosphatidylinositol trisphosphate (PIP<sub>3</sub>), which can be generated from phosphatidylinositol bisphosphate (PIP<sub>2</sub>) via phosphorylation by the phosphoinositide 3-kinase (PI3K) [45]. To activate PI3K, the costimulatory molecule B7 on the APC needs to bind its receptor (CD28) on the T cell. This binding leads to phosphorylation of the intracellular domain of CD28, which recruits and activates PI3K [45]. In addition, the produced PIP<sub>3</sub> leads also to the activation of the protein kinase Akt, which in turn leads to upregulation of

cell metabolism and enhances cell survival [46]. The described mechanism is the reason why naïve CD8 T cells are not activated by just any cell that presents a pMHC-I complex on its surface that fits to the specificity of the TCR. Instead, a mature APC, which has upregulated costimulatory molecules like B7, is needed to confirm that the detected peptides originated from a potentially harmful source.

For optimal CD4 or CD8 T cell responses, three signals are believed to be required. Signal 1 is provided by recognition of the pMHC complex by the TCR, signal 2 via co-stimulation and signal 3 by cytokines, which ensure survival of the activated T cells and influence its differentiation [47, 48]. It is also possible to activate naïve CD8 T cells *in vitro* by adding antibodies directed against CD3 (signal 1) and CD28 (signal 2) [49]. As soon as the CD8 T cell is fully activated, recognition of signal 1 alone is enough for a cytotoxic T cell to kill a target cell [1].

### **1.3 The adaptive immune system can protect against reinfection**

In addition to the relatively limited breadth of the innate immune system's receptor repertoire, it does not "learn" from an infection. Consequently, if only the innate immune system existed, people who live in areas where a certain pathogen is met very frequently would regularly get sick. However, a reinfection with the same pathogen leads to an adaptive immune response that is much faster and stronger than the primary response [48]. This is the case because the primary response entails strong proliferation of antigen-specific lymphocytes—and while 90–95% of T and B cells present at the peak of expansion die after the pathogen clearance, the number of antigen-specific lymphocytes that persist long-term substantially exceeds the number of antigen-specific lymphocytes present before primary infection. This numerical increase of antigen-specific memory lymphocytes is one of the key reasons why secondary immune responses are faster and stronger than primary immune responses [48]. For this reason, a reinfection with the same pathogen is often cleared before the individual recognizes that there was an infection at all.

Memory T and B cells can persist in the body for many years—potentially even life-long—based on rare homeostatic cell divisions [50-52]. These memory lymphocytes explain why children usually get infected with chickenpox only once and are the underlying mechanism of vaccinations [53].

To be able to further improve vaccination strategies, it is necessary to better understand how naïve lymphocytes differentiate into short- and long-lived subsets and how the expansion and contraction of these subsets is regulated.

### **1.3.1 CD8 T cell memory is provided by specialized subsets**

Activated murine  $\alpha\beta$  CD8 T cells can be grouped into at least four different subsets, which are distinct in migratory behavior, longevity and effector functions: T central memory ( $T_{CM}$ ) cells, T effector memory ( $T_{EM}$ ) cells, T resident memory ( $T_{RM}$ ) cells and short-lived effector cells (SLECs) [54, 55].

$T_{CM}$  cells are very long-lived. They do not migrate into tissues but circulate between blood and secondary lymphatic organs. To be able to do that, they express the chemokine receptor CCR7, which directs them to the lymphatic system, and the adhesion molecule L-selectin (CD62L) which can bind to glycosylation-dependent cell adhesion molecule-1 (GlyCAM-1) on high endothelial venules (HEVs) of lymph nodes, thereby facilitating transmigration through HEVs into lymph nodes [55, 56].  $T_{CM}$  cells display weak killing capacity. Their expression of effector molecules like granzyme B and perforin, which contribute to killing of target cells, is very low. Their main task is to recirculate between blood and secondary lymphatic organs until their cognate antigen is presented to them again due to reinfection with the same pathogen. In such cases they start to proliferate vigorously and while part of their offspring differentiates into more cytotoxic  $T_{EM}$  cells and SLECs a small fraction retains the phenotype and functional capacity of  $T_{CM}$  cells [57-59]. Serial transfer and re-infection experiments have shown that a single activated  $T_{CM}$  cell, indeed possesses the stem cell-like capacity to self-renew and, in parallel, generate a diverse offspring of more differentiated T cells. In these experiments, single  $T_{CM}$  cells were harvested

from immune mice, transferred into naive secondary recipients, and re-exposed to infection. The resulting T cell families (i.e. all T cells derived from the same individual T<sub>CM</sub> cell) were rested for 2 months. Then single T<sub>CM</sub> cells were again sorted via flow cytometry, adoptively transferred to new recipients and tested for their re-expansion, differentiation and self-renewal potential [60]. These experiments showed that single T<sub>CM</sub> cells undergoing primary or secondary expansion were equally potent at fulfilling these tasks. This work shows that T<sub>CM</sub> cells akin to tissue stem cells have the long-term capacity to maintain an “epitope-specific tissue” i.e. an epitope specific T cell population [60, 61].

In contrast to T<sub>CM</sub> cells, T<sub>RM</sub> and T<sub>EM</sub> cells do not express CCR7 and CD62L and cannot migrate back into the lymph nodes via HEVs [62]. T<sub>RM</sub> cells were discovered just a few years ago [63]. As their name already indicates, they reside in tissues (e.g., skin). Due to their residence in barrier organs, they can encounter pathogens very soon after infection and are able to produce effector molecules and cytokines, thus enabling them to kill infected cells before the pathogen invades deeper into the body. Apart from their location, they are distinguishable from the other CD8 T cell subsets by their expression of CD69 and CD103. Although CD69 is expressed on virtually all T cells as an activation marker after priming, its expression is usually lost within a few days. CD103 is an adhesion molecule that most likely helps T<sub>RM</sub> cells to reside in the tissues.[54, 63]

T<sub>EM</sub> cells express CD127 and CD27 on their surface [57, 59]. CD127 is the  $\alpha$  chain of the interleukin-7 receptor and enhances proliferation in response to interleukin-7 (IL-7), whereas CD27 is an important co-stimulatory receptor that is activated via CD70 expressed on DCs [64, 65]. Compared to T<sub>CM</sub> cells, the number of T<sub>EM</sub> cells decreases more rapidly within the weeks to months after pathogen clearance [66], but they express more effector molecules than T<sub>CM</sub> cells [55, 57, 59]. It has been suggested that they can be further divided into CX3CR1<sup>high</sup>

	<u>characteristic markers</u>	<u>killing capacity</u>	<u>longevity</u>
	CD62L, CCR7, CD27, CD127	low	long-lived
	CD27, CD127	intermediate	intermediate
	CD69, CD103	intermediate / high	intermediate
	KLRG1, CD25	high	short-lived

**Fig. 1: Subsets of CD8 T cells**

cells which do not migrate to the extravascular space and CX3CR1<sup>intermediate</sup> cells that can enter the extravascular space, migrate through the tissue and return to the draining lymph nodes via the afferent lymph [67]. However, due to the lack of the memory markers CD27 and CD127 on CX3CR1<sup>high</sup> cells, it is also possible that the putative CX3CR1<sup>high</sup> T<sub>EM</sub> cells are actually SLECs (see below). For vaccination strategies against aggressive viruses which replicate fast, it can be helpful to preferentially induce effector memory T cells and apply booster vaccinations to gain high numbers of preformed T<sub>EM</sub> cells with instant effector functions [68].

SLECs constitute the fourth subset. They have lost the memory markers CCR7, CD62L, CD127 and CD27 and migrate to inflamed peripheral tissues to fight infection. In the case of an inflammation, they are attracted by the chemokines that are secreted e.g., by macrophages and can invade the infected tissues through the

activated endothelium. SLECs are the most potent killers among CD8 T cells. However, as the name already indicates, they are short-lived and die during the contraction phase [69].

## 1.4 The pathway of differentiation

During an adaptive immune response, antigen-specific CD8 T cell populations can expand approximately 10 000-fold [70]. After the pathogen is cleared, roughly 95 % of T cells present at the peak of expansion die, and only memory T cells survive [48]. Before the contraction phase, the T cell response is dominated by cells that express effector molecules and are efficient in killing target cells. Furthermore, the inter-division times of CD8 T cells during the expansion phase can be very fast. *In vitro*, inter-division times were measured at approximately 6-8 hours per cell division [71] *In vivo*, inter-division times were also measured and estimated at 6-8 hours but differed greatly depending on the type of infection and the time point at which cell cycle speed was measured [72-75].

T memory cells, on the other hand, are low in immediate cytolytic capacity and divide very slowly after clearance of infection, with one division per 50 days in mice [76] and one division per over 450 days in humans [77]. While various data show that the segregation into T memory precursors (MPs) and SLECs already begins during the expansion phase of a T cell immune response [69, 78-80], it has not been possible to directly tie these differentiation processes to the fundamental changes in proliferation activity that occur in parallel. In addition, it remains incompletely resolved in which developmental order SLECs and MPs arise.

Three major models to describe this process have been proposed (Fig. 2):

1. SLECs and MPs arise in parallel without one subset preceding the other one.
2. MPs emerge by de-differentiation from SLECs
3. SLECs emerge by differentiation from MPs.

I will briefly introduce these distinct models and their implications for memory T cell development in the next section.

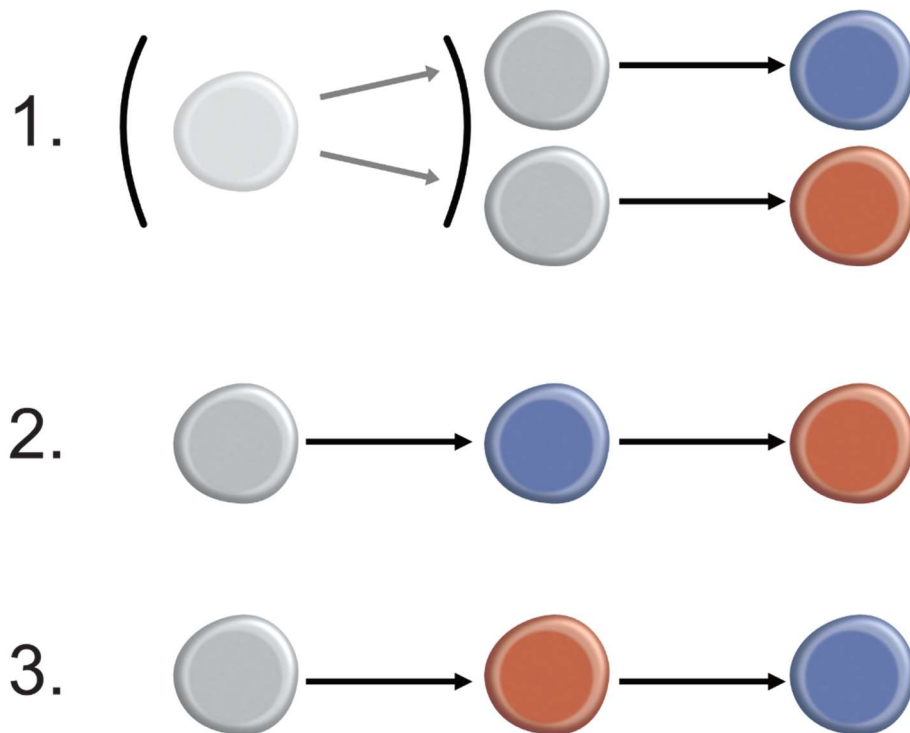


**Fig. 2: Possible pathways of differentiation. Grey:** naïve or undifferentiated cell. **Blue:** effector cell. **Red:** memory cell. **1.** Effector and memory cells arise in parallel from different or the same (light cell) progenitor. **2.** Memory cells arise from effector cells. **3.** Effector cells arise from memory cells.

#### 1.4.1 Effector and memory cells arise in parallel

In theory, the problem of which subset differentiates into which other subset would be provided by the so-called 'One cell, one fate' hypothesis [81]. According to this model, a naïve CD8 T cell will either generate MPs or SLECs but not both (Fig. 3). The 'One cell, one fate' hypothesis is opposed to the 'One cell, multiple fates' hypothesis [81] that assumes that all major CD8 T cell subsets can arise from the same naïve T cell.

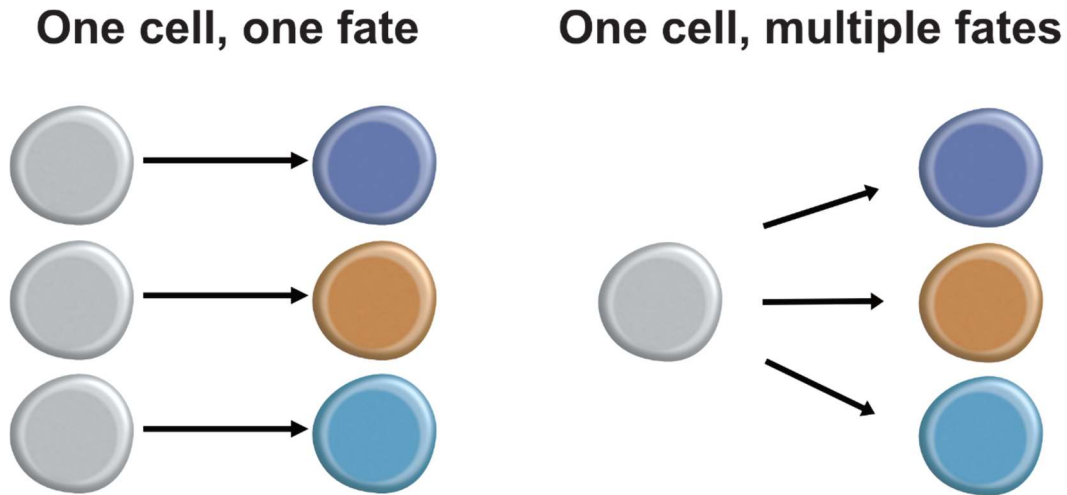


**Fig. 3: 'One cell, one fate' or 'One cell, multiple fates'.** Different subtypes of CD8 T cells could either be generated by different progenitor cells (One cell, one fate) or a single naïve T cell is able to generate different phenotypes in parallel (One cell, multiple fates)

An elegant solution for generating MPs and SLECs from the same naïve T cell without one subset preceding the other could be provided by asymmetric cell division. This specific mode of cell division has already been shown to play a substantial role in differentiation and maintenance of other tissues and cell types like neurons, satellite cells of muscles, or

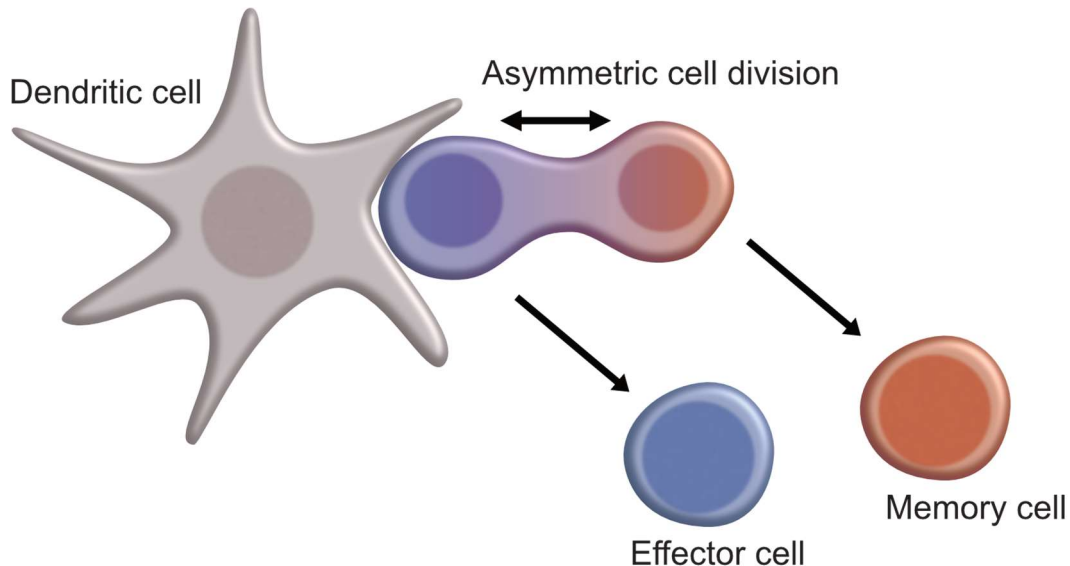


**Fig. 4: Asymmetric cell division.** During activation the synapse between the dendritic cell (DC) and the activated cell could lead to an unequal distribution of fate determining factors along the axis between the DC and the cell (color gradient). The gradient is believed to result in a proximal effector cell and a distal memory cell after the first division.

hematopoietic stem cells [79, 82-85]. In this model, asymmetric distribution of proteins on the cell surface and inside the cytoplasm along the axis between the T cell and the priming DC results in an asymmetric distribution of fate determining agents onto the two daughter cells that arise after the first cell division [83] (Fig. 4). The progeny of the proximal daughter cell will mainly differentiate into SLECs, while the distal daughter cell will mostly generate MPs. [82, 83].

#### 1.4.2 MPs emerge from SLECs

The 'linear differentiation' hypothesis derives from the observation of the dominance of cells with effector functions during the expansion phase and the peak of expansion, as well as from the dominance of memory cells after the contraction phase (Fig. 5). It states that SLECs differentiate further into MPs and these into memory T cells [86, 87].

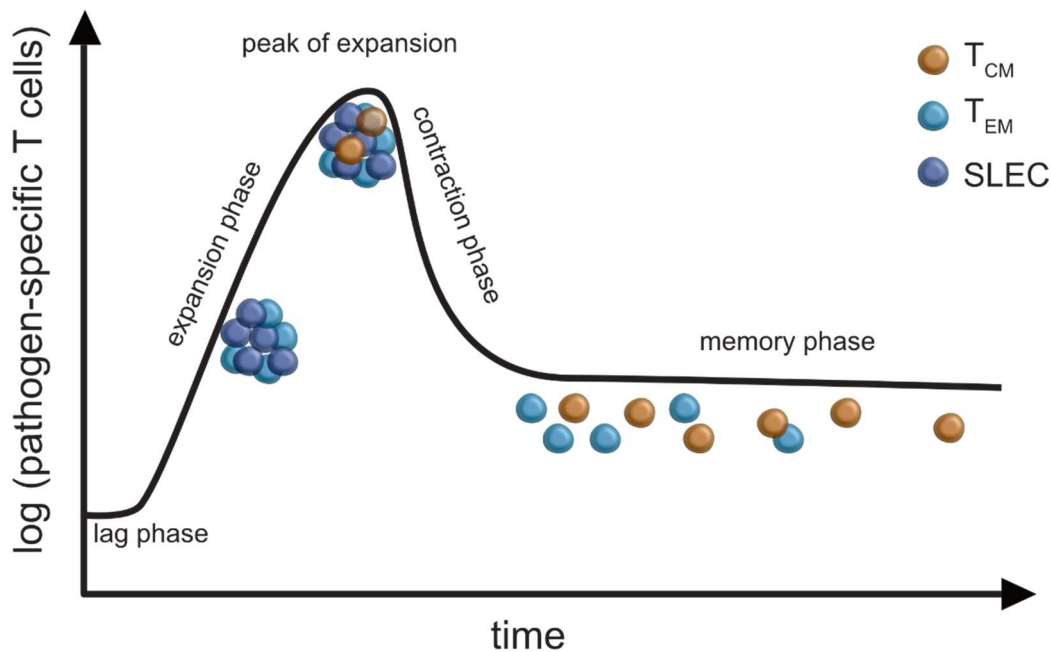


**Fig. 5: The phases of a CD8 T cell response are dominated by different phenotypes.** The expansion phase and the peak of expansion are dominated by short-lived effector cell (SLECs) and effector memory cells (T<sub>EM</sub>). When roughly 95 % of the T cells die during the contraction phase, mainly effector-memory and central memory cells (T<sub>CM</sub>) are left over.

### 1.4.3 SLECs emerge from MPs

According to the decreasing potential hypothesis [87], naïve T cells become memory or memory precursor cells after activation. Memory T cells can expand upon reinfection and replenish all T cell subsets. Thus, they have similarities with naïve T cells as opposed to short-lived effector T cells. During the expansion phase, the T cells receive different pro-inflammatory and effector-promoting signals that drive differentiation away from a memory phenotype (Fig. 6). The low number of memory cells that survive the contraction phase consists of those cells that received fewer differentiating signals [4, 78, 87, 88].

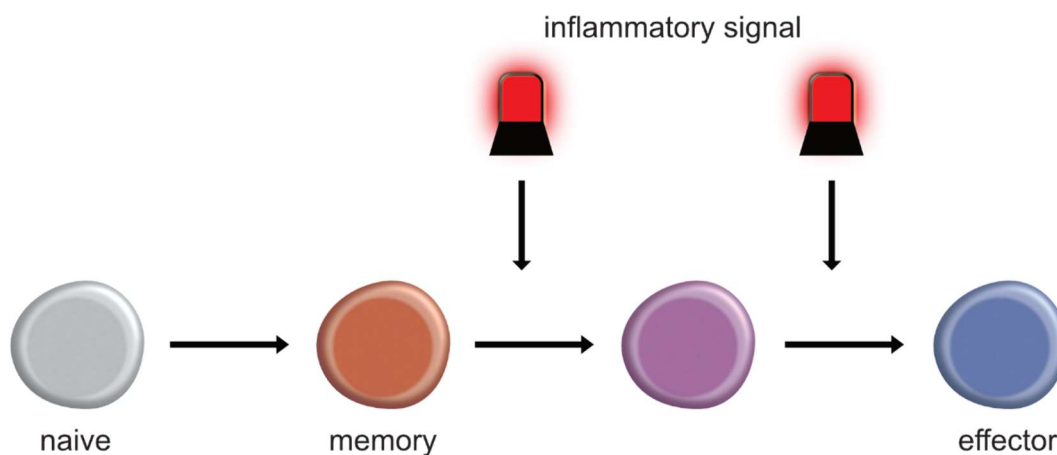


**Fig. 6: Decreasing Potential hypothesis.** Pro-inflammatory signals accumulate and lead to differentiation of low differentiated memory or memory precursor cells into terminally differentiated effector cells.

Similar to the 'decreasing potential' hypothesis, the 'stochastic model of progressive differentiation' [89-91] assumes the occurrence of events that drive the progression from MPs into terminally differentiated SLECs. However, these events are not necessarily external instructing signals but can also be stochastic variations within the cells that change, for example, the responsiveness of a particular cell to an instructing signal. Furthermore, this model explains the distribution over time of effector cells and memory precursor cells by different proliferation rates of central memory precursor cells (TCM<sub>ps</sub>) (slow cycling), effector memory precursor cells (TEM<sub>ps</sub>) (fast cycling) and SLECs (even faster cycling) already before the peak of expansion [89] (Fig. 7).

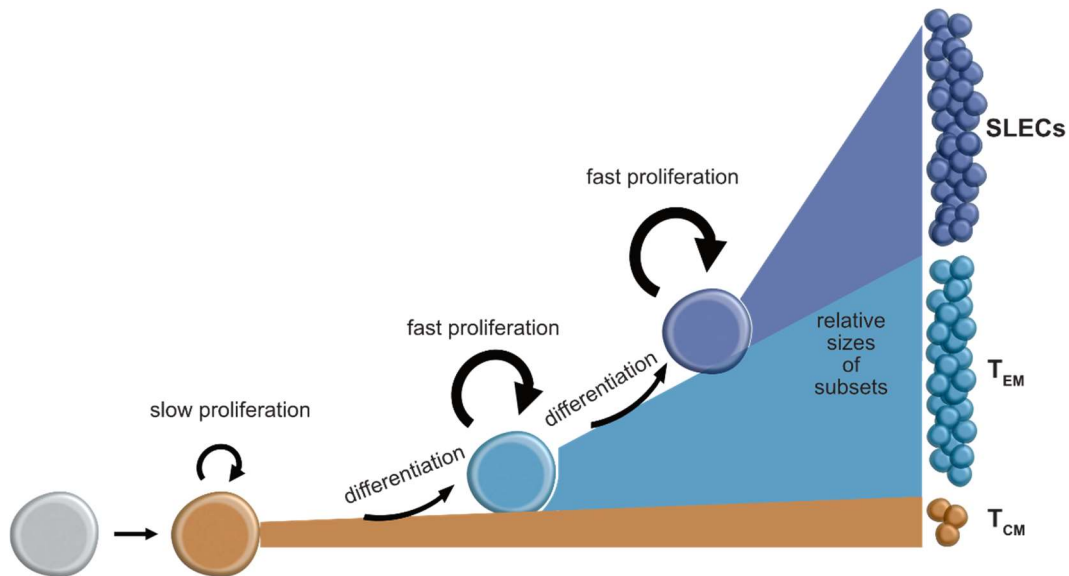


**Fig. 7: Stochastic model of progressive differentiation.** After activation naïve CD8 T cells differentiate into  $T_{CM}$  precursor cells with a slow proliferation rate. In a stochastic fashion, a  $T_{CM}$  precursor cell may differentiate further into an  $T_{EM}$  precursor cell. This differentiation step is associated with an increase in the proliferation rate of the differentiated cell and its progeny. During a further differentiation event, a  $T_{EM}$  precursor cell may differentiate into a SLECs. The proliferation rate of SLECs was suggested to be even a little higher than for  $T_{EM}$  precursor cells.

The high diversity of current hypotheses that try to explain memory generation in CD8 T cells shows that there is a key aspect about CD8 T cell differentiation that we don't understand despite years of research. Thus, the order in which CD8 T cell subsets differentiate is one aspect that will be addressed in this thesis.

## 1.5 How are fate decisions made?

Resolving the order in which the T cell subsets differentiate still leaves the question open of why and how the phenotype is changed.

A few possibilities have already been introduced together with the pathways of differentiation (e.g., external instructing signals, stochastic variations, distinct responsiveness towards the same signal, unequal distribution of proteins during cell division). The 'progressive differentiation' model suggests that the priming event might already imprint the fate of all daughter cells of the primed T cell [92-94]. A strong activation signal such as that

provided by a high affinity TCR or a strong costimulation would result in effector-prone descendants [58, 95]. In more recent publications, the differentiation was claimed to be coupled to proliferation [96, 97]. In a single cell-derived progeny that has gone through many cell divisions, the likelihood of each cell within this progeny to differentiate into a SLEC is believed to be very high, whereas few cell divisions would result in memory-prone progenies (Fig. 8B). This ‘division-linked differentiation’ hypothesis is in conflict with the ‘differentiation-linked proliferation’ hypothesis (Fig. 8A) of the ‘stochastic model of progressive differentiation’ in which distinct proliferation rates are acquired by differentiation into the T cell subset that is assigned to the respective proliferation rate [89].

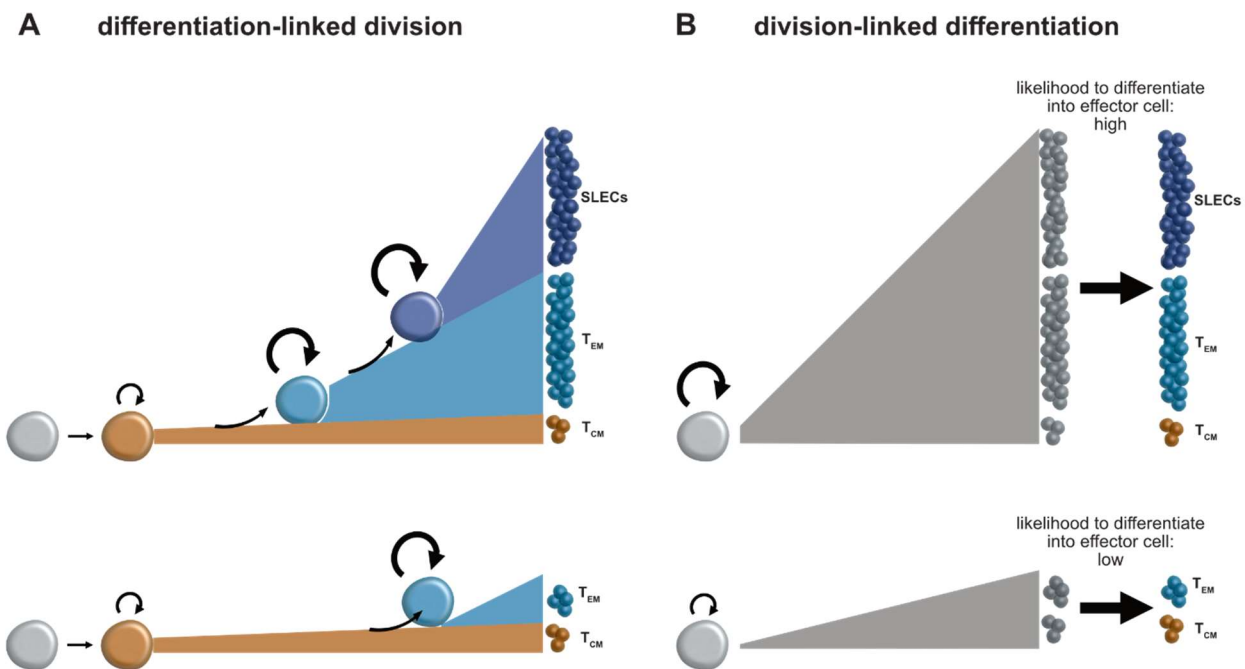


**Fig. 8: Differentiation-linked division vs. Division-linked differentiation.** **A:** Differentiation-linked division. Distinct division speeds are assigned to different phenotypes. Differentiation into a  $T_{EM}$  or SLEC increases division speed. Early differentiation into effector cells leads to large effector-prone populations (upper panel). Late differentiation into effector cells leads to small memory-prone populations (lower panel). **B:** Division-linked differentiation. Due to different but homogenous division speeds or early vs. late division cessation, the T cells have passed through many (upper panel) or just a few (lower panel) cell divisions. The higher the cell number is, the higher is the likelihood for the respective T cell to differentiate into an effector cell.

Understanding the relationship between phenotype and division speed in combination with the pathway of differentiation is crucial for the improvement of vaccinations and immune therapies because knowledge would enable us to enhance prediction quality of the sizes of memory and effector populations at different time points.

## **1.6 Call for new methods**

The variety of opinions about T cell development shows that it is very challenging to get the information that is required to resolve the differentiation pathway. A method that is widely used in immunological research and has already provided an enormous contribution to our understanding of the immune system is flow cytometry.

### **1.6.1 The gold standard in immunology**

In flow cytometry an aliquot of cells (e.g., from a blood sample or a biopsy) is co-incubated with antibodies against structures on the surfaces of the cells. The antibodies are conjugated with different fluorescent dyes. When the cells are analyzed individually in the flow cytometer by dilution in a narrow beam of sheath buffer, the fluorescent dyes that are bound to the cells via the antibodies are excited and the emitted light is measured [98]. Cells of a certain subset are usually equipped with combinations of surface antigens that are specific for this kind of cell. Thus, the emitted light reveals which antigens are expressed by the analyzed cell and allows for the determination of the phenotype or the subset of the cell [98].

However, the value of flow cytometry for the investigation of T cell differentiation pathways is limited due to the fact that the T cells have to be taken out of their habitat and give only a snapshot of the phenotypes at the time point of analysis. Dynamic changes or the ancestry and relationships between the measured cells are not unveiled by flow cytometry.

### 1.6.2 Live-cell imaging

A method that can map dynamic changes and ancestry of cells is continuous live-cell imaging. This assay has already been used successfully to delineate differentiation pathways of hematopoietic stem cells [99]. The principle behind live-cell imaging is to equip a microscope with an incubation chamber and produce a time-lapse movie of living cells. If the gap between two consecutive pictures is short enough, the identity of the cells is preserved, and the movements and cell divisions can be tracked [100, 101]. With those data, whole genealogical trees (also known as family trees) can be generated and the time between two consecutive cell divisions (= 'cell cycle speed' or 'inter-division time' (idt)) can be calculated for each individual cell [99, 100]. Furthermore, it has been shown that fluorophore-conjugated antibodies can be added in very low concentrations to the cultured cells [99], so that the cell is not influenced by the bound antibodies and the concentration of free-floating antibody is low enough to enable detection of specifically bound antibodies. The expression of the respective epitopes can be measured by live-cell imaging associated fluorescence microscopy [100]. By the combination of the genealogical data, the inter-division times and the phenotypic data, provided by the antibody staining, all required information should be provided to comprehend the differentiation from naïve T cells into memory and effector cells.

## 2 Aim of this thesis

During an adaptive immune response, naïve T cells that bind to their cognate antigen are induced to rapidly proliferate. In well-defined settings of infection or vaccination, the burst size derived from an epitope-specific T cell population is reliably regulated and can be closely predicted. However, single-cell fate mapping has shown that this reliable regulation at the population-level is based on an averaging of highly variable response behaviors of individual T cells. In response to the same infection or vaccination, clonal expansion of individual T cells harboring identical T cell receptors (TCRs) was found to vary across more than three orders of magnitude. Immune responses of single CD8 and CD4 T cells derived from an endogenous, polyclonal TCR repertoire have also shown strong variation in clonal expansion. Thus, on the single-cell level, response variation appears to be a fundamental feature of T cell immune responses. How this variation comes about, remains, however, incompletely understood. Computational modelling based on single-T-cell derived response patterns, measured at day 8 after *Listeria monocytogenes* infection in vivo, has suggested that differences in clonal expansion are due to differences in cell-cycle speed of responding T cells. However, *in vitro* studies that monitored cell-cycle speed of activated T cells directly rather supported a regulation of the time to first division and/or the time to division cessation as major factors influencing clonal burst size. Furthermore, computational modelling of *in vivo* immune responses has suggested that distinct division speeds develop in distinct subsets contained within the same single-T-cell derived progeny—with long-lived memory precursors (MPs) and short-lived effector cells (SLECs) showing slow and fast division speeds, respectively. However, such a segregation into distinct division activities within the same clone has not been observed directly. Instead, tracing cell proliferation *in vitro* has shown that T cells belonging to the same single cell-derived clone show highly concordant division activity—characterized by a synchronized timing of divisions and division cessation. However, these analyses were limited to studying the first 3–4 T cell divisions, were explicitly focused on

reducing the influence of further stimuli beyond initial T cell priming, and did not attempt a phenotypic characterization of developing T cells.

Thus, based on the current literature, it remained unresolved:

1) how much distinct division speeds contribute to the variable expansion of single-T-cell derived clones

2) how division speed is influenced by antigenic and cytokine-based stimuli available beyond priming

3) whether distinct division speeds develop and are maintained in separate subpopulations of the same clone

and

4) whether distinct division speeds coincide with MP and SLEC phenotypes.

It is these questions that I aimed to answer in the course of this dissertation. To do so I expanded single naïve CD8 T cells *in vitro* over a period of five days and performed live-cell imaging of the single cell-derived progenies. This enabled me to track the fates of all cells, create genealogical trees and directly extract the division speeds of all individual cells. I addressed the influence of antigenic and cytokine-based stimuli beyond priming by establishing similar experiments in which the availability of TCR-stimuli was restricted to the first 24 h and cytokines were added to the culture. Finally, to investigate whether distinct division speeds coincide with MP and SLEC phenotypes, live-cell imaging was performed in combination with fluorescent antibodies against subset-related markers.

## 3 Material and Methods

### 3.1 Materials

#### 3.1.1 Chemicals and Reagents

<b>Chemicals/Reagents</b>	<b>Provider</b>
Ammonium chloride (NH <sub>4</sub> Cl)	Sigma, Taufkirchen, Germany
Assay Diluent (for ELISA)	eBioscience, San Diego, California, USA
Avidin HRP	Thermo fisher scientific, Waltham, USA
Bovine serum albumin (BSA)	GE Healthcare, Munich, Germany
BrefeldinA (Golgi Plug)	BD Biosciences, Heidelberg, Germany
Capture antibody (for ELISA)	eBioscience, San Diego, California, USA
CellTrace Violet™ Cell Proliferation Kit	Thermo fisher scientific, Waltham, USA
Coating buffer (10x for ELISA)	eBioscience, San Diego, California, USA
Cytofix/Cytoperm	BD Biosciences, Heidelberg, Germany
Ethanol	Klinikum rechts der Isar, Munich, Germany
Ethidium-monoazide-bromide (EMA)	Molecular Probes, Leiden, Netherlands
Ethylenediaminetetraacetic acid (EDTA)	Roth, Karlsruhe, Germany

---

Fetal calf serum (FCS)	Biochrom, Berlin, Germany
	Thermo fisher scientific, Waltham, USA
Fixation viability dye eFluor 780	eBioscience, San Diego, California, USA
Heparin-Natrium-25000	Ratiopharm, Ulm, Germany
Hydrochloride (HCl)	Roth, Karlsruhe, Germany
Ionomycin	Sigma, Taufkirchen, Germany
SIINFEKL-peptide	Peptides & elephants, Hennigsdorf, Germany
Phorbol-myristate-acetate (PMA)	Sigma, Taufkirchen, Germany
Phosphate buffered saline (PBS)	Biochrom, Berlin, Germany
Propidium iodide (PI)	Invitrogen, Carlsbad, CA, USA
RPMI 1640	PAA Laboratories, Pasching, Austria
	Thermo fisher scientific, Waltham, USA
RPMI 1640 without phenol red	Thermo fisher scientific, Waltham, USA
Sodium azide	Sigma, Taufkirchen, Germany
Sodium chloride (NaCl)	Roth, Karlsruhe, Germany
Stop solution (for ELISA)	Thermo fisher scientific, Waltham, USA
Streptavidin-PE	eBioscience, San Diego, California, USA
Substrate solution (for ELISA)	eBioscience, San Diego, California, USA

Trypan Blue	Sigma, Taufkirchen, Germany
Washing buffer (for ELISA)	eBioscience, San Diego, California, USA

### 3.1.2 Antibodies (anti-murine)

<u>Epitope</u>	<u>Fluorochrome</u>	<u>Clone</u>	<u>Provider</u>
CD3	-	145-2C11	BD Biosciences, Heidelberg, Germany
	APC	145-2C11	Biolegend, San Diego, USA
	FITC	17A2	BD Biosciences, Heidelberg, Germany
	PE-Cy7	145-2C11	Biolegend, San Diego, USA
CD8	APC	5H10	Thermo fisher scientific, Waltham, USA
	APC-Cy7	53.6.7	Biolegend, San Diego, USA
	FITC	53-6.7	Biolegend, San Diego, USA
	Pacific Blue	53.6.7	Biolegend, San Diego, USA
	Pacific Orange	5H10	Thermo fisher scientific, Waltham, USA
	PE	53-6.7	Biolegend, San Diego, USA
	PE-CF594	53-6.7	BD Biosciences, Heidelberg, Germany
	PE-Cy7	53-6.7	Biolegend, San Diego, USA
	PerCP-Cy5.5	53-6.7	Biolegend, San Diego, USA
CD19	PE-CF594	1D3	BD Biosciences, Heidelberg, Germany
	PE/Dazzle 594	6D5	Biolegend, San Diego, USA
CD25	APC	PC61.5	BD Biosciences, Heidelberg, Germany
	Alexa488	PC61.5	Thermo fisher scientific, Waltham, USA
	PE	PC61.5	Thermo fisher scientific, Waltham, USA

CD27	APC	LG7.F9	Thermo fisher scientific, Waltham, USA
	PE	LG7.F9	Thermo fisher scientific, Waltham, USA
	PE-Cy7	LG.7-F9	Biolegend, San Diego, USA
CD28	-	37.51	BD Biosciences, Heidelberg, Germany
CD44	APC	IM7	Biolegend, San Diego, USA
	FITC	IM7	Biolegend, San Diego, USA
	PE	IM7	Biolegend, San Diego, USA
CD45.1	APC	A20	Biolegend, San Diego, USA
	APC-Cy7	A20	Biolegend, San Diego, USA
	BV421	A20	Biolegend, San Diego, USA
	BV650	A20	Biolegend, San Diego, USA
	BV785	A20	Biolegend, San Diego, USA
	FITC	A20	Biolegend, San Diego, USA
	Pacific Blue	A20	Biolegend, San Diego, USA
	PE	A20	Biolegend, San Diego, USA
	PE-Cy7	A20	Biolegend, San Diego, USA
	PE/Dazzle 594	A20	Biolegend, San Diego, USA
	PerCP-Cy5.5	A20	Biolegend, San Diego, USA
CD45.2	APC	104	Biolegend, San Diego, USA
	BV650	104	Biolegend, San Diego, USA
	FITC	104	Biolegend, San Diego, USA
	Pacific Blue	104	Biolegend, San Diego, USA
	PE	104	Biolegend, San Diego, USA
	PerCP-Cy5.5	104	Biolegend, San Diego, USA

CD62L APC	MEL-14	Biolegend, San Diego, USA
FITC	MEL-14	Biolegend, San Diego, USA
Pacific Blue	MEL-14	Biolegend, San Diego, USA
PE	MEL-14	Biolegend, San Diego, USA
PE-Cy7	MEL-14	Biolegend, San Diego, USA
CD69 FITC	H1.2F3	Biolegend, San Diego, USA
CD90.1 APC	HIS51	Thermo fisher scientific, Waltham, USA
APC-eF780	HIS51	Thermo fisher scientific, Waltham, USA
eF450	HIS51	Thermo fisher scientific, Waltham, USA
FITC	HIS51	Thermo fisher scientific, Waltham, USA
PE	HIS51	Thermo fisher scientific, Waltham, USA
PerCP-Cy5.5	HIS51	Thermo fisher scientific, Waltham, USA
CD90.2 APC	53-2.1	Thermo fisher scientific, Waltham, USA
APC-Cy7	53-2.1	BD Bioscience, Heidelberg, Germany
APC-eF780	53-2.1	Thermo fisher scientific, Waltham, USA
eF450	53-2.1	Biolegend, San Diego, USA
BV785	30-H12	Biolegend, San Diego, USA
CD127 PE	A7R34	Biolegend, San Diego, USA
IL2 -	JES6-5H4	Thermo fisher scientific, Waltham, USA
KLRG1 APC	2F1	Thermo fisher scientific, Waltham, USA
PE	2F1	Thermo fisher scientific, Waltham, USA
PE-Cy7	2F1	Biolegend, San Diego, USA

### 3.1.3 Buffers

<b>Buffer</b>	<b>Recipe</b>		
Ammonium chloride Tris (ACT)	0.17 M	NH <sub>4</sub> Cl	
	0.3 M	Tris-HCl, pH 7.5	
FACS buffer	1x	PBS, pH 7.5	
	0.5 % (w/v)	BSA	
Phosphate buffered saline (PBS) powder	9.55 g/l	Dulbecco's	PBS

### 3.1.4 Equipment

<b>Equipment</b>	<b>Model</b>	<b>Provider</b>
Cytometer	Cyan ADP Analyser	Beckman Coulter, Fullerton, USA
	MoFlo Legacy Cell Sorter	Beckman Coulter, Fullerton, USA
	MoFlo XDP Cell Sorter	Beckman Coulter, Fullerton, USA
	FACSAria III Cell Sorter	BD Biosciences, Heidelberg, Germany
	CytoFLEX Flow Cytometer	Beckman Coulter, Fullerton, USA
	CytoFLEX S Flow Cytometer	Beckman Coulter, Fullerton, USA
	CytoFLEX LX Flow Cytometer	Beckman Coulter, Fullerton, USA

---

Centrifuge	Biofuge fresco	Haraeus, Hanau, Germany
	Multifuge 3 S-R	Haraeus, Hanau, Germany
	Sorvall® RC 26 Plus	Haraeus, Hanau, Germany
	Varifuge 3.0 RS	Haraeus, Hanau, Germany
	Biofuge stratos	Haraeus, Hanau, Germany
Incubator	Cytoperm 2	Haraeus, Hanau, Germany
	Minitron	Infors, Bottmingen, Switzerland
	BE 500	Memmert, Schwabach, Germany
Bio Safety Cabinets	HERA safe	Haraeus, Hanau, Germany
Hemocytometer	Neubauer	Schubert, Munich, Germany
Water Bath	LAUDA ecoline 019	Lauda, Königshofen, Germany
pH-meter	MultiCal® pH 526	WTW, Weilheim, Germany
Weighting Scale	CP 124 S	Sartorius, Göttingen Germany

Microscope	EVOS FL Auto II	Thermo fisher scientific, Waltham, USA
Plate reader	SpectraMax i3x	Molecular Devices, San Jose, USA

### 3.1.5 Software

<b>Software</b>	<b>Provider</b>
Affinity Designer	Serif Ltd., Nottingham, UK
EndNote	Microsoft, Redmond, USA
FlowJo	BD Biosciences, Heidelberg, Germany
GraphPad Prism	GraphPad Software, La Jolla, USA
Microsoft Office	Microsoft, Redmont, USA
Summit V4.5	Beckman Coulter, Fullerton, USA
The Tracking Tool	ETH Zurich, Basel, Switzerland
qTFy	ETH Zurich, Basel, Switzerland
TTT Converter	ETH Zurich, Basel, Switzerland
fasTER	ETH Zurich, Basel, Switzerland
STATTTs	ETH Zurich, Basel, Switzerland
Visual Basic	Microsoft, Redmont, USA
MetaMorph	Molecular Devices, San José, USA
CytExpert	Beckman Coulter, Fullerton, USA

## 3.2 Methods

### 3.2.1 Transfer of T cells

For the transfer of T cells, spleen or blood was taken from donor mice which expressed a combination of congenic markers<sup>1</sup> that was different from the pattern expressed by the recipient mice and a single-cell suspension was produced as described below. Depending on the T cell subset that was to be transferred, a fitting staining panel was established, and the cells were stained as described below. However, the concentrations of several staining antibodies were chosen in lower concentrations compared to staining for flow cytometry to prevent that antibodies on the surface of the cells influence the behavior of the stained cells. This was especially the case for  $\alpha$ -CD25 and  $\alpha$ -CD62L. In addition to the donor cells, cells from blood or spleen of feeder mice were prepared. The feeder mice expressed the same congenic markers as the recipient cells and were used to enhance the transfer of low cell numbers. Feeder blood or spleen was processed as donor blood or spleen but not stained with antibodies. Instead, they were diluted in sterile filtered FCS to a concentration of  $4 \times 10^5$  cells/200  $\mu$ l. 200  $\mu$ l of this cell suspension were pipetted into wells of a 96-well V-bottom plate (1 well à 200  $\mu$ l for each recipient mouse) and the plate was centrifuged shortly for 30 secs at 1500 rpm. The stained donor cells were sorted on top of the feeder cells in FCS by the in-house FACS core facility on a MoFlo Legacy or XDP cell sorter. Subsequently, the plate was centrifuged again for 30 secs and the cells were injected i.p. into the recipient mice.

### 3.2.2 Infection with *Listeria monocytogenes*

5 mL of BHI medium were filled into a test tube and 1 mL was transferred into a cuvette as a negative control. 10-20  $\mu$ l of *L.m.*-OVA stock solution were added to the remaining BHI medium. The tube was vortexed shortly and incubated for 4.5-6 h at 37° C under perturbation. 1 mL of bacteria suspension was carefully pipetted into a fresh cuvette and the OD<sub>600</sub> was

---

<sup>1</sup> Congenic markers (e.g., CD45.1 and CD45.2) are proteins on the surface of cells for which different isoforms exist. Those isoforms are not immunogenic to mice which express the other isoform but you can discriminate between the isoforms by antibody staining and flow cytometry. Thus, it is possible to determine which cells in a recipient mouse originate from the donor mouse and which originate from the recipient mouse.

measured in a photometer. The number of bacteria per mL were calculated using the following semi-empirical formula:

$$c_{L.m.} = 12 \cdot 10^8 \cdot \frac{OD_{600}}{ml}$$

Depending on the respective experiment, the bacteria were diluted in cold and sterile PBS until the desired infection dose was adjusted to an injection volume of 200  $\mu$ l. For experiments with wt *Listeria* the infection dose for primary infections was 2000 cfu in 200  $\mu$ l per mouse. Due to the lower virulence of *L.m.-OVA*, the infection dose for primary infections with *L.m.-OVA* was 5000 cfu and  $2 \times 10^5$  for rechallenge infections. The resulting suspension was injected into a tail vein. To control for the infection dose, an appropriate amount of cell suspension was plated onto agarose gels containing BHI. The plates were incubated at 37° C for 1-2 days and the number of colonies was counted. During the infection the mice were monitored regarding weight loss and health.

### 3.2.3 Single-cell suspension from spleen or lymph nodes

Infected or naïve C57BL/6 mice were euthanized by cervical dislocation. If lymph nodes were required, inguinal, mesenteric, brachial and axillary lymph nodes were taken, collected in a tube containing 1.5 mL RPMI complete and mashed through a cell strainer (grid size 40-100  $\mu$ m) into a petri dish. Spleens were similarly pressed through a cell strainer. Mashed organs were transferred into a fresh 15 mL falcon tube and RPMI complete was added until a total volume of 10 mL per tube was reached. Cells were pelleted for 5-6 min at RT and 1500 rpm. Supernatant was removed by aspiration through a Pasteur pipette and pellets were resuspended in 5 mL ACT buffer at room temperature. To lyse erythrocytes, the cell suspension was incubated in ACT at RT for 5 min. Subsequently lysis was stopped by the addition of 9 mL cold RPMI. If mice had been infected, RPMI complete was also used for this step. Next, cells were pelleted for 5-6 min at 4° C and 1500 rpm and washed again with 10 mL cold RPMI. An aliquot of 10  $\mu$ l was taken to determine the cell number in a Neubauer counting chamber, and the cells were stored on ice until progression with further protocols.

### 3.2.3 Single-cell suspension from blood

50-200  $\mu$ l blood were taken from the donor mice and mixed with approximately 10  $\mu$ l heparin. The blood was diluted in 10 mL ACT buffer at room temperature, and erythrocytes were lysed for 10 min. Subsequently, the tube was centrifuged for 6-7 min at RT and 1500 rpm and the supernatant was aspirated. The pellet was suspended in further 5 mL of ACT buffer, and erythrocytes were lysed for another 5 min at RT. At the end of the incubation time, lysis was stopped by the addition of 9 mL cold RPMI media, and the tube was centrifuged for 6-7 min at 4° C and 1500 rpm. The cells were washed with 2-5 mL cold FACS buffer and centrifuged for 6-7 min at 4° C and 1500 rpm. For antibody staining cells were suspended in 300  $\mu$ l FACS buffer.

### 3.2.4 Staining for flow cytometry

Cells were pelleted for 5-6 min at 4° C and 1500 rpm and washed with 10 mL FACS buffer. Subsequently the cells were pelleted again and resuspended in fresh FACS buffer, resulting in a concentration of  $10^8$  cells/mL based on the counting results with the Neubauer counting chamber. For staining, the cell suspension was transferred into a 96-well V-bottom plate. Depending on the demands of the experiment, another number of wells was filled with 100  $\mu$ l cell suspension per well, containing  $10^7$  cells. For experiments in which no cells were transferred into the mice, just one well per sample was used. For experiments in which populations of cells with a congenic marker had been transferred, usually 2 wells/sample were stained, and when single cells had been transferred, 4 wells were prepared for staining. In addition to the samples, a few wells were prepared for single color and unstained controls to be able to compensate for the spillovers of different fluorescence channels at the flow cytometer. For this purpose, cells from all samples were pooled (if available), and 10-50  $\mu$ l of the resulting cell suspension was pipetted into each unstained or single color well.

The cells were pelleted for 3 min at 4° C and 1500 rpm, and supernatant was discarded by a swift movement of the plate up-side down. To block Fc $\gamma$ -

receptors<sup>2</sup>, unconjugated  $\alpha$ -Fc $\gamma$ -antibody (Fc-block) was dissolved 1:200 in FACS buffer, and cells were resuspended in 100  $\mu$ l of the resulting solution. The plate was incubated for 20 min on ice. For experiments in which it was not planned to read in the cells at the flow cytometer on the same day, the cells were stained with EMA to discriminate between alive and dead cells<sup>3</sup>. In those cases, EMA-stock solution was diluted 1:1000 into the prepared FACS/Fc-block buffer prior to addition to the cells. The incubation step was conducted below a light source to allow for covalent binding of EMA. Subsequent to the incubation, 100  $\mu$ l FACS buffer were added into each well, and the cells were pelleted for 3 min at 4° C and 1500 rpm. The supernatant was discarded, and the cells were washed with 200  $\mu$ l FACS buffer.

For each channel used at the flow cytometer, 0.5-1  $\mu$ l of an antibody solution containing the respective fluorescent label and specificity for an epitope expressed by a sufficient number of cells in the samples was added to 100  $\mu$ l of FACS buffer into the SC-well dedicated to the respective channel. For the wells that contained the samples, a master mix was prepared that contained all antibodies of the respective staining panel diluted in FACS buffer at a concentration specific for the respective antibody. 100  $\mu$ l of the resulting master mix were pipetted into each sample well, and then the cells were resuspended and incubated for 30 min on ice in the dark to prevent bleaching of the fluorescent dyes. After the incubation time, 100  $\mu$ l FACS buffer were added into each well, the cells were pelleted again for 3 min at 4° C and 1500 rpm and resuspended in 200  $\mu$ l FACS buffer.

If no EMA was used for the staining of dead cells, 100  $\mu$ l of PI-stock solution, diluted 1:200 in FACS buffer were added into each well (also US and SC wells). The cells were resuspended and incubated for another 3 min. After incubation, 100  $\mu$ l FACS buffer were added into each well, and cells were

---

<sup>2</sup> Fc $\gamma$ -receptors are expressed by certain cell types (e.g. B cells, macrophages, NK cells, DCs), and bind to the constant region of antibodies. Thus, they could also bind to the constant region of fluorescent-dye conjugated antibodies that we use for detection of markers on the cell surface, thereby leading to false positive events.

<sup>3</sup> PI and EMA are dyes that can cross the perforated cell membrane of dead cells and intercalate with DNA. While this process is reversible for PI, EMA binds covalently to DNA via a light induced reaction, thus enabling us to discriminate between live and dead cells even days after staining and fixation.

pelleted for 3 min at 4° C and 1500 rpm. Subsequently all wells were washed again with 200 µl FACS buffer. If EMA was used for the staining of dead cells, the step containing PI was replaced by washing the cells another time with 200 µl FACS buffer and instead of suspending the cells in 200 µl FACS buffer after the last washing step, they were fixed by resuspension in FACS buffer containing 0.5 % PFA.

The cells were stored at 1-4° C in the dark and filtered through a nylon mesh prior to reading in at a flow cytometer.

If cells were stained not for analysis but were planned to be sorted for transfer *in vivo* or *in vitro*, they were not fixed with PFA or stained with EMA or PI, but PI stock solution was added 1:200 to the cells in FACS buffer directly prior to sorting.

### 3.2.5 CTV staining

A single-cell suspension was established, and the cells were washed twice with PBS. The cells were counted, and the concentration was adjusted to max.  $10^6$  cells/mL. Subsequently, 1 mL of the cells were pelleted and resuspended in 500 µl pre-warmed PBS. 20 µl DMSO were added to one fresh vial of CTV, resulting in a stock solution of 5 mM CTV. 2 µl of the stock solution were mixed with 500 µl pre-warmed PBS, and the staining solution was added to the cell suspension while vortexing the sample. Subsequently, the cells were incubated for 20 min at 37° C protected from light in a water bath. When the incubation time was over, at least 5 mL pre-warmed RPMI + 10 % FCS were added, and the cells were incubated at 37° C for further 5 min to remove any free dye from the solution. The cells were centrifuged at 1500 rpm for 6 min and resuspended in 1 mL pre-warmed RPMI. Subsequently, the cell suspension was stained for cell sorting as described above. To be able to determine the number of cell divisions after analysis via flow-cytometry, an aliquot of freshly CTV-stained cells was stored at 4° C until analysis as a control for the undivided peak.

### 3.2.6 Single-cell expansion (continuous stimulation)

For continuous single-cell expansion, stock solutions of antibodies against CD3 and CD28 were diluted 1:50 in sterile PBS, and 6  $\mu$ l of the resulting coating reagent were pipetted into each well of a small volume 384-well plate. Those plates were incubated over night at 4° C. Approximately 4 h prior to the cell sort, 10  $\mu$ l sterile filtered FCS were added to the wells and further incubated for 3.5 h at 4° C. In the meantime, cells from blood of a OT-I Rag1<sup>-/-</sup> mouse were prepared for sorting as described above and stained with antibodies against CD8 and CD44. The medium for single-cell expansion was prepared (RPMI complete without phenol red + 25 U/mL IL-2 + 10 ng/mL IL-12), the content of the plate was thrown off, and the wells were refilled with 15-20  $\mu$ l of the prepared medium for single-cell expansion. Into those wells a single living naïve OT-I cell (PI<sup>-</sup>, CD44<sup>low</sup>, CD8<sup>+</sup>) was sorted at a MoFlo Leagacy or XDP cell sorter. The plate was incubated at 37° C, 95 % H<sub>2</sub>O and 5 % CO<sub>2</sub>.

### 3.2.7 Single-cell expansion (discontinuous stimulation)

To stimulate the T cells just for 24 h with  $\alpha$ -CD3 and culture them further without signal 1, a large-volume 384-well plate was coated with  $\alpha$ -CD3/ $\alpha$ -CD28 in PBS. For each well, 10  $\mu$ l of coating reagent were used. Further procedure was as described for continuous stimulation with the following changes: Instead of 10  $\mu$ l FCS, 20  $\mu$ l sterile filtered FCS were used per well and instead of naïve single cells, 10 000 naïve OT-I cells were sorted into each well. The plate was cultured for 24 h at 37° C, 95 % H<sub>2</sub>O and 5 % CO<sub>2</sub>.

Meanwhile, a small-volume 384-well plate was prepared as described in the continuous-stimulation section, but the coating reagent contained just  $\alpha$ -CD28 in PBS and no  $\alpha$ -CD3. Depending on the respective experiment the medium for single-cell expansion was made of RPMI complete without phenol red +25 or 250 U/mL IL-2 with or without 10 ng/mL IL-12.

When 24 h incubation time were over, the cells from the large-volume 384-well plate were transferred into a 96-well V-bottom plate and pooled via several rounds of centrifugation (5 min at 4° C and 1500 rpm) and resuspension in a smaller volume of cold FACS buffer until all cells fit into

one well. The cells were suspended in 200  $\mu$ l FACS buffer, 2  $\mu$ l  $\alpha$ -CD8 antibody (conjugated to eF450) and 0.6  $\mu$ l  $\alpha$ -CD44 antibody (conjugated to FITC) were added to the wells, mixed and incubated on ice in the dark for 30 min. PI was added prior to the sorting, and a single activated (CD8<sup>+</sup>, CD44<sup>high</sup>) OT-I cell was sorted into each well. Subsequently, the plate was incubated at 37° C with 5 % CO<sub>2</sub> and 95 % H<sub>2</sub>O.

### 3.2.8 Single-cell expansion (splenocyte cultures)

To expand T cells in a more physiological environment, CD8 T cells were also expanded in the presence of splenocytes. For this purpose, a single-cell suspension from the spleen of a wt C57BL/6 mouse and another single-cell suspension from blood of an OT-1 Rag1<sup>-/-</sup> mouse was made. The combination of congenic markers expressed by the OT-1 mouse had to be distinct from the phenotype of the wt mouse. After ACT lysis, the splenocytes were suspended in 5 mL RPMI and split into 5 wells of a 12 well plate. 1  $\mu$ l of 1 $\mu$ g/ $\mu$ l SIINFEKL peptide in DMSO was added to the cells to load them with the cognate epitope for OT-1 cells and the cells were incubated at 37° C with 5 % CO<sub>2</sub> and 95 % H<sub>2</sub>O for 60 min. When the incubation time was over, the cells were transferred back into a 15 mL Falcon tube and washed twice with 10 mL RPMI. Cells were counted in a Neubauer counting chamber and diluted in RPMI complete + 25 U/mL IL-2 to a final concentration of 10<sup>5</sup> cells per 200  $\mu$ l FCS. 200  $\mu$ l of the resulting cell suspension were filled into each well of a 96-well V-bottom or U-bottom plate.

In parallel, the cells from the OT-1 blood were prepared for sorting of naïve CD8 T cells as described in the sections “Staining for flow cytometry” and “Single-cell expansion from blood”. Subsequently, a single naïve CD44<sup>low</sup> and CD8<sup>+</sup> cell was sorted into each well with the SIINFEKL-pulsed splenocytes and cultured at 37° C, 5 % CO<sub>2</sub> and 95 % H<sub>2</sub>O. Due to the high cell density compared to feeder free single-cell expansion, half of the medium was exchanged every 1-2 days.

### 3.2.9 Enzyme-linked immunosorbent assay (ELISA)

One day prior to analysis, a NUNC maxi sorb 96 well plate was coated with capture antibody. For that purpose, 50  $\mu$ l coating buffer containing the antibody diluted as noted on the antibody vial was applied to each well and the plate was covered, sealed and incubated overnight at 4° C. On the next day, the wells were aspirated, washed 5 times with wash buffer (<250  $\mu$ l/well) and following the last washing step, residual buffer was removed by blotting the plate on absorbent paper. Subsequently 100  $\mu$ l of 1x Assay Diluent were added into each well and incubated for 1 h at RT. The plate was washed again 5 times as described before for the coating buffer. Fresh standards containing 0, 25 and 250 U/mL IL-2 were prepared in Assay Diluent. 50  $\mu$ l of the prepared standards and 50  $\mu$ l of supernatant from sample wells were pipetted into different wells, the plate was covered and sealed again and incubated for 2 h at RT or at 4° C over night. After incubation time, the plate was aspirated and washed again 5 times with wash buffer. 50  $\mu$ l/well of detection antibody diluted in 1x Assay Diluent were added into each well, and the plate was sealed and incubated for 1 h at RT. After aspiration and 5 additional washing steps, 50  $\mu$ l/well Avidin-HRP diluted in 1x Assay Diluent were added into each well and incubated for another 30 min a RT. The plate was washed 7 times as described before, but this time, the wells were left for 1-2 min prior to aspiration. 50  $\mu$ l/well substrate solution were added into each well, and after 15 min at RT 25  $\mu$ l/well of stop solution were added to stop the reaction. Finally, the OD at 450 nm and 570 nm was measured on a Plate Reader, and the values at 570 nm were subtracted from the values at 450 nm. The values of the standard wells were used to compile a calibration line and to determine the IL-2 concentrations in the samples.

## 4 Results

### 4.1 Establishment of a feeder-cell free single-cell culture

In this thesis, the development from naïve CD8 T cells into memory and effector T cells and their proliferation was investigated. To this end, an *in vitro* system was established, in which single CD8 T cells could be cultured under strictly defined and simple conditions. A technical requirement for this culture system was that it should allow direct observation of proliferation and differentiation of individual cells via live-cell imaging. These controlled conditions allowed the addition of different factors one by one to the culture, thereby analyzing the potential of those external stimuli to reconstitute the variability of CD8 T cells.

To find the simplest conditions under which expansion of single CD8 T cells is possible, we started with complex culture conditions that, at least partly, mimicked an *in vivo* system, and then reduced the complexity of the culture conditions stepwise. We anticipated that this procedure would also show which simplification step had the largest impact on the variability of immune responses derived from single CD8 T cells.

The first culture condition that was tested relied on whole splenocytes from C57BL/6 mice as APCs and *in vitro* infection of these cells with *Listeria monocytogenes* (*L.m.*) expressing chicken ovalbumin (OVA). Naïve OT-1 Rag1<sup>-/-</sup> cells with CD45.1 as congenic marker were used as responding CD8 T cells. OT-1 T cells express a transgenic TCR that recognizes OVA in the context of the MHC class I haplotype H2K<sup>b</sup>. By fluorescent antibody staining against CD45.1 and CD45.2, one can discriminate between offspring of OT-1 CD45.1 cells (CD45.1<sup>+</sup>) and the wt feeder cells (CD45.2<sup>+</sup>), which largely do not respond to OVA as antigen.

Unfortunately, the usage of live bacteria was not suitable for *in vitro* culture due to their rapid expansion, acidification of culture media and killing of splenocytes (data not shown).

The most complex setting that was successfully established in our lab for the activation of OT-1 cells via APCs was based on splenocytes, which were pulsed with SIINFEKL-peptide. Flow cytometric analysis of these cell mixtures after 3 days revealed that the activation of OT-1 cells was successful, as indicated by the high expression of activation markers (e.g., CD44, CD69 and CD25) and the increase in number of OT-1 cells (data not shown). Furthermore, the differentiation into different T cell subsets seemed to be intact, taking into account the distribution of the memory/effector markers CD62L and CD27 (

Fig. 9), although the fraction of CD62L<sup>low</sup> cells was lower in the cell culture assay. This reduced differentiation into effector T cells might have been caused by a lack of inflammatory signals that promote effector differentiation. Analysis of cell numbers at different time points showed that clonal expansion was a little reduced, as the mean clone size was estimated to lie between 100 and 1000 cells on day 5 p.i. (Fig. 10 and [89]). Interestingly, the variability in the size of single cell-derived progenies was also just slightly reduced compared to

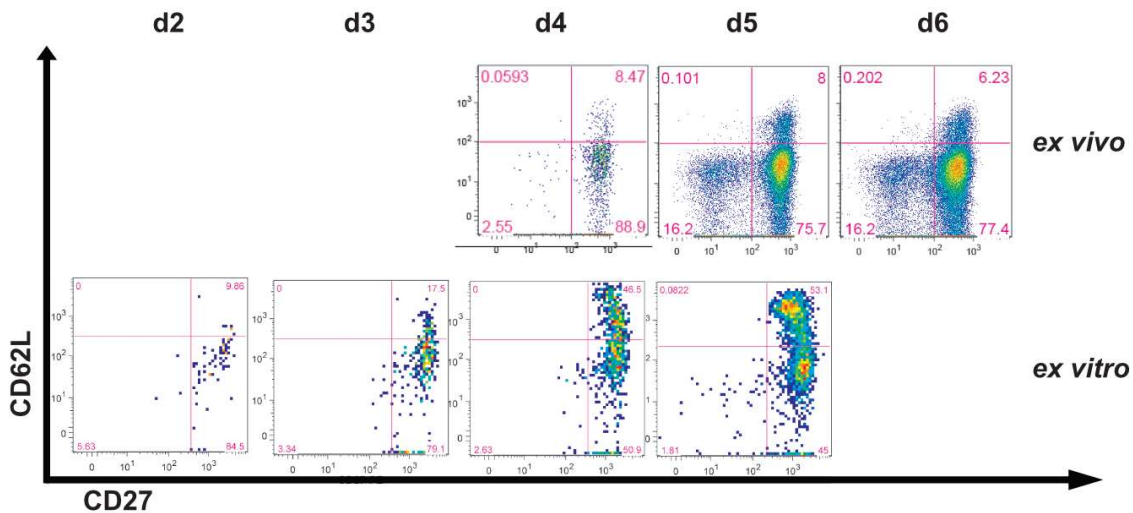


**Fig. 9: Expansion of cells *in vitro* leads to similar phenotypes as *in vivo*.** **Upper panel:** 100 000 (d4), 10 000 (d5) or 1000 (d6) naïve OT-I cells were transferred into mice that were infected with L.m.-OVA. The phenotypes were investigated by flow cytometry of splenocytes on d 4, 5 and 6 p.i. **Lower panel:** 100 naïve OT-I cells were cultured in the presence of 10<sup>5</sup> SIINFEKL-pulsed splenocytes and the phenotype was analyzed by flow cytometry on d 2, 3, 4 and 5 after sorting.

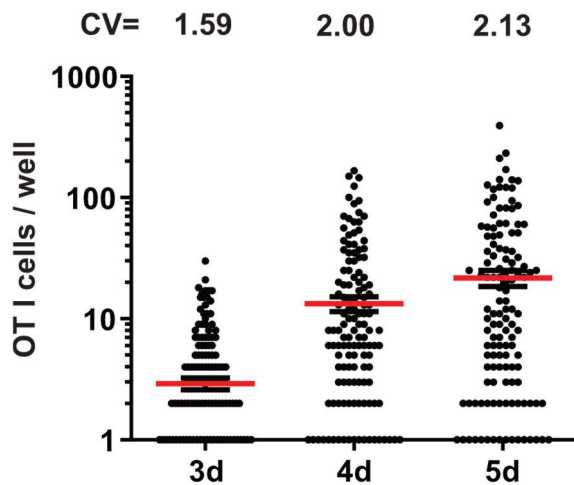


**Fig. 10: Expansion of single OT-I cells *in vitro* is extremely variable.** A single naïve OT-I cell was cultured in the presence of  $10^5$  SIINFEKL-pulsed splenocytes. Size of single cell-derived progenies was determined by flow cytometry after 3, 4 and 5 days. Coefficients of variation are indicated above.

*in vivo* expanded T cells. The coefficient of variation (CV) that was expected to lie between 2 and 3 from day 3 to day 7, based on *in vivo* observations [89], was measured at 1.59, 2.00 and 2.13 on day 3, 4 and 5, respectively *in vitro* (Fig. 10). These results indicate that even in a petri dish, a substantial part of the complexity and variability of CD8 T cell responses can be generated, thus enabling us to manipulate individual factors in these cultures and dissect their impact on the generation of diversity.

Almost all assays performed on the proliferation and differentiation of CD8 T cells suffer from the limitation that the T cells have to be killed or at least modified and taken out of the organ or culture for analysis. Thus, it is usually not possible to analyze the same cell at different time points for several days in a row and keep the information about the identity of the cell. When proliferation is investigated, longitudinal information is very important because cell numbers alone give no information about the time point when proliferation has stopped and whether all measured cells proliferated with the same intermediate speed or whether the result is a composition of many slow-dividing and a few fast-dividing cells.

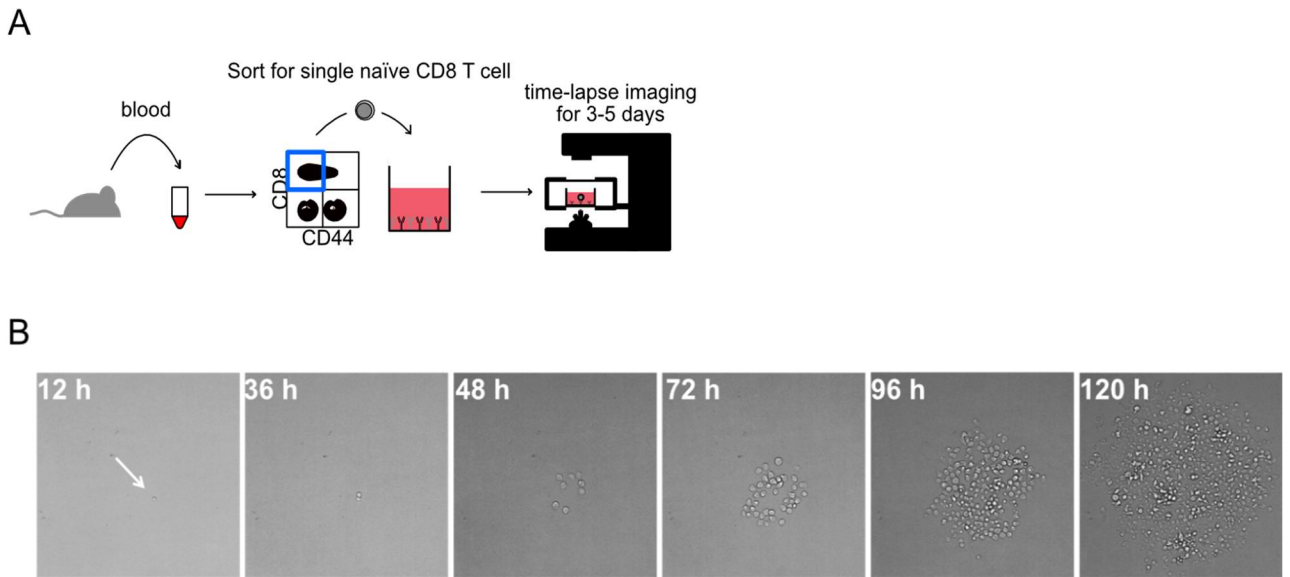


**Fig. 11: Single CD8 T cells can be expanded for at least 5 days *in vitro*.** (A) Blood was taken from an OT-I mouse and sorted for naïve CD8<sup>+</sup>, CD44<sup>low</sup> cells. A single naïve OT-I cell was sorted into a well that was coated with  $\alpha$ CD3 and  $\alpha$ CD28 in the presence of 25 U/mL IL-2. The cell culture plate was transferred to a live-cell imaging microscope and imaged for the next three to five days. (B) Pictures, taken at different time points from the same single cell-derived progeny.

To overcome these limitations, we established a feeder-cell free, single-cell culture where it was possible to take pictures of the T cells at different time points and to follow their movements and cell divisions. To activate the cells, antibodies against CD3 and CD28 were bound to the surface of the plate, providing a strong and permanent stimulus (Fig. 11A). Subsequently, the plate was transferred into a live-cell imaging microscope, which is a combination of a microscope with an incubator. The pictures shown in Fig. 11B were taken from the same well at different time points and show the development from a single cell (12 h) to a large colony of cells (120 h) that are all offspring of the cell shown in the first picture.

To investigate the variability in size of different single cell-derived progenies, the number of cells after five days was counted for all single cell-derived progenies and is plotted in Fig. 12A. Despite the highly controlled starting conditions, which were as equal as possible for all single naïve sorted T cells, the sizes of the single cell-derived colonies reached from 10 to almost 10 000 daughter cells. To investigate the phenotype of these *in vitro*

generated single cell-derived progenies, they were harvested at the end of the experiment and analyzed via flow cytometry. Based on these analyses, we found a negative correlation between the size of the single cell-derived progenies and the fraction of cells within these progenies that express memory-associated markers like CD62L and CD27 (Fig. 12B-C). The expression of the effector and activation-associated marker CD25 was higher in large single cell-derived progenies (Fig. 12D). These data indicate that the memory vs. effector differentiation bias of small vs. large single cell-derived progenies observed *in vivo* [89] is preserved in a well-controlled *in vitro* setting.

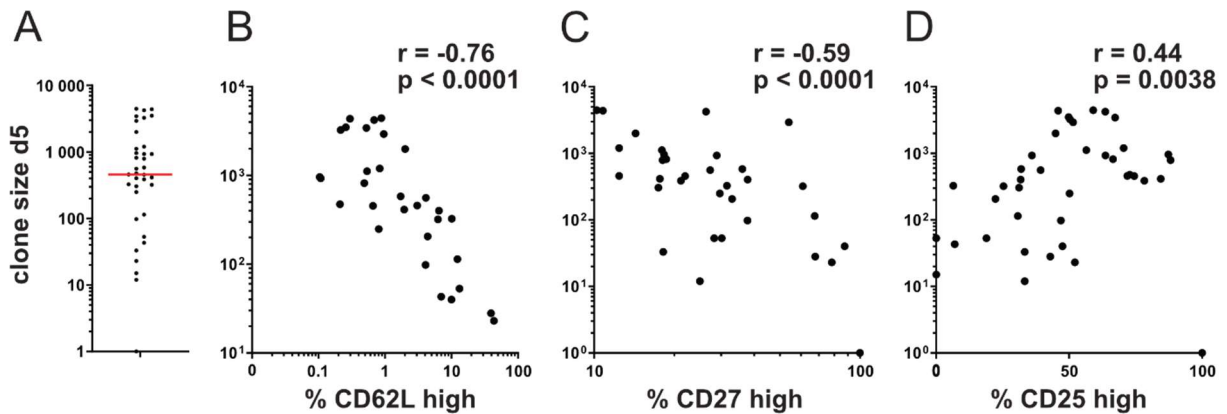


**Fig. 12: The outcomes of single cell-derived progenies are very variable – even under well-defined *in vitro* conditions.** Cells from Fig. 11 were analyzed by flow cytometry on day 5 p. activation. **(A)** Cell numbers of single cell-derived progenies. red: median. **(B-D)** Cell numbers of single cell-derived progenies are plotted against the percentage of CD62L, CD27 or CD25 expressing cells within the T-cell clone. Spearman correlation coefficients  $r$  are indicated.

To further investigate whether the variability in progeny size was caused mainly by different times to first division, T cell numbers were also counted at earlier time points and representative growth curves are plotted in Fig. 13A. As can be seen from the lines rising later in the plot, early vs. late onset of proliferation could influence the size of a single cell-derived progeny. An early vs. late cessation of division has also been suggested as a main driver of different clone sizes due to the imprinting of so-called division destinies [102, 103]. However, under constant anti-CD3 and anti-CD28 mediated

stimulation no division cessation was observed throughout the 6 days of observation. Thus, divisions cessation could not contribute to single-cell variability at least in this *in vitro* setting. In addition to different starting times, different slopes of the growth curves were visible, indicating distinct proliferation rates. To check whether proliferation rates indeed varied between the single-cell clones, the duplication rate was calculated (Fig. 13B). The results suggested that cell-cycle speed itself was also a relevant factor for setting apart the clonal expansion derived from distinct founder T cells. This was also the case in experiments where not just one, but two naïve T cells were sorted into the same well. Since offspring from the two founder cells proliferated in the same micro-milieu, well-to-well variation of extrinsic expansion conditions can be largely excluded as a major factor for inducing single T cell-derived variation.

The small differences in the measured duplication rates can sum up quite drastically because one duplication more per day already means 128-times more cells after 7d, and two duplications more per day would in theory result in 160 384 times as many cells after 7d.

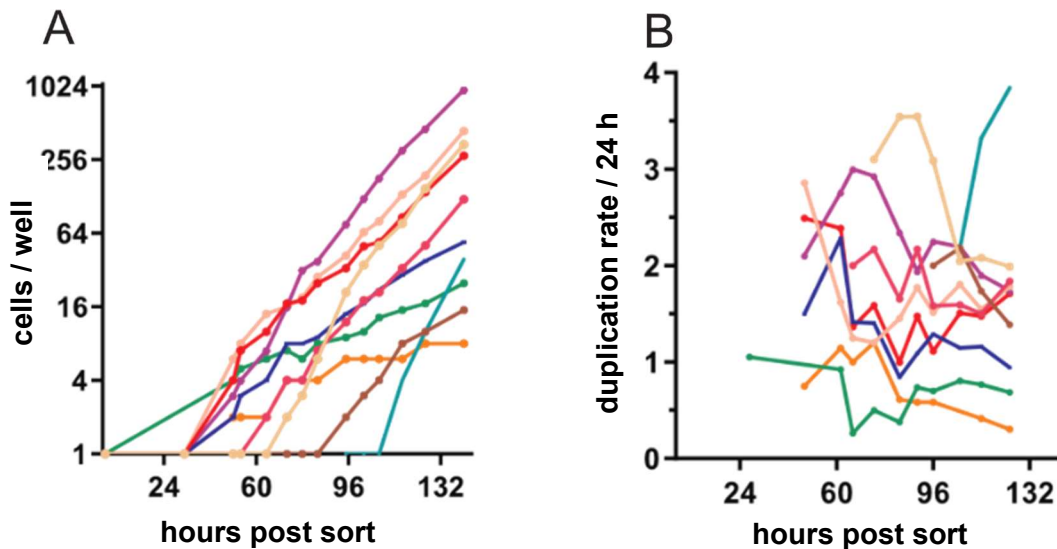


**Fig. 13: Single cell-derived progenies can expand with different proliferation rates.** (A) Cells from an experiment as shown in Fig. 11 were imaged and counted at different time points during expansion. The cell numbers were plotted against the time point. (B) The number of times, the cell number doubled during 24 h, was calculated by taking the cell numbers of four consecutive measurements, dividing the last cell number by the first cell number, building the logarithm to the basis 2, dividing the result by the time between the early and the late time point and multiplying the result by 24 h.

Through live-cell imaging, we were also able to determine the exact duration between two subsequent cell divisions (inter-division times) of all cells within a single cell-derived progeny (Fig. 14). This confirmed our observation that the T cells divide with different proliferation speeds. The fastest cell divisions had inter-division times of 5-6 h, whereas the slowest cell divisions could take 24 h. The median inter-division time was approximately 8 h, and the mean 8.6 h. In line with previous reports, the time until the first cell division was much longer, with a median division time of approximately 36 h (Fig. 14 left). During the first 24 h, no cell divisions were observed. Almost all times to first division ranged between 30 h and 48 h hours. With a mean inter-division time of 8.6 h (for subsequent divisions), we would expect that the 18-hour delay, from early to late onset of proliferation, would allow early starters to execute two more divisions or grow 4-fold larger than late starting T cell progenies. This difference is quite small compared to the potential effect that we have estimated for different proliferation rates and is insufficient to explain the almost 200-fold variation in progeny size observed by day 5 after activation (Fig. 13A).

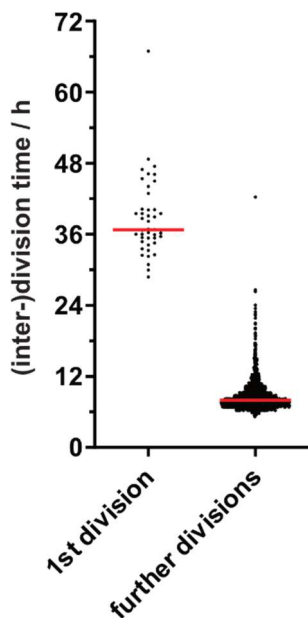


**Fig. 14: The first cell division needs more time than the subsequent divisions.** Single naïve ( $CD44^{low}$ )  $CD8^+$  T cell were sorted into separate wells of an  $\alpha CD3/CD28$ -coated 384-well plate and imaged for 5 days in a live-cell imaging microscope. The fate of each cell was tracked and the inter-division times were determined.

## 4.2 Functionality

While SLECs and MPs can be reliably identified at the peak of expansion by their expression of effector vs. memory markers, discerning these subsets turned out to be more complicated during the first days after activation *in vitro*.

To test whether T cells from the feeder-cell free cultures already showed distinct *in vivo* functions, they were sorted out of the cultures on day 6 after activation according to their expression of the memory marker CD62L and were transferred into naïve C57BL/6 mice (Fig. 15). Under those conditions, CD62L<sup>low</sup> effector cells would be expected to die during the following weeks, whereas CD62L<sup>high</sup> memory cells could outlive them for a long time without infection of the mouse and re-expand upon infection with *L.m.*-OVA 5 weeks later. Consequently, when the offspring of transferred cells on d8 after infection were detected, a high cell number in the memory group and a low cell number in the effector group would show successful and early differentiation into different subsets. The control with cells that were sorted *ex vivo* from mice that had been infected with *L.m.*-OVA 6d before the T cell transfer (Fig. 15 black) showed that, as early as d6, CD62L can be used to discriminate between memory and effector cells. However, when the same experiment was conducted with cells from a feeder-cell free culture, a difference in the survival and subsequent proliferation could not be detected (Fig. 15 red). Interestingly, a direct comparison between cells which were sorted from culture and infected mice, respectively, showed that cells from culture were recovered in much higher numbers after transfer into resting and re-challenged mice than cells that were activated *in vivo* (Fig. 15 red vs. black). This increased recovery and the higher percentage of CD62L<sup>high</sup> cells *in vitro* that was observed in

Fig. 9 indicate that the differentiation into terminally differentiated effector cells is decreased in the used *in vitro* setting.

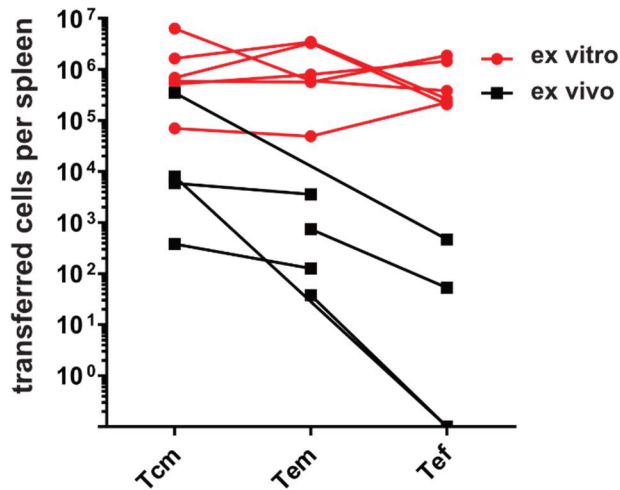


**Fig. 15: Under continuous stimulation, *in vitro* differentiated T cells do not show subset-associated survival and expansion upon transfer *in vivo*.** **Red:** OT-I cells with different combinations of the congenic markers CD45.1/2 and CD90.1/2 were stimulated as in Fig. 11 A and sorted on day 6 for central memory precursor (Tcm, CD62L<sup>high</sup>, CD27<sup>high</sup>), effector memory precursor (Tem, CD62L<sup>low</sup>, CD27<sup>high</sup>) and effector T cells (Tef, CD62L<sup>low</sup>, CD27<sup>low</sup>). **Black:** As a control, OT-I cells were activated *in vivo* via infection with L.m.-OVA and also sorted on day 6 for the different subsets. 100 cells per subset were co-transferred into resting mice, which were infected with L.m.-OVA after five weeks and the offspring of the transferred cells were detected by flow cytometry on d8 p.i..

### 4.3 Establishment of a feeder-cell free single-cell culture without continuous stimulation

Shedding complicates the use of CD62L as a marker for memory cells. The protease ADAM-17 mediates shedding of CD62L [104, 105], which usually occurs approximately 4 h after activation via TCR stimulation [106]. The complete molecule is re-expressed after around two to three days [106]. The shedding is thought to enable the migration from the lymphatics into infection sites, but the proliferation enhancing effects of CD62L shedding have also been discussed [107]. Consequently, continuous signaling via  $\alpha$ CD3 on the surface of the culture plate may also lead to further shedding. Thus, it was possible to sort for pure CD62L<sup>high</sup> cells, but for CD62L<sup>low</sup> cells it was not clear, whether this population was contaminated by T cells having only transiently shed CD62L from the surface.

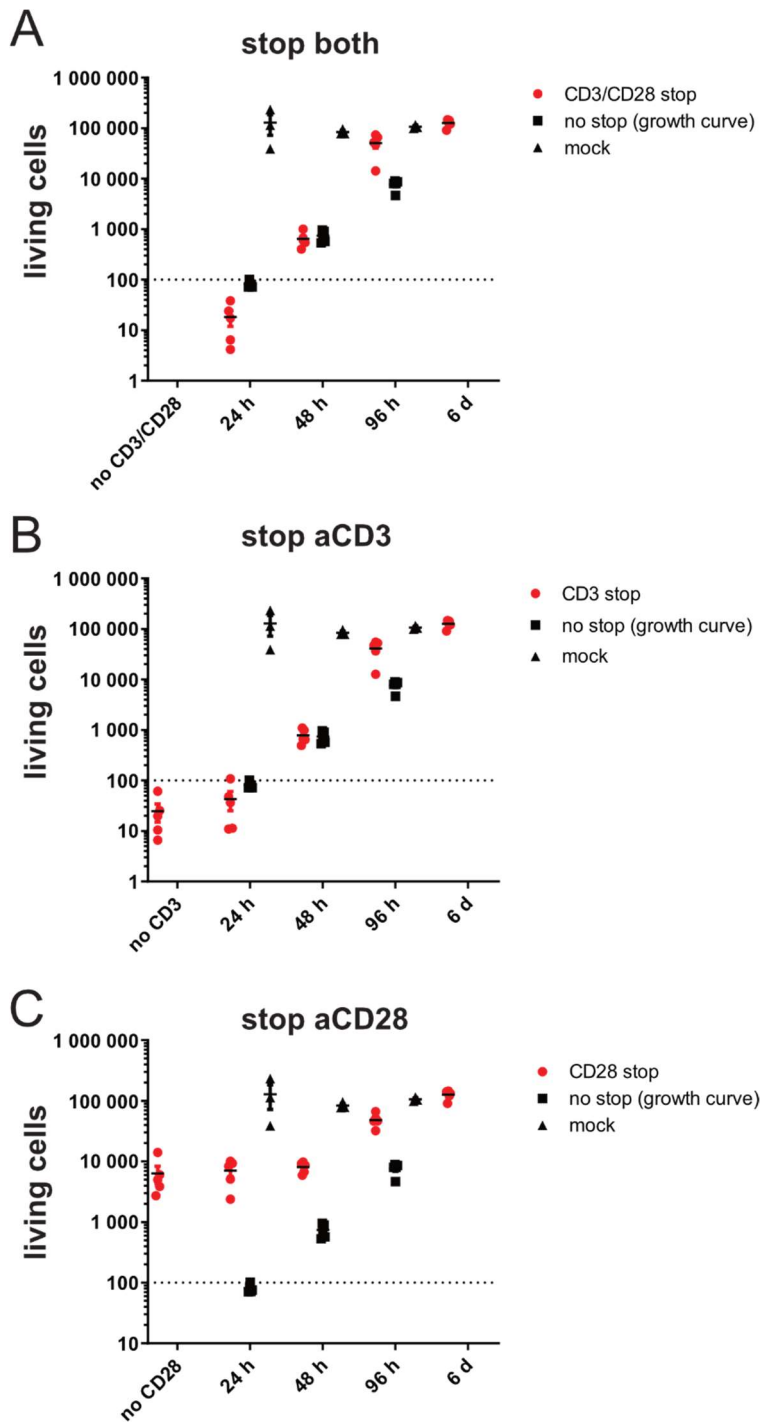


**Fig. 16: Abrogation of stimulation via  $\alpha$ CD3 results in reduced cell numbers.**

100 cells were activated as in Fig. 11. At indicated time points, cells were taken out of the well and transferred either into wells with further  $\alpha$ CD3/CD28 stimulation (mock control) or further cultured without  $\alpha$ CD3/CD28 (A), without  $\alpha$ CD3 (B), or without  $\alpha$ CD28 (C). The cell numbers were always determined on day 6 p. activation. To compare with the cell numbers that were reached at the time of transfer, a few wells were analyzed at the time points of transfer (no stop (growth curve)).

In a first attempt, we tried to prevent shedding by adding TAPI-2, an inhibitor of ADAM-17 [108], to the culture. Due to the fact that it was not possible to keep the cells alive for several days in the presence of the inhibitor (data not shown), this approach had to be rejected. Another approach was to limit the time frame in which the cells received signals from  $\alpha$ CD3, thus reducing the events which could lead to shedding. A further advantage of reducing the contacts to  $\alpha$ CD3 is that the setting would be more physiological compared to permanent  $\alpha$ CD3 stimuli.

To elucidate how long  $\alpha$ CD3 and  $\alpha$ CD28 were required to enable sustained proliferation of CD8 T cells, small populations of naïve T cells were activated for different amounts of time with  $\alpha$ CD3/ $\alpha$ CD28 and then transferred into fresh wells lacking  $\alpha$ CD3 and/or  $\alpha$ CD28 coating (Fig.16). After the transfer into fresh wells, cells were further incubated for a total incubation time of 6 days and the cell number was determined. To be able to calculate how much proliferation was possible from the time point at which the stimulation was abrogated, the number of cells with continuous stimulation at all the time points when cells were transferred was measured (growth curve).  $\alpha$ CD3 seemed to be very crucial for proliferation throughout the expansion phase. When  $\alpha$ CD3 was removed, only weak proliferation was observed for the remaining days of culture (Fig. 16A-B). Removal of  $\alpha$ CD28 had no additional effect on the cell number if  $\alpha$ CD3 was also missing. If only  $\alpha$ CD28 was removed, this led to a reduction of cell numbers when removal occurred within the first 48 hours but had no effect when performed later. (Fig. 16C). These data indicate that  $\alpha$ CD28 affects proliferation only in the presence of  $\alpha$ CD3 and only during the first 48 h.

We planned to perform live-cell imaging experiments with the single-cell cultures in order to follow the fate of a CD8 T cell from the naïve state to the differentiation into memory and effector cells with all cell divisions. The first cell division usually occurs after around 1.5 days after activation. If the cells were to be removed from the stimulus and transferred to a well without  $\alpha$ CD3 after more than 36 h, the observation of the proliferation of a single cell into a single cell-derived progeny would be interrupted and important information about the identity of the cells would be lost. Thus, we decided to use  $\alpha$ CD3 just for activation of the cells during the first 24 h and then sort

the activated cells again into plates without  $\alpha$ CD3 before the first cell division occurred.

To overcome the limitation of too weak proliferation under these conditions and to investigate their impact on proliferation, different combinations of cytokines were added to the culture (Fig. 17). IL-2, IL-7, IL-12 and IL-15 are known to enhance viability or proliferation of CD8 T cells *in vivo* and were tested regarding their impact on cell number in feeder-cell free cultures. Interestingly, none of the cytokines was able to allow for proliferation in the absence of IL-2 (Fig. 17A left). IL-2 alone enabled proliferation and the number of recovered T cells after 4 days could be increased by adding more IL-2. Combinations of IL-7 and IL-12 with IL-2 resulted in higher cell numbers than IL-2 alone, with IL-12 + IL-2 resulting in the highest cell numbers (Fig. 17A right). In addition, the combination of IL-12 and IL-2 was the only one that also increased the expression of CD25 (Fig. 17B). Because CD25 enhances the sensitivity to IL-2, this is an explanation for why IL-12 needs to be combined with IL-2 to increase proliferation. The effect of cytokines on proliferation and CD25 expression was no longer detectable, when the cells were cultured under continuous stimulation via  $\alpha$ CD3/ $\alpha$ CD28 (data not shown).

To test whether the concentration of 25 U/mL IL-2 was constant throughout a whole experiment, an IL-2 ELISA was performed with the supernatant after four days of cultivation with different numbers of starting cells (Fig. 18). In this experiment, no change of IL-2 concentration was observed, indicating that degradation, consumption and synthesis of IL-2 did not occur to a degree that interfered with total IL-2 levels in culture.

The antibodies against  $\alpha$ CD3 and  $\alpha$ CD28 in the continuous stimulation setting were very helpful for live-cell imaging experiments because they attached the cells to the surface of the plate. Without this attachment, the movements of the T cells were found to be too fast to ensure reliable tracking. Consequently, the lack of attachment in the short stimulation setting had to be compensated. Two approaches were

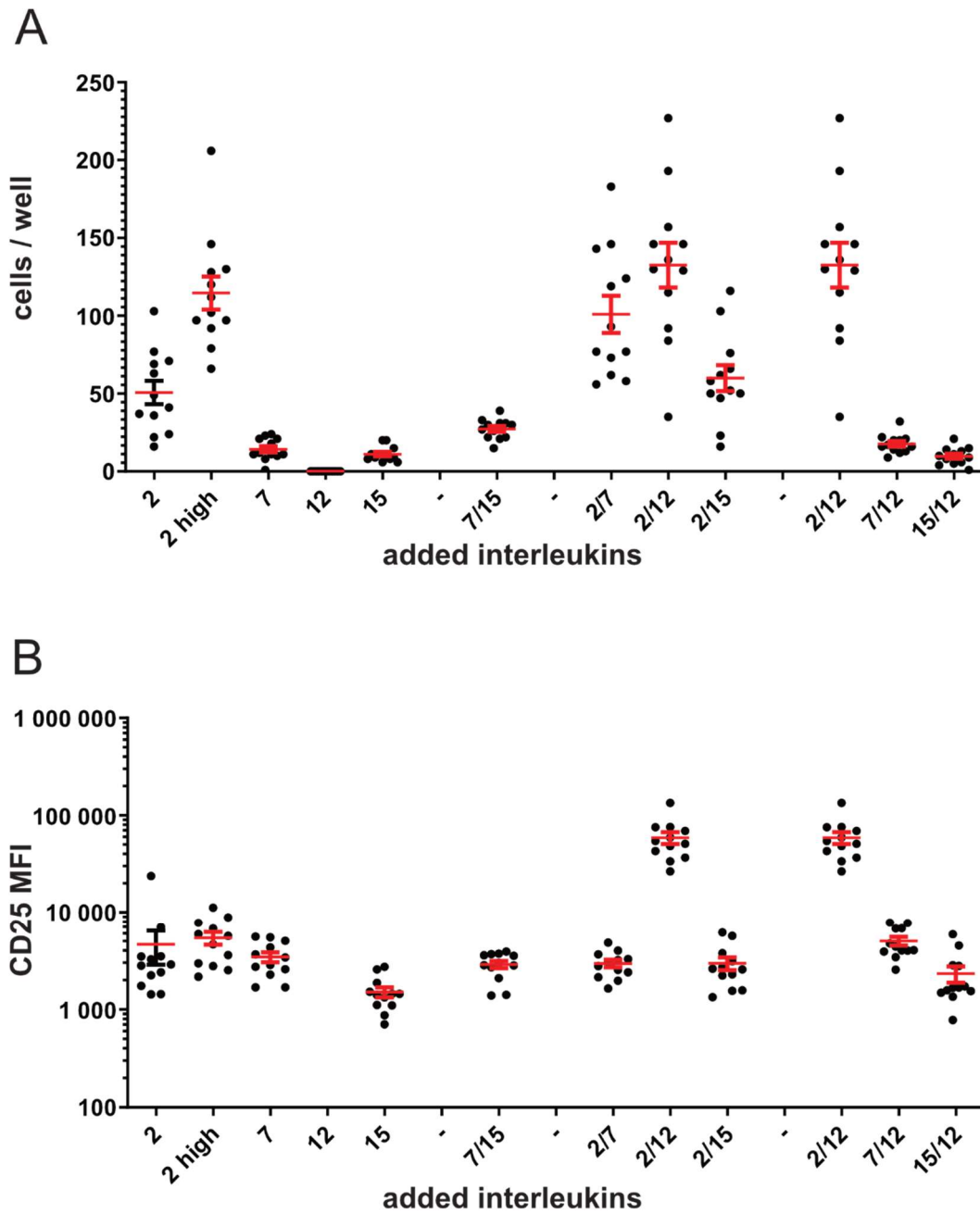


**Fig. 17: IL-7, 12 and 15 cannot enhance proliferation in the absence of IL-2, and IL-12 upregulates the expression of CD25.** 10 cells were activated for 24 h, and then transferred into wells without antibody coating, but with different combinations of cytokines. The offspring were analyzed on d 4 p. activation by flow cytometry. IL-2: 25 U/mL, IL-2 high: 250 U/mL, IL-7, 12, 15: 10 ng/mL, each. **(A)** Cell number of 10 cell-derived progenies. **(B)** Mean expression of CD25. Red: mean + SEM

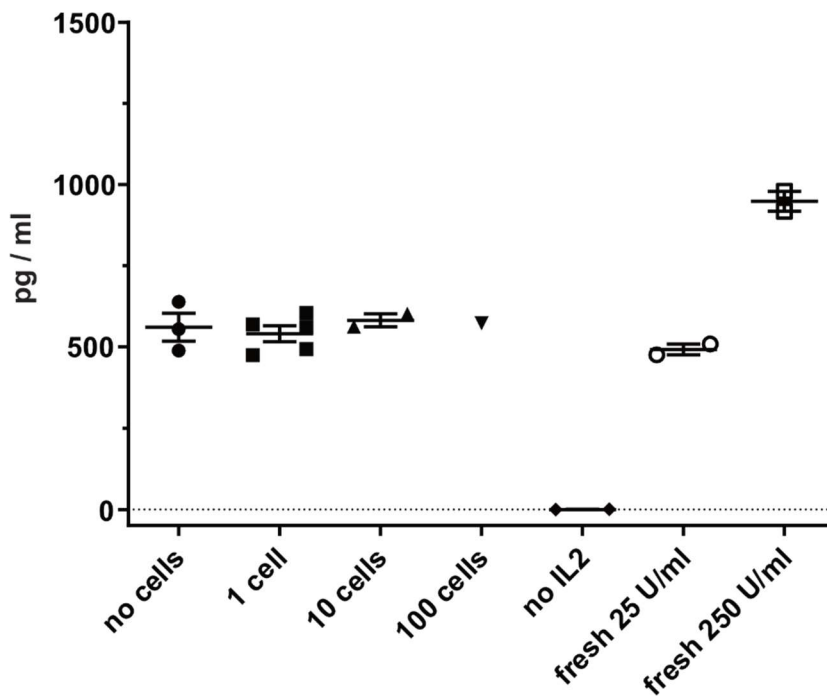


**Fig. 18: Levels of IL-2 in the medium are stable.** Cells were activated for 24 h, and 0, 1, 10 or 100 cells transferred into wells with 25 U/mL IL-2, and cultured for a further three days. IL-2 in the supernatant was detected by ELISA. As a control, culture medium without cells containing no, 25 or 250 U/mL freshly added IL-2 were measured.

tried to solve the problem. The first approach was to increase the viscosity of the medium by the addition of  $\alpha$ -methylcellulose. Unfortunately, this did not reduce the migration of the cells to a degree where tracking was possible, and the optical properties of the medium were impaired, which would have hampered tracking further (data not shown). The second approach was to coat the culture plate with adhesion molecules or antibodies against epitopes that have not been reported to have a direct impact on T cell proliferation and differentiation. The adhesion molecules that were tested were fibronectin, retronectin, poly-L-lysine and ICAM-1. Of those four molecules, only ICAM-1 improved the attachment of the cells to a degree that live-cell imaging seemed possible. As a consequence, a few of the live-cell imaging experiments were conducted with ICAM-1 as the adhesion molecule, while a stronger adhesion molecule was searched for,

because the resulting family trees were often incomplete due to loss of T cell identity or wandering to the edges. CD45.1, CD45.2, CD90.1 and CD90.2 are often used as congenic markers in *in vivo* cell-transfer studies. CD90.2 and especially CD90.1 showed improved attachment, but counting of the cells showed that CD90.2 cells divided less compared to CD90.1 cells, and cell numbers were reduced when the epitope of the antibody that was used for coating was also present on the attached cells (Fig. 19). While the effect of  $\alpha$ CD28 as coating reagent was weaker compared to  $\alpha$ CD3/ $\alpha$ CD28, it was still the most promising candidate to enable T cell tracking in live-cell imaging. However, CD28 is a cofactor during T cell activation and thereby able to modulate T cell responses. Nevertheless, the experiments have shown that no effect of  $\alpha$ CD28 on T cell proliferation and differentiation was detected when  $\alpha$ CD3 was not present in addition. Therefore, it was further used as adhesion molecule for live-cell imaging.

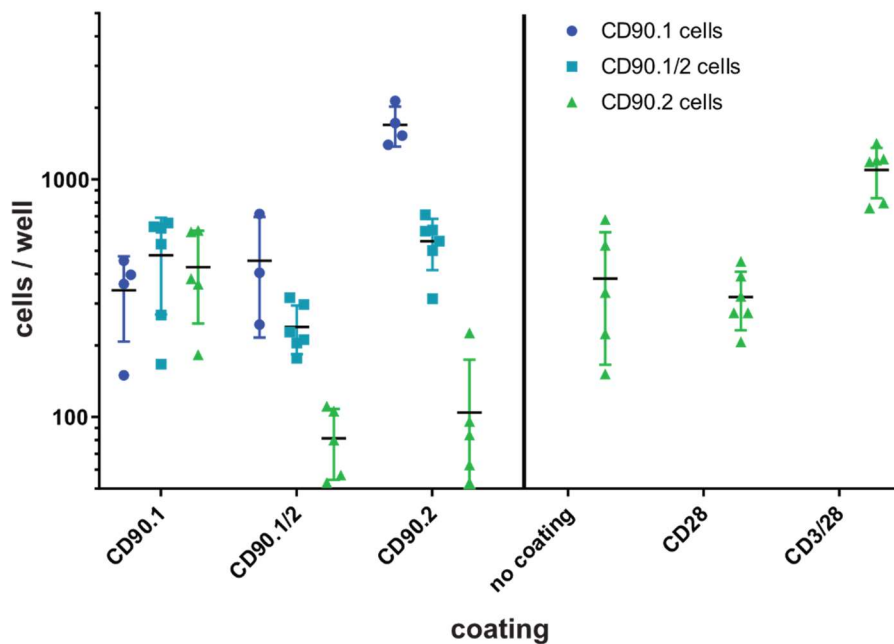


**Fig. 19: CD90.1 and CD90.2 cells show reduced proliferation when the respective antibody is bound to the culture plate.** The culture plate was coated with different combinations of antibodies, and 50 activated cells (CD90.1, CD90.1/2 or CD90.2) were sorted into each well by limiting dilution. After 3d, cells were counted by flow cytometry. Colors indicate the phenotype of the cells that were transferred to the coated wells.

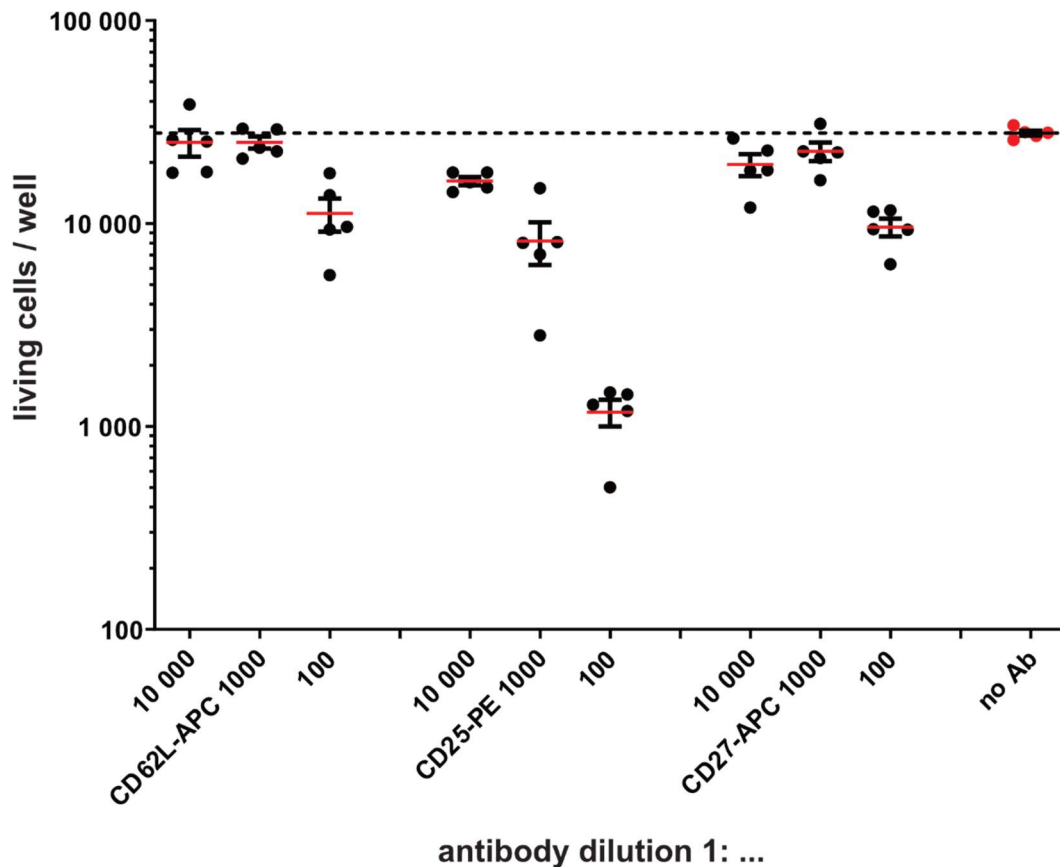


**Fig. 20: High concentrations of  $\alpha$ CD25 in culture can interfere with T cell proliferation.** 100 cells per well were cultured under continuous stimulation via plate-bound  $\alpha$ CD3/CD28. Fluorescent antibodies were added to the culture medium as indicated. After 5d, the cells were counted by flow cytometry.

To be able to connect the inter-division time of a cell in live-cell imaging to a phenotype, the phenotype must be visible under the microscope. For that purpose, it is possible to add fluorescent antibodies to the culture that bind to the molecule of interest [109]. Concentrations have to be adjusted so that the density of dye-conjugated antibodies is low in the medium (to reduce background signal) but quickly increases at the location of antigen binding (to ensure rapid detection of the molecule of interest once it is upregulated). In addition, sufficient antibody concentrations must be available to replenish digested antibody and compensate for bleaching. In addition, it has to be shown that binding of the staining antibody itself does not change the results. Especially in the case of CD25, it is possible that proliferation is hampered due to blocking of IL-2 signaling by the antibody. Indeed, the

results show that high concentrations of  $\alpha$ CD25 lead to reduced proliferation (Fig. 20). However, the effect was very small when dilutions of 1:10 000 or lower were used. For  $\alpha$ CD62L, even dilutions of 1:1000 were without consequence for T cell expansion. Taking these measurements into account, a dilution of 1:20 000 for  $\alpha$ CD25 and 1: 10 000-20 000 for  $\alpha$ CD62L was used for live-cell imaging experiments.

#### **4.4 Investigation of inter-division times within and between T-cell families under continuous stimulation**

For the measurement of inter-division times in single cell-derived progenies under continuous stimulation, blood from OT-1 Rag1<sup>-/-</sup> mice was taken and sorted for naïve (CD44<sup>low</sup>) CD8 T cells. In doing so, a single cell was sorted into each well of a 384-well plate that was coated with  $\alpha$ CD3/ $\alpha$ CD28 to activate the cells. To get a deeper insight into the expansion of single cells, “The Tracking Tool” was used. “The Tracking Tool” is a software that was developed by Timm Schroeder’s group at the ETH Zurich to build family trees for cells with data from live-cell imaging experiments [100]. The user manually tracks all cells at all time points and indicates their cell divisions while the software creates a family tree out of these data and produces a table containing all inter-division times as an output. In those family trees, the time is plotted on the Y-axis and each cell is plotted as a vertical line ( Fig. 21). The length of the lines indicates the time between two cell divisions (inter-division time). Horizontal lines show the time point of a cell division and connect the two daughter cells which were generated by the cell division to their mother cell, which ended in the respective cell division. The number of cell divisions, which a particular cell in the tree has experienced is called its generation. Accordingly, there is just one cell in generation 0, two cells in generation 1, four cells in generation 2, up to 8 cells in generation 3, etc.

In Fig. 22, two representative family trees are shown. One of the trees is very small with long inter-division times (right tree), whereas the other tree

is very big and has much shorter inter-division times (left tree). Consequently, there was large inter-clonal heterogeneity. Moreover, there

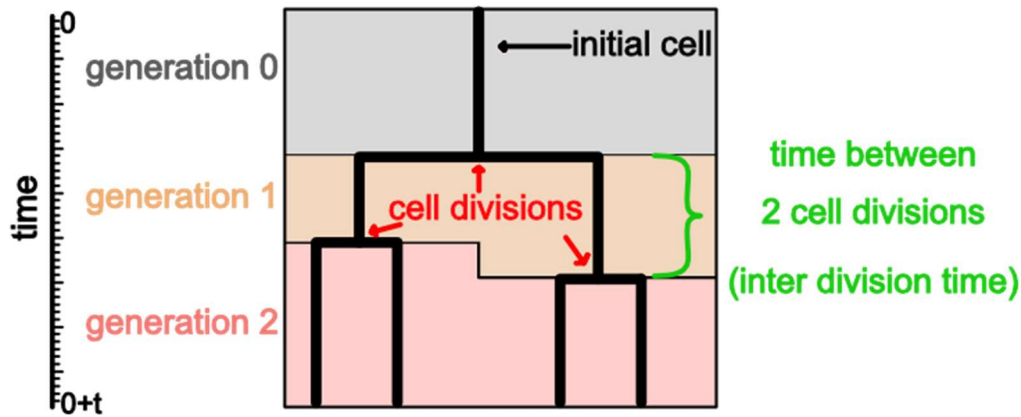


**Fig. 21: Schematic family tree of a single T cell.** By tracking single cells in live-cell imaging, genealogical trees of T cells can be generated. Each vertical line represents a cell. The vertical lines indicate the inter-division times, and sister cells are connected by horizontal lines that also indicate the time points of cell divisions. The number of cell divisions is called the generation of the cell. Cells that did not yet divide are in generation 0.

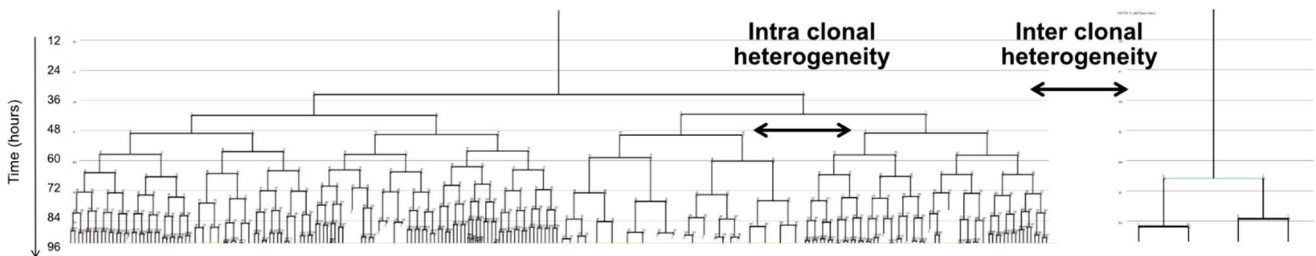


**Fig. 22: Under continuous stimulation, there is huge intra- and inter-clonal variability.** Two representative family trees that were generated by single-cell expansion and live-cell imaging are shown.

was also a whole branch within the large tree that was composed of longer inter-division times than most of the inter-division times in the other branches, showing that there was, in addition to inter-clonal heterogeneity, also wide intra-clonal heterogeneity. Interestingly, the inter-division times within a tree are more closely correlated between sibling cells than between mother and daughter cells (Fig. 23), speaking in favor of a longitudinal

differentiation process along branches as opposed to, e.g., asymmetric cell divisions. Fig. 24A shows the distribution of all inter-division times in all trees

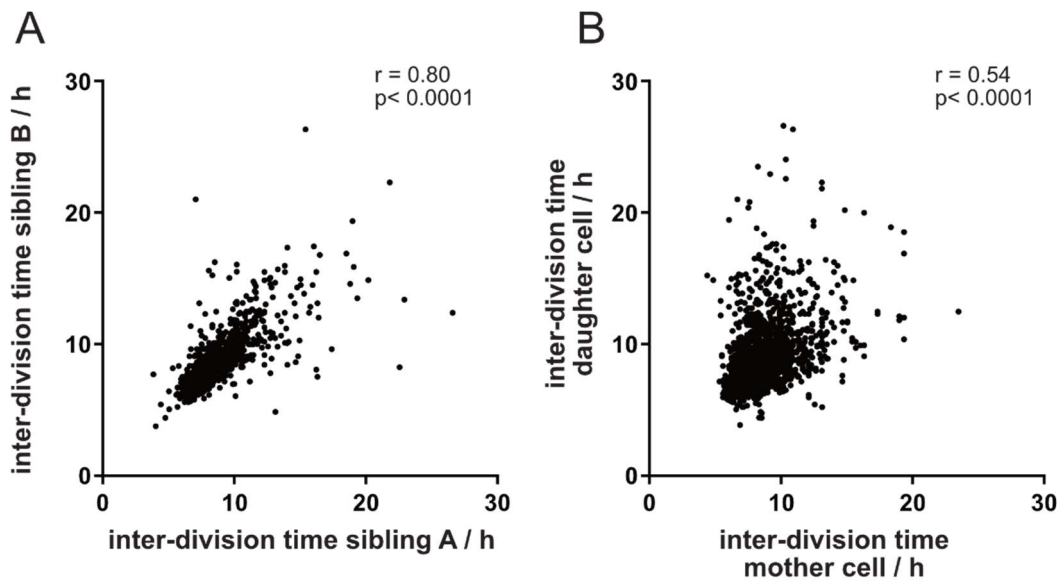


**Fig. 23: Inter-division times of sibling cells are more closely correlated than between mother and daughter cells.** Inter-division times from Fig. 14 were plotted against the inter-division times of their (A) direct daughter cells or (B) sibling cells. The spearman coefficients  $r$  are indicated.

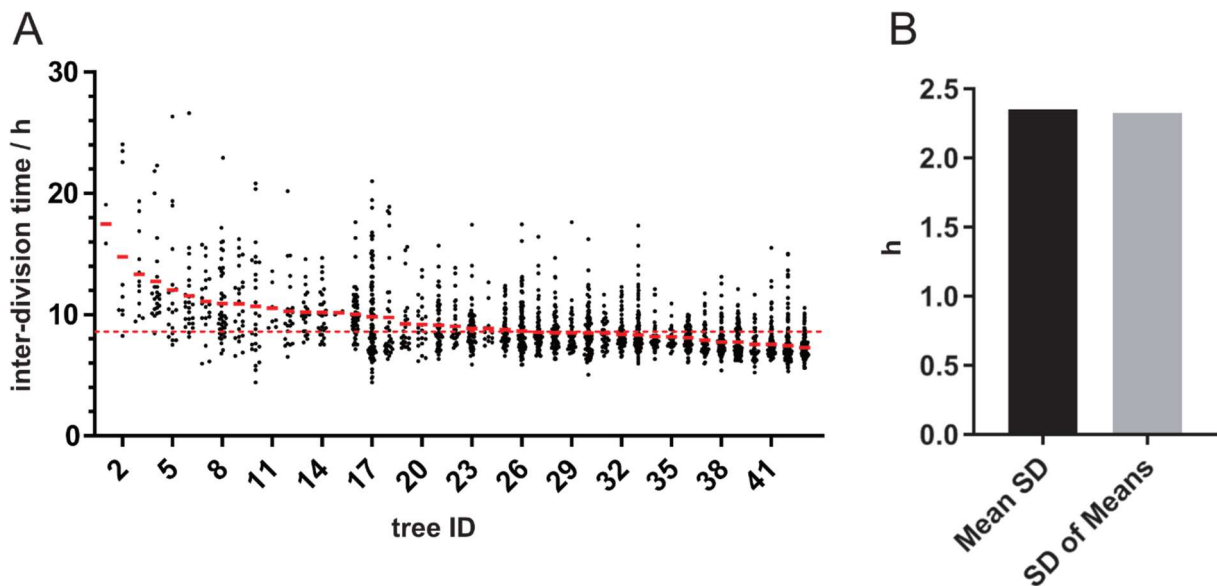


**Fig. 24: Intra- and inter-clonal variability of inter-division times contribute similarly to total variability.** (A) The inter-division times of all cells in 43 different single cell-derived progenies are plotted. Red bars: medians, red dotted line: mean of all cells (B) The mean of the standard deviations of inter-division times within trees (intra-clonal variability) (black) are compared to the standard deviation of the mean inter-division times of the different trees (inter-clonal variability) (grey).

of a representative experiment. To investigate whether the inter-clonal or the intra-clonal variability contributes more to the total variability, the mean standard deviation of all inter-division times within all the individual trees (intra-clonal variability) (Fig. 24B black) was compared with the standard deviation of all mean inter-division times of all trees (inter-clonal variability) (Fig. 24B grey). Interestingly, both intra-clonal and inter-clonal variability had a similar contribution to the total variability.

#### 4.5 Investigation of inter-division times with short stimulation in the presence or absence of IL-12

For experiments with only 24 h of stimulation with  $\alpha$ CD3/ $\alpha$ CD28, OT-1 blood was taken and sorted for naïve CD8 T cells as described for the continuous stimulation setting, but they were not single-cell sorted. Instead, 10 000 naïve CD44<sup>low</sup> CD8<sup>+</sup> T cells were sorted for activation into a large volume 384-well plate that was coated with  $\alpha$ CD3/ $\alpha$ CD28 and incubated for 24 h. Twenty-four hours was a time point that was long enough to activate the cells before they divided. After 24 h, the cells were sorted again, but this time we sorted for CD8<sup>+</sup> T cells that expressed the activation marker CD44. Of these activated T cells, a single cell was sorted into each well of a low base 384-well plate that was coated with ICAM-1 or  $\alpha$ CD28 for adhesion but not with  $\alpha$ CD3. Subsequently, the briefly-stimulated cells were imaged in the absence of further antigen-like stimuli in a live-cell imaging microscope (Fig. 25).

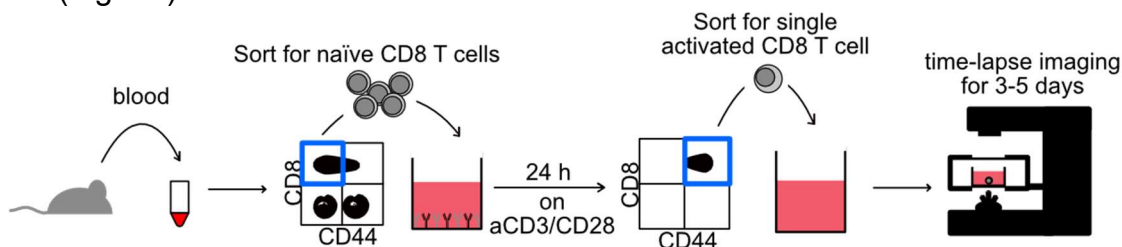


**Fig. 25: Live-cell imaging under short stimulation conditions.** Blood was taken from an OT-1 mouse and sorted for naïve CD8 T cells. 10 000 cells/well were activated for 24 h with plate-bound  $\alpha$ CD3/CD28 and 25 U/mL IL-2. Cells were sorted again for activated (CD44<sup>high</sup>) cells and a single cell was given in each well of a 384-well plate that was coated with ICAM-1 or  $\alpha$ CD28 to enable attachment. The cells were imaged for 3-5 days in a live-cell imaging microscope.

The representative trees in Fig. 26 show that trees from a short stimulation setting were smaller with longer inter-division times, compared to trees from a continuous stimulation setting. Plotting all inter-division times from all cells under the three conditions revealed that cells in the short stimulation setting without IL-12 were the slowest cells, addition of IL-12 increased the proliferation rate, and cells which received continuous stimulation had the shortest inter-division times (Fig. 27). Interestingly, the fastest cell divisions occurred quite precisely between five and six hours in all three cases, whereas the range for slow-dividing cells was very large. Analysis of the mean inter-division times of the trees showed that also with short stimulation, the mean inter-division times of different trees were very variable, thus speaking for a huge inter-clonal variability (Fig. 28A). These differences of just a few hours in the mean proliferation rate of different trees could hypothetically translate to differences in total cell number ranging from less than a hundred to almost a million cells, if the rates were kept constant for a whole week (Fig. 28B).

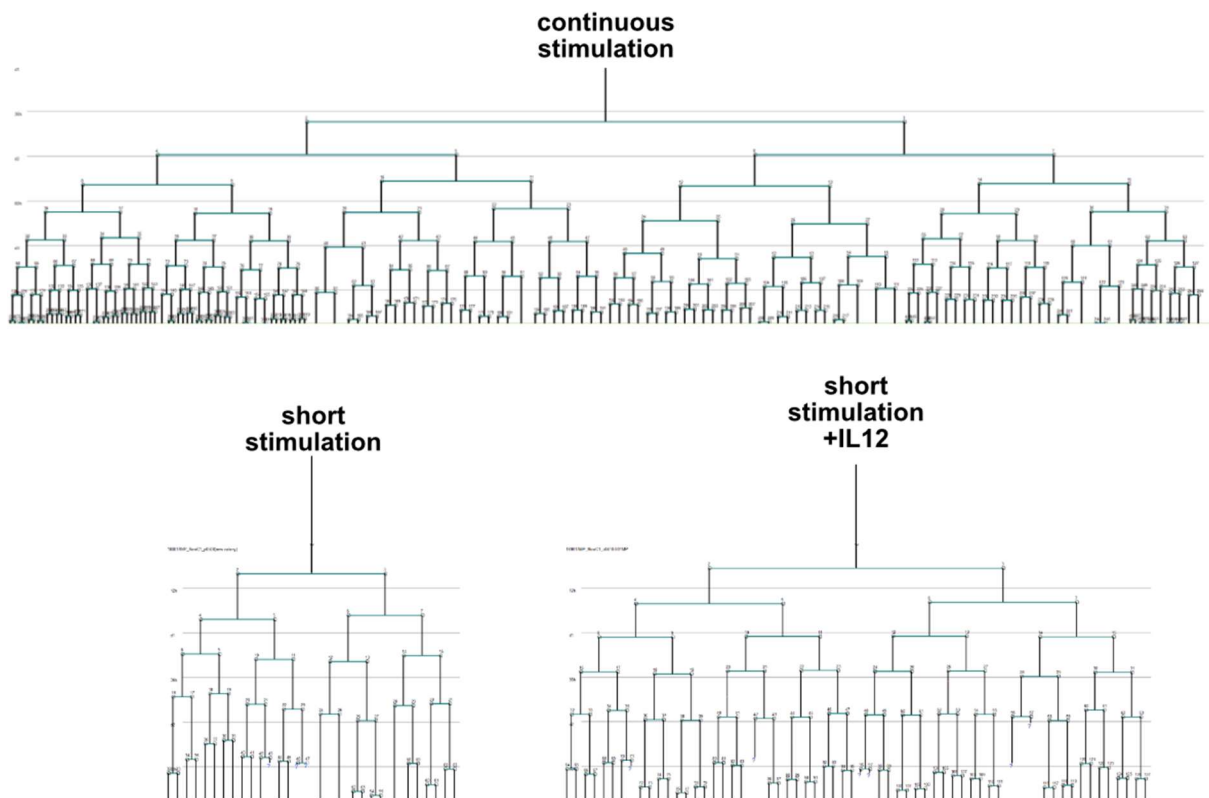


**Fig. 26: Representative trees from continuous stimulation, short (24 h) stimulation without IL-12 and short stimulation with subsequent cultivation in 10 ng/mL IL-12.**

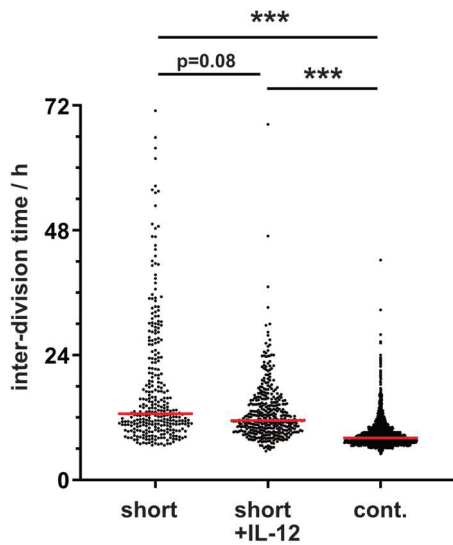


**Fig. 27: Continuously-stimulated cells have the shortest inter-division times, followed by short stimulation + IL-12 and short stimulation without IL-12.** Red: median inter-division time. For statistical analysis, Kruskal-Wallis Multiple comparison test was used. \*\*\*  $p < 0.0001$ .

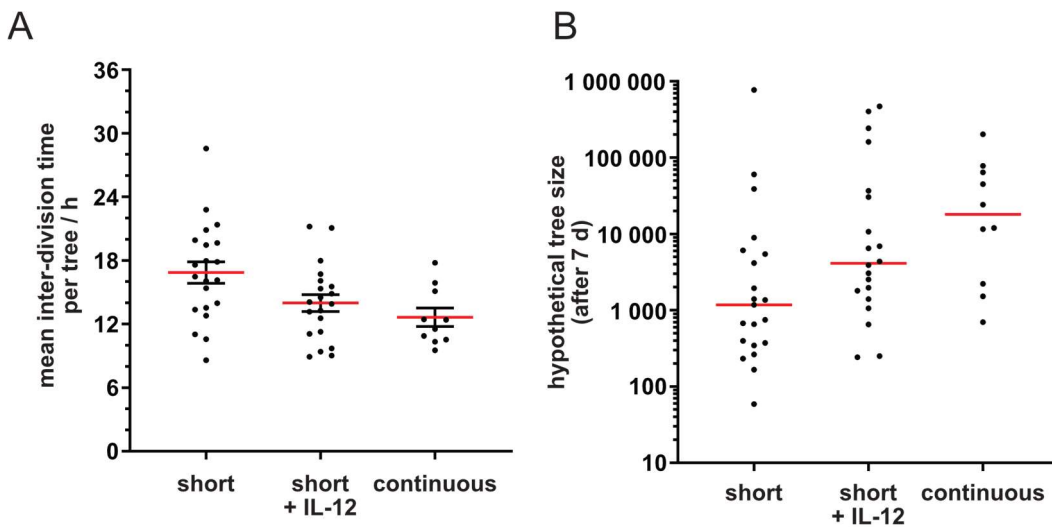


**Fig. 28: Small differences in mean inter-division time can amplify into substantial differences in the size of a single cell-derived progeny.** (A) Mean inter-division times of trees from data in Fig. 27. Red: mean inter-division time. (B) Hypothetical clone size after 7 days if the mean proliferation rate were kept constant. Red: median inter-division time.

## 4.6 CD25 expression in fast and slow dividing cells

Addition of IL-12 and TCR signaling can both lead to upregulation of CD25. To check whether the upregulation of CD25 was responsible for the different inter-division times in the short, short + IL-12, and continuous stimulation settings, live-cell imaging was repeated in the presence of a fluorescent antibody against CD25. After tracking of the trees, the data and images were loaded in qTfy and the pixel intensities of antibody-labelled cells were measured. As a result, so called heat-tree plots were generated and a table was created that contained the fluorescence intensities.

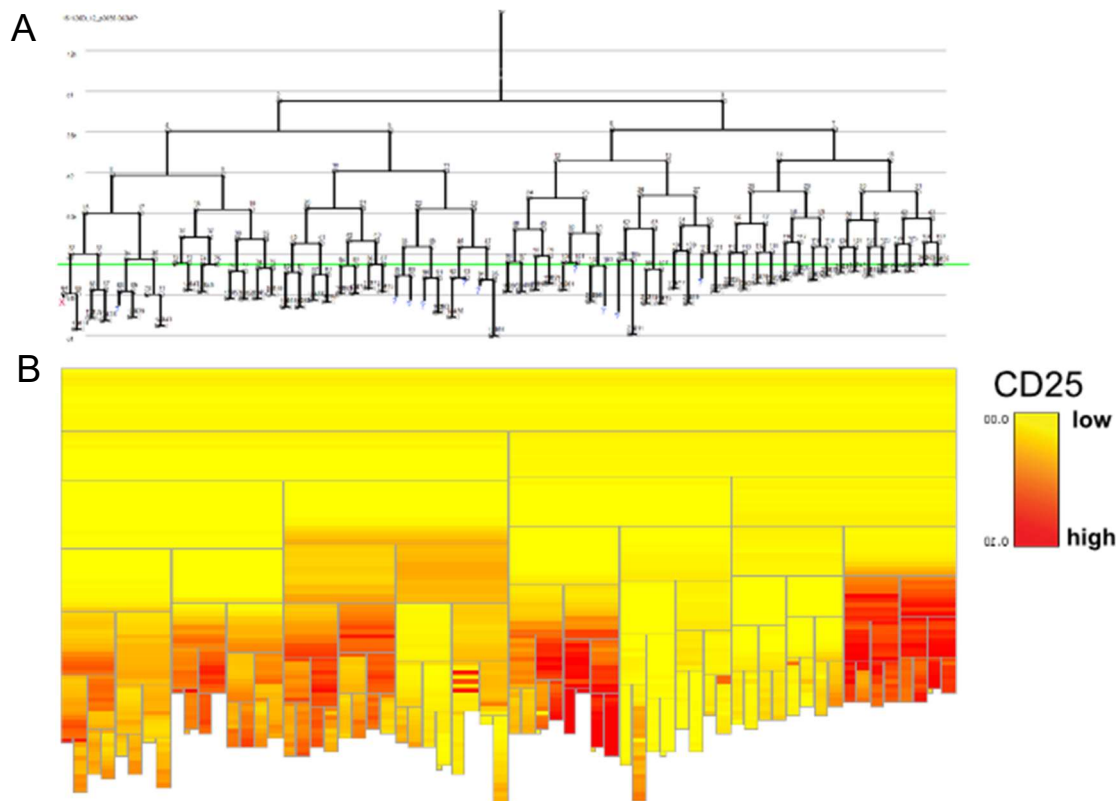


**Fig. 29: CD25 is preferentially expressed by fast-dividing cells.** (A) A representative family tree (continuously stimulated). (B) The same tree as a heat-tree plot. Yellow indicates low expression of CD25. Red indicates high expression of CD25. Each box represents a cell from the tree in (A). The height of the boxes is a measure of inter-division times.

A representative heat-tree plot from the continuously stimulated setting is shown in Fig. 29B. Each cell from the family tree (Fig. 29A) is presented as a box. The height of the respective box is a measure for the inter-division time. The daughter cells of a cell are depicted as boxes that are put directly below their mother cell and together have the same width as their mother-cell box. Thus, the widths of the boxes are bisected with every generation. The CD25 expression is color-coded on a linear scale. Shades of yellow indicate low CD25 expression, whereas shades of red indicate high CD25 expression. After a phase with similar CD25 expression all over the tree, the tree separated into parts (branches) with higher and lower CD25 expression. As can be seen by the endpoints of the boxes, the branches that were composed of more red boxes (more CD25 expression) ended earlier, indicating faster inter-division times. The inter-division times of this tree were correlated with the mean CD25 expression levels in Fig. 30A. The spearman correlation with a correlation coefficient of  $r = -0.47$  shows negative correlation between the expression of CD25 and the length of the cell cycles. Plotting of the spearman coefficients of all measured trees from the continuously stimulated setting showed that most of the trees had a negative correlation between inter-division time and CD25 expression (Fig. 30B).

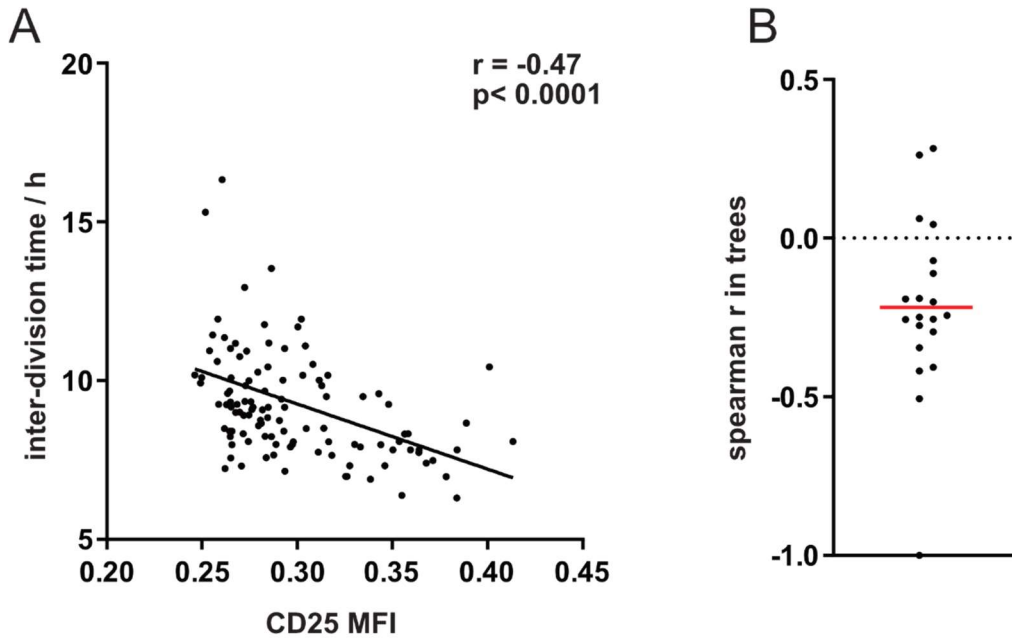


**Fig. 30: Intra-clonal distribution of CD25 weakly correlates with cell-cycle speed. (A)** Spearman correlation of cells from tree in fig. X is shown. **(B)** Spearman r for all investigated trees under continuous stimulation.

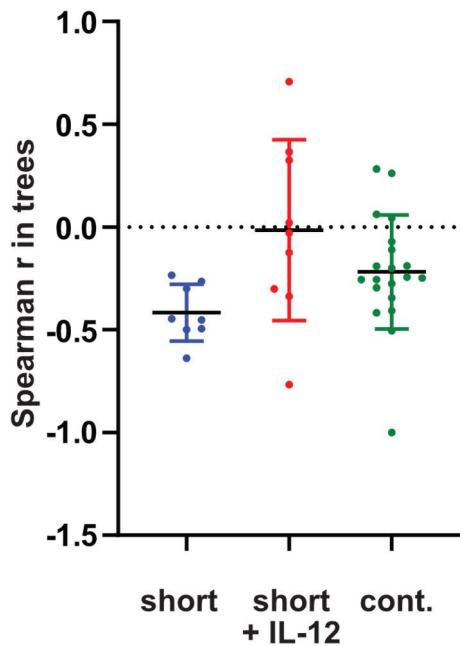


**Fig. 31: Correlation between inter-division time and expression of CD25 is strongest in the shortly-stimulated setting and weakest when IL-12 was added.** The spearman correlation coefficients for all investigated trees from all three experimental settings are shown.

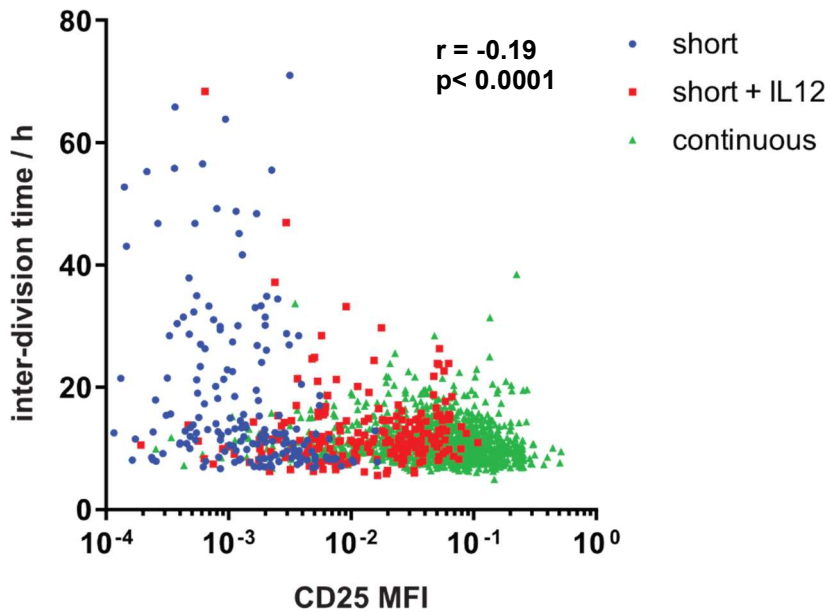


**Fig. 32: Inter-division times and CD25 expression of continuously, shortly and shortly + IL-12 stimulated cells.** Blue circles: short stimulation. Red squares: short stimulation and cultivation in the presence of 10 ng/mL IL-12. Green triangles: continuously stimulated cells.

When CD25 expression was also investigated for the shortly stimulated settings and the spearman coefficients were calculated for all trees, the shortly stimulated trees showed a stronger correlation between inter-division times and CD25 expression, but addition of IL-12 abrogated this correlation almost completely (Fig. 31). When the data from all three groups were combined, there was also a negative correlation between the inter-division times and CD25 expression levels (Fig. 32). But the cells from the shortly stimulated setting without IL-12 clustered at low CD25 expression levels with long inter-division times (blue circles), the setting with IL-12 clustered at intermediate-high expression levels with shorter inter-division times (red squares), and the cells from the continuously stimulated setting clustered at the highest CD25 levels with the shortest inter-division times (green triangles). Further insight into the correlation between inter-division times and CD25 was gained by separating the data sets into the respective generations of the cells (Fig. 33). Although the cells already showed different CD25 expression levels during the first generations, their inter-division times were still narrowly distributed and quite fast. However, in the fourth generation, the inter-division times became more broadly distributed and,

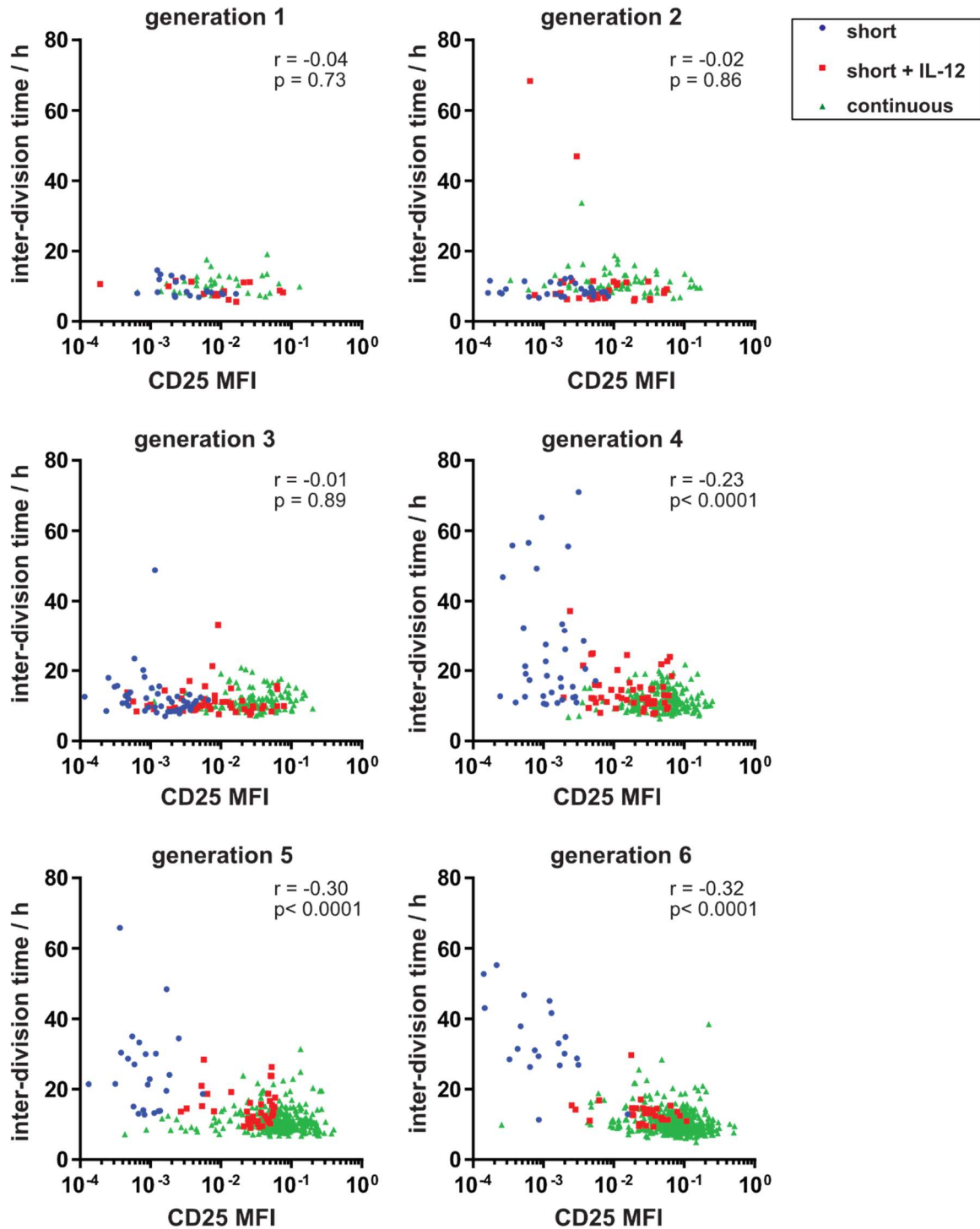


**Fig. 33: Correlation between CD25 and inter-division time depends on the generation and the stimulation conditions.** The inter-division times of all cells from all investigated trees of all three experimental settings were separated according to their generation, and their inter-division times were plotted against their CD25 expression. **Blue:** short stimulation without IL-12. **Red:** short stimulation with IL-12. **Green:** continuous stimulation.

the correlation between CD25 and inter-division time became significant (Fig. 33 generation 4). Comparing the spearman coefficients within individual trees of all three conditions showed that the correlations were similar in all three cases but most stable and strong in the setting where no IL-12 or  $\alpha$ CD3 increased CD25 expression (Fig. 31). Together these data show that in addition to the upregulation of CD25 by IL-12 and  $\alpha$ CD3, which led to an increased proliferation rate throughout the whole trees (Fig. 32 and Fig. 33), there were also additional differences in CD25 expression within trees under all three conditions that correlated with further intra-clonal variability of inter-division times (Fig. 31).

#### **4.7 Development of inter-division times over time**

Analysis of CD25 expression and its correlation with inter-division times has revealed that inter-division times and their regulation are not constant across time. Consequently, we further investigated the change in inter-division times over time.

While the inter-division times were almost constant during the time of observation in the continuous stimulation setting, the mean division time significantly slowed down after reaching generation 3 in the short stimulation + IL-12 and especially the short stimulation without IL-12 setting (Fig. 34). In parallel to this slowing down, the variation of inter-division times appeared to increase across generations 1 through 6. Analysis of the standard deviations (Fig. 35) and coefficients of variation (CV) within each tree (Fig. 36) showed that there was indeed a substantial increase in variability of inter-division times, especially after the third or fourth cell division. Furthermore, comparing the SDs with the respective CVs showed that, although the absolute variability in the continuously stimulated setting was smaller compared to short stimulation, the CVs were just slightly smaller (Fig. 35 and Fig. 36). Accordingly, the variability in relation to the mean inter-division time in different conditions was similar.

To investigate whether distinct inter-division times were stably maintained within distinct subtrees of the same single cell-derived progeny, inter-division times beyond the third cell division were grouped according to their

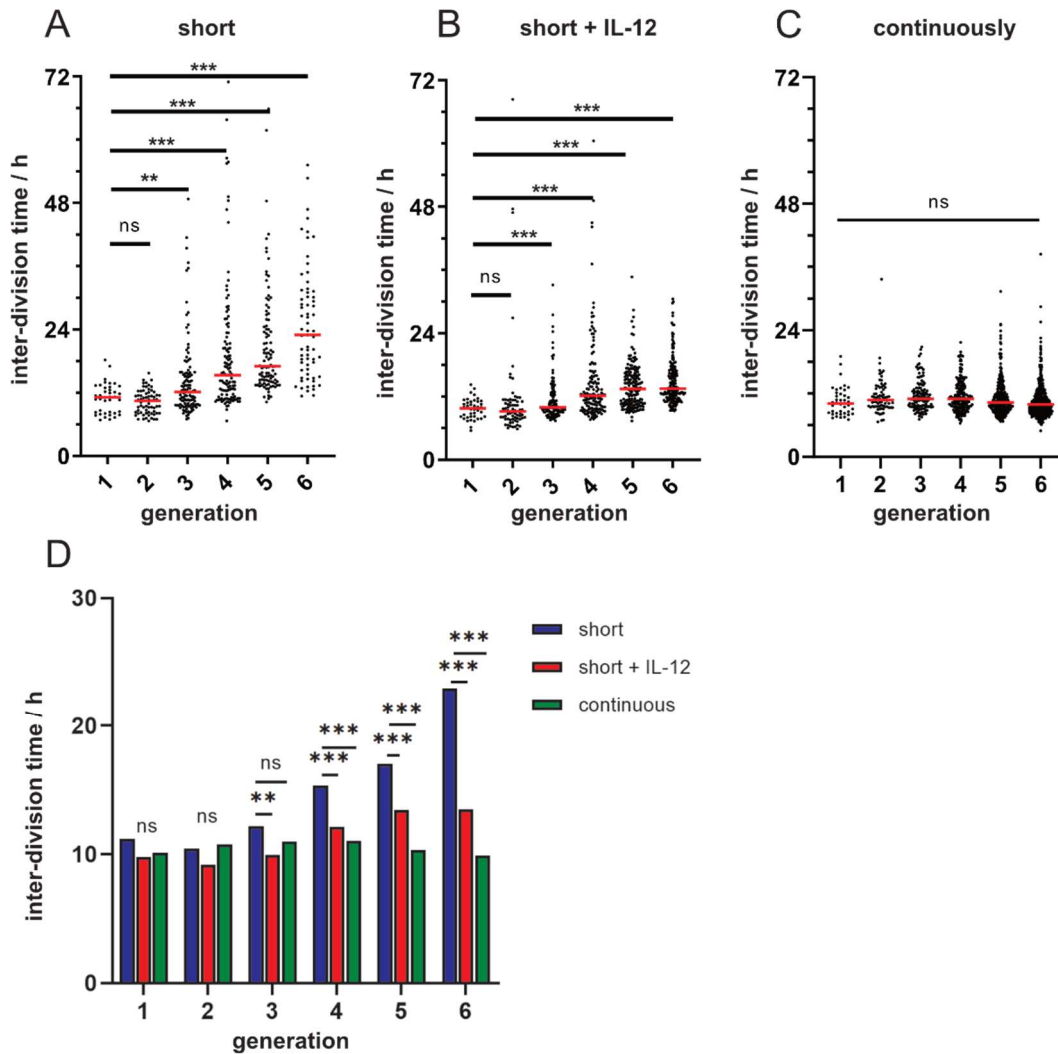


**Fig. 34: With short stimulation, the cells slow down with each generation and the variability of inter-division times increases. (A-C)** Inter-division times of all cells are plotted to their respective generations for all three settings. Red line indicates median. **(D)** Mean inter-division times from all three conditions in direct comparison. Statistical analysis: Dunn's multiple comparison test. \*\*  $p < 0.01$ , \*\*\*  $p < 0.001$

origin from one of four 2<sup>nd</sup> generation daughter cells into subtree #1–4 (Fig. 37A). Comparison of the inter-division times in the four subtrees of each progeny revealed that more than 30% of trees separated into fast and slow cycling branches that harbored significantly different inter-division times (Fig. 37). We did not perform this analysis for shortly stimulated cohorts because there were not enough offspring of the 2<sup>nd</sup> generation subtrees to perform proper statistical analysis due to the longer inter-division times after the third cell division (Fig. 34)

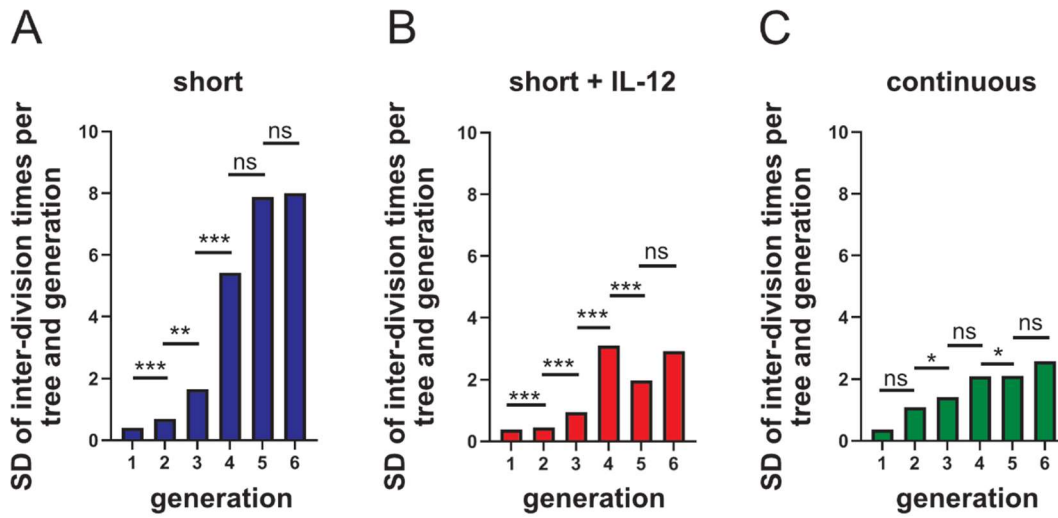


**Fig. 35: Standard deviations of inter-division time within individual trees increase during the first few cell divisions.** Data from Fig. 34 were separated into the different trees, and the mean standard deviations of inter-division times within the trees were calculated within each generation. F-test: \*  $p < 0.05$ , \*\*  $p < 0.01$ , \*\*\*  $p < 0.001$

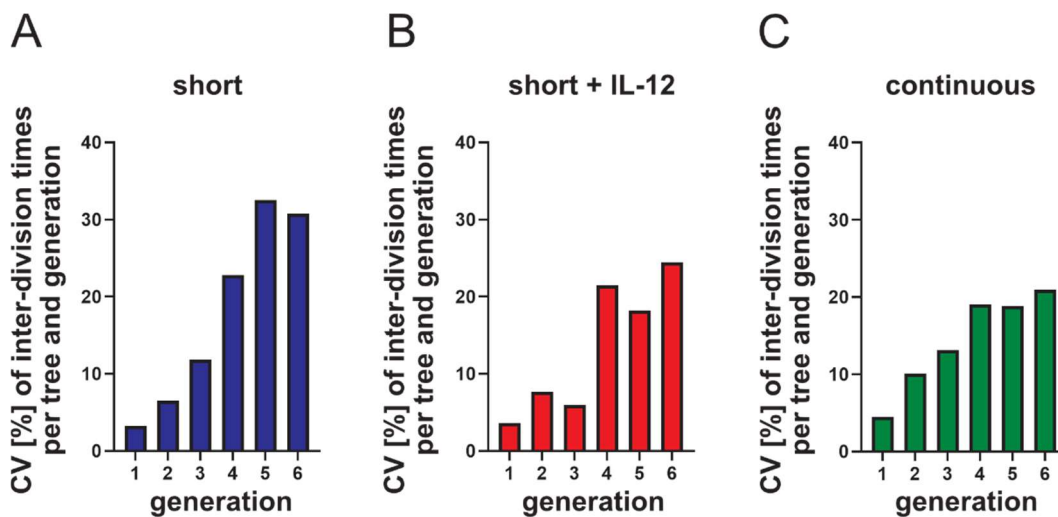


**Fig. 36: Variability of inter-division time within individual tree increases after a few cell divisions.** Data from Fig. 34 were separated into the different trees, and the mean coefficient of variation of inter-division times within the trees were calculated within each generation.



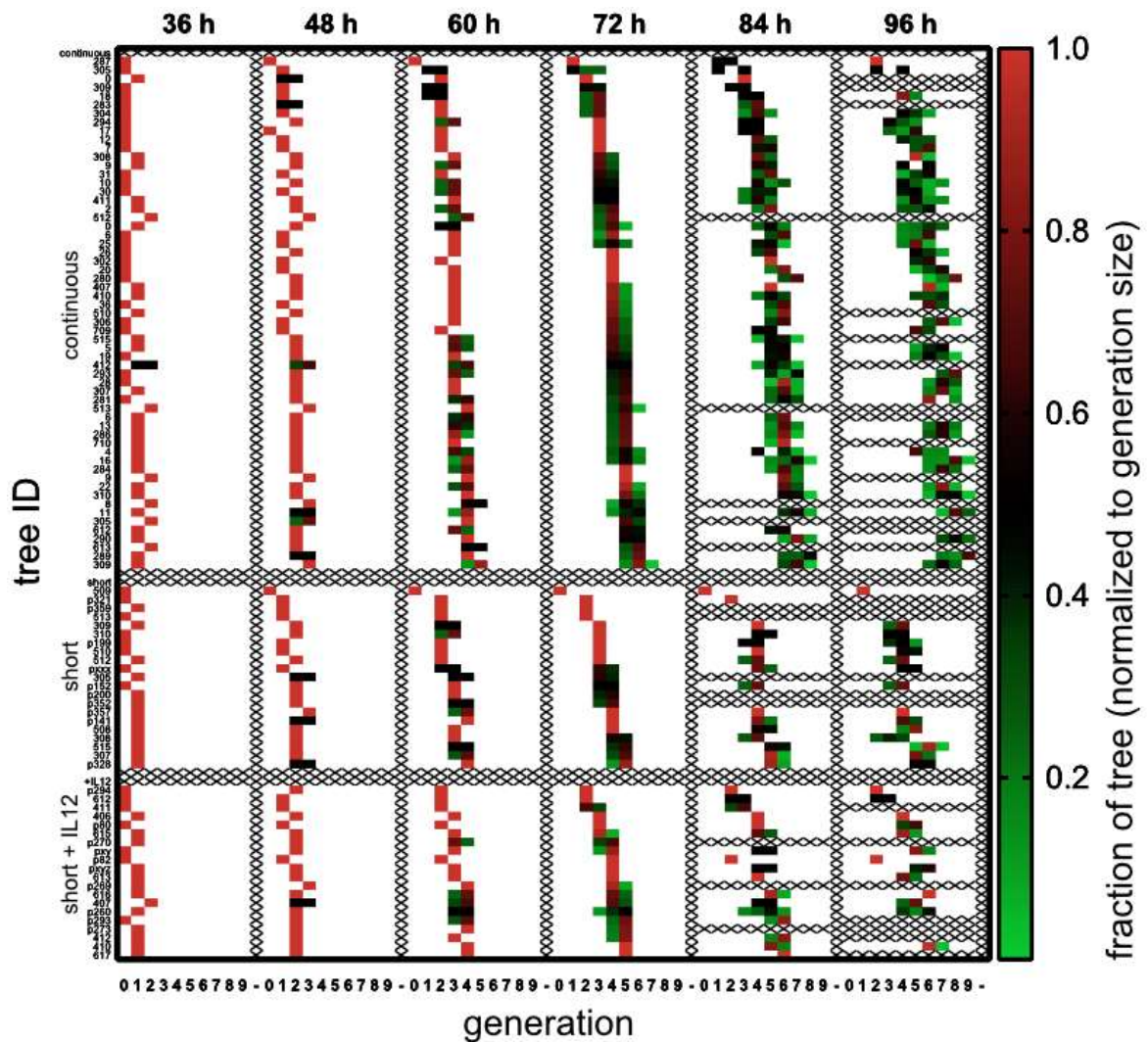


**Fig. 39: Ranges are very small during the first 72 h but diverge in later generations.** For all three conditions it is shown how the individual cells within a tree are distributed over the generations at different time points. Each square represents the cells of a tree that are in the respective generation at the given time point. The redder the box is, the higher is the fraction of the tree in the respective generation. Samples from the continuous stimulation setting are depicted in the upper part. Below that are the short stimulation samples. The short stimulation + IL-12 samples are depicted in the bottom part.

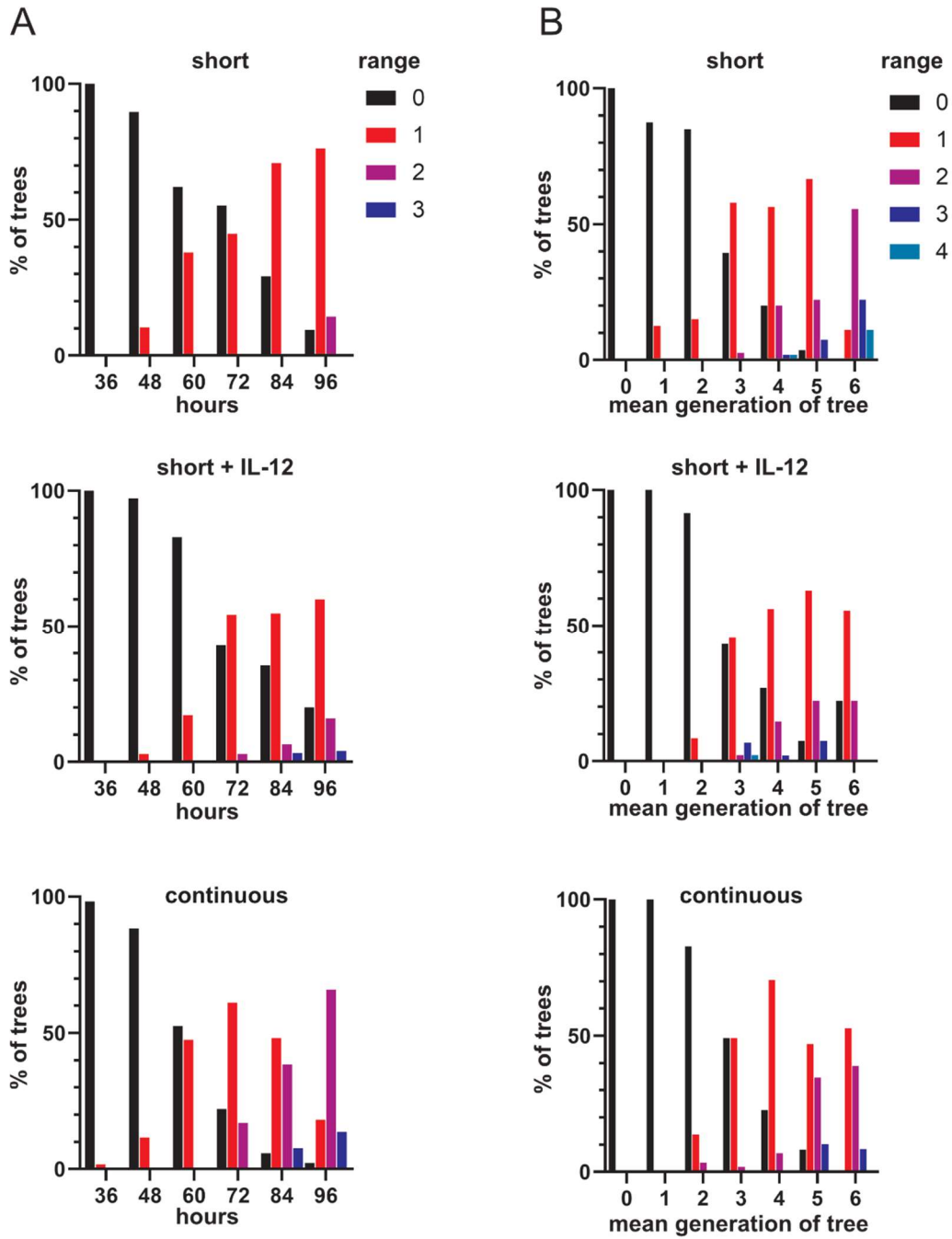


**Fig. 40: Ranges diverge faster when cells divide fast, but they diverge similarly when the ranges are plotted in relation to the mean generation of the tree. (A)** The ranges of all trees were determined at the indicated time points. black: range 0, red: range 1, purple: range 2, blue: range 3, cyan: range 4. **(B)** For every 12 h, the mean generations of the trees were calculated and the respective ranges were determined.

A necessary consequence of such distinct proliferation speeds maintained in distinct subtrees is that over time, a single cell-derived progeny will distribute across a range of generations. An elegant study has recently used cell proliferation dyes to investigate such heterogeneity in cell divisions but found T cell division to be concordant and single cell-derived progenies to be distributed across a maximum of two generations [102]. However, this analysis had been limited to investigating mainly the first 2–4 cell divisions. Interestingly, we observed similar initial concordance at early time points but found that T cells spread out across multiple generations later on. The distance between cells positioned in distinct generations has been termed “range” (Fig. 38). Cells within the same division peak would have a range of “0”, cells in two peaks next to each other would have a range of “1” and so forth. For the family trees in this work that have not been generated by cell proliferation dye assays but by live-cell imaging, the range at a given time point can be calculated by finding the cell within a tree with the most cell divisions (highest generation) and subtracting from the generation number the generation of the viable cell with the least cell divisions (lowest generation) at the same time point.

Fig. 39 shows how the ranges of individual trees develop over time. The colors of the boxes indicate the fraction of the tree that is in the respective generation. Completely red boxes mean that all cells of the tree were in that generation, black means half of the cells were found to be in that generation, and green indicates that just a few cells were in that generation. Hence, trees that contain only one box must be always red. In addition, the color code is corrected for incomplete trees and for generations. Correction for generation means that each cell from generation 1, in which only two cells are possible, could contribute with 0.5 to the fraction of cells in the respective generation. Cells which were in generation 3 (max. 8 cells possible) contributed with 0.125 per cell and so forth. The results show that there were almost no trees detected with a range larger than 1 during the first 3 days. After that, however, the ranges increased drastically.

In the continuously stimulated setting, the inter-division times were shorter. Therefore, more cell divisions with potentially different inter-division times were possible within a given time frame. To correct for the different speeds

between individual trees and under the three tested conditions, the division progress of each tree was measured every 12 h and the ranges for different division progresses were calculated. The division progress was defined as the mean generation at a given time point. Because the generations have a different maximum number of cells, a similar correction as for calculation of the fraction of tree was used. Accordingly, a tree with 1 cell (out of **max. 2**) in **generation 1** and 2 (out of **max. 4**) cells in **generation 2** would result in a mean generation of 1.5 ( $1/2 \times 1 + 2/4 \times 2$ ).

Under conditions which promote fast cell divisions (e.g., continuous stimulation), the ranges rise faster as a function of the time than under conditions that promote slow cell divisions (e.g., short stimulation without IL-12) (Fig. 40A). Fast dividing trees can pass through more cell divisions within the same time than slow dividing trees. Correction for this effect by plotting the ranges not against the time point but against the mean number of cell divisions at a given time point (Fig. 40B) leads to similar kinetics under all three conditions. This indicates that the variability of inter-division times within single cell-derived trees is preserved in relation to the overall proliferation rate under different conditions (Fig. 40B). Or in other words, the relative but not absolute difference between fast and slow cells within a tree is similar, regardless of whether the overall proliferation rate of the respective tree is high or low.

#### **4.8 Expression of the memory-related marker CD62L in fast vs. slow dividing cells**

Due to activation-induced shedding, CD62L cannot be used in the continuously stimulated setting, and also with short stimulation, the first few days are not reliable. Nevertheless, CD62L is the most desired marker for live-cell imaging because mathematical modelling of single cell-derived data had predicted that CD62L would discriminate best between fast and slow-dividing T cell subsets [89]. In addition, a negative correlation between CD62L and size of expanded progeny had also been found *in vitro* in the continuous stimulation setting (Fig. 12B). However, both settings could not

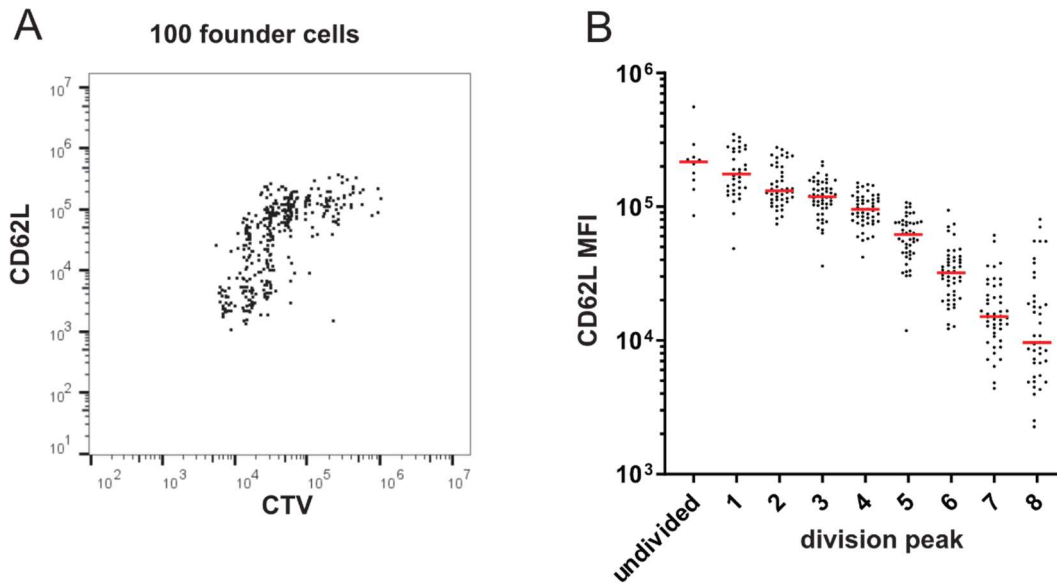


**Fig. 41: CD62L low cells divide within the same time more often than CD62L high cells.** (A) Representative CTV-plot of the offspring of 100 OT-I cells that had been stained with CTV and activated for 24 h. After further 3 days of cell culture, the cells were stained for CD62L and analyzed by flow cytometry. (B) On the basis of the vertical lines in the CTV-plot, the number of cell divisions for each cell in the plot can be estimated. The mean CD62L expression within each division peak is shown for all 100 cell-derived progenies.

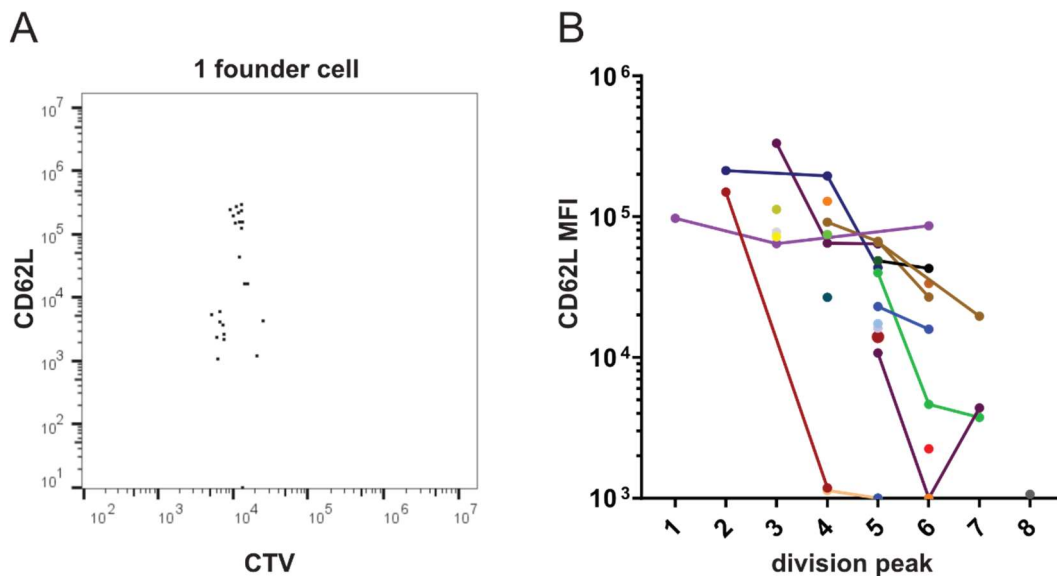


**Fig. 42: Downregulation of CD62L is correlated with the number of cell divisions within the same single cell-derived progeny.** (A) Representative CTV-plot as in Fig.29 but from a single progenitor cell. (B) CD62L expression in division peaks as in Fig.29 B. In addition, division peaks of the same single-cell tree are drawn in the same color and connected with a line.

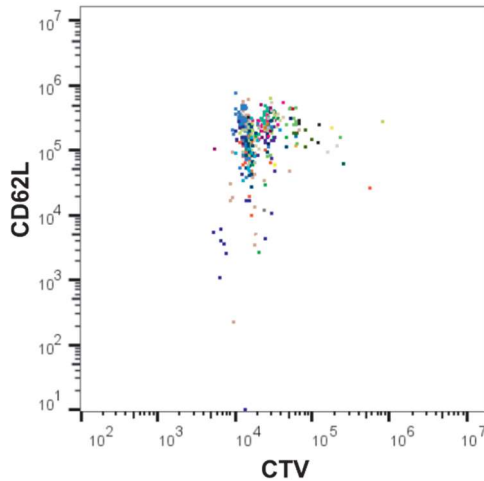


**Fig. 43: Overlay of 30 single-cell CTV-plots.**

resolve whether CD62L<sup>+</sup> T cells indeed proliferated slower or simply entered the cell cycle later, or exited it earlier than their CD62L<sup>-</sup> counterparts.

By staining responding T cell populations (derived from 100 cells) with CTV and anti-CD62L, we found that CD62L<sup>hi</sup> T cells had indeed divided less often by day 4 after *in vitro* priming (Fig. 41A–B). Importantly, CD62L<sup>hi</sup> and CD62L<sup>lo</sup> T cells that were derived from the same founder cell also showed distinct proliferation activity, as shown in the representative CTV plot of a single cell-derived progeny in Fig. 42A. The division peak on the right (i.e. less divided cells) shows higher CD62L staining intensity than the division peak on the left (i.e. more divided cells). Thus, the correlation is also true within single cell-derived progenies and was further quantified for all cells from the short-stimulated setting in Fig. 42B. By combining the CTV plots from 30 single cell-derived progenies, a CTV plot was generated that looks similar to a population-derived CTV plot (Fig. 43).

A possible explanation is that T cells with high levels of CD62L stop dividing earlier than other cells, or that the T cells lose CD62L after a certain number of cell divisions. To confirm or reject these hypotheses, live-cell imaging experiments in the presence of an antibody against CD62L were necessary. In Fig. 44, the accumulated inter-division times from all trees in the short stimulation settings with and without IL-12 are shown. The cells which were high for CD62L showed indeed longer inter-division times. The median inter-

division time of CD62L low cells in the data set without IL-12 was almost exactly the same as in the data set with IL-12, whereas the CD62L high cells divided slower when no IL-12 was added. Separating the data sets into individual trees shows that also within the trees, the CD62L high cells divided slower than the CD62L low cells (Fig. 45).

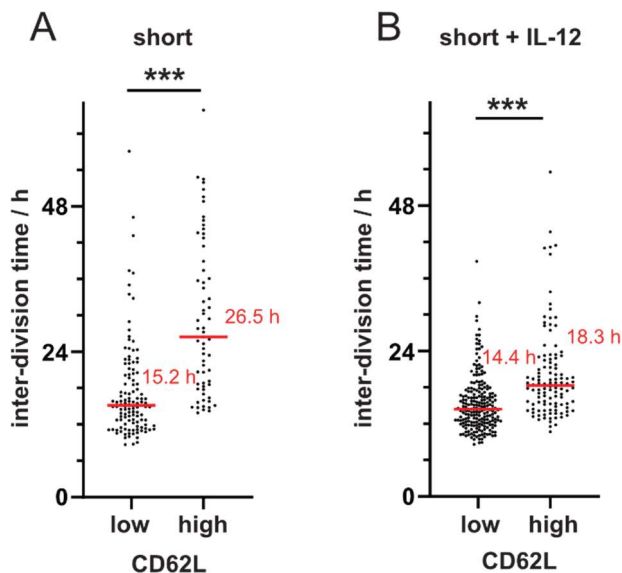


**Fig. 44: Slow-dividing cells are CD62L high.** Live-cell imaging was conducted in the presence of fluorescent antibodies against CD62L, and the fluorescence was measured every 12 h. Red numbers and lines indicate the median inter-division times. Statistical analysis: Student's T test. \*\*\*  $p < 0.001$ .

In Fig. 34 it was demonstrated that the cells divided slower with every further generation if no continuous stimulation was available. Taking into account the activation-induced shedding of CD62L during the first T cell divisions after activation, the correlation could be an artefact, because CD62L high cells were only detected at time points when all cells divided slower. To control for this bias, the inter-division times of CD62L high and CD62L low cells were plotted against the time when the respective cell divided (Fig. 46). As a result, there was also a separation into slow cycling CD62L high cells and fast cycling CD62L low cells at time points when both cell types were present and there was a slowdown of inter-division times over time for both

subsets, but on a different level. These effects were stronger when no proliferation-enhancing IL-12 was added.

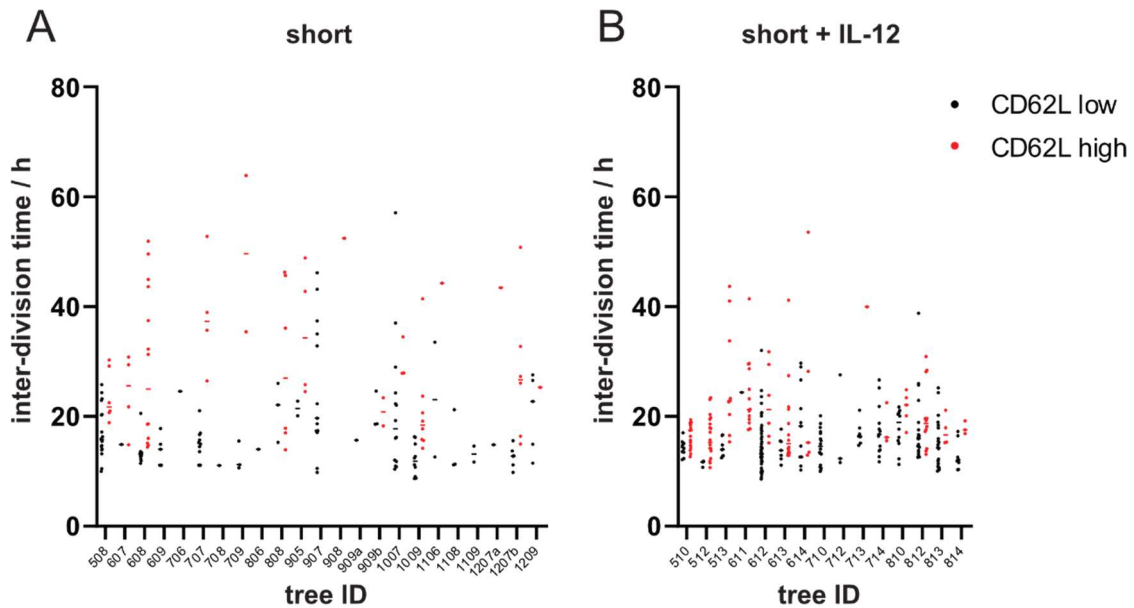


**Fig. 45: Also within the same single-cell tree, CD62L high cells divide slower than CD62L low cells.** Data from Fig. 34 but segregated into the individual T cell trees. Black dots were CD62L low, red dots were CD62L high.

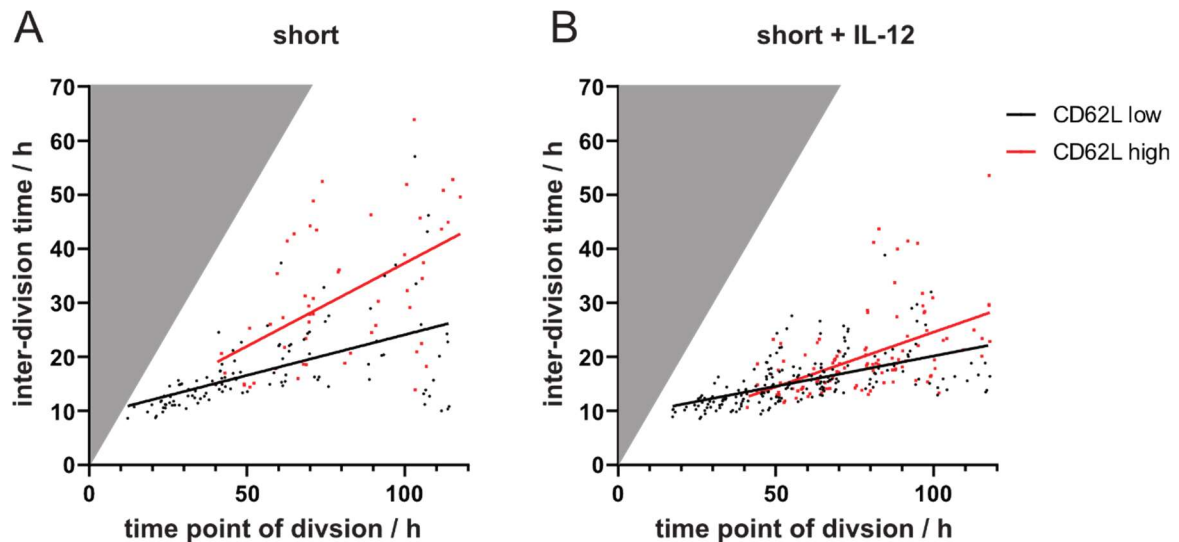


**Fig. 46: CD62L high cells are more affected by slowing down of cell-cycle over time, and IL-12 reduces the difference in inter-division times of CD62L high and low cells.** The inter-division times from Fig.32 were plotted against the time point when the respective cell divided. Black: CD62L low. Red: CD62L high. Grey areas indicate areas where no data points are possible because cells cannot divide earlier than the length of their inter-division time.

## 5 Discussion

The differentiation into memory and effector cells is a key feature of the adaptive immune system. It enables the organism to build up a strong defense against acute infections on the one hand and to protect against reinfection with the same pathogen for many years on the other hand. How the different T cell subsets are created from naïve precursor cells is still a subject of vivid discussions. By transferring a single naïve CD8 T cell into a recipient mouse which was infected with *L.m.-Ova* and detecting the offspring of this single cell, Stemberger et al. showed that all three subsets (TCMs, TEMs and SLECs) can be generated from just one naïve T cell [110]. Although this experiment impressively shows that a single naïve T cell can produce all major T cell subsets, it does not exclude the possibility that the potential of each precursor cell to produce predominantly memory or effector cells is different. It has been suggested that the affinity of a TCR to its epitope might influence the expansion and differentiation of T cells, and many studies have shown that this may play an important role [111-113]. However, by using a combination of congenic mouse strains, Buchholz and colleagues were able to multiplex the single-cell transfer approach and thereby, map the fate of multiple naïve OT-1 T cells and their progeny *in vivo* [89]. Even under these conditions, in which all T cells harbor the same transgenic TCR, the outcomes after 12 days of infection were very variable, with many small single cell-derived progenies that consisted of just a few hundred mainly memory-differentiated cells, and a few very large progenies that consisted of up to  $10^5$  cells, which were mainly effector-differentiated.

Mathematical analysis of studies in which the fates of single naïve T cells were investigated *in vivo*, suggested the diversification into fast cycling SLECs and slow cycling memory precursor cells within the same single cell-derived progeny already early during the acute infection as a source for this variability [89]. However, to evaluate whether this hypothesis is correct, a

few critical and sophisticated questions were still not directly addressed. These questions, which I aimed to answer were:

- 1) How much do distinct division speeds contribute to the variable expansion of single T cell-derived clones?
- 2) How is division speed influenced by antigenic and cytokine-based stimuli available beyond priming?
- 3) Do distinct division speeds develop, and are they maintained in separate subpopulations of the same clone?
- 4) Do distinct division speeds coincide with differentiation of MP and SLEC phenotypes?

In the following sections, I will first discuss to what extent my results could shed light on these questions, and in the last sections I will examine how these results can improve our understanding of T cell differentiation.

## **5.1 Distribution of cell-cycle speed and phenotype during the early phase of the immune response**

### **5.1.1 Contribution of distinct division speeds to the variable expansion of single T cell-derived clones**

Although the culture conditions were well-defined throughout the experiment, the variability in the size of the single cell-derived progenies on day 4 after activation was considerable. To evaluate the source of this variability, a few variables have to be taken into account: the time to first division, the subsequent inter-division times and division cessation. Cessation of division and apoptosis were not observed during the observation period to an appreciable degree. Nevertheless, it cannot be excluded that division cessation would further increase the variability at a later time point. Measurements of the inter-division times showed that the time to first division was indeed variable and took, with roughly 36 h much longer than the subsequent cell divisions (Fig. 14). However, comparing the variability in size that was caused by different onsets of proliferation to the variability that was generated by different inter-division times showed that

both were contributing to overall variability, but the impact of division speed was substantially higher (Fig. 13 and Fig. 14).

#### **5.1.1.1 Concordance of trees**

These results are not in line with publications suggesting that the variable outcomes of single cell-derived progenies are generated by concordantly growing trees in combination with division cessation within the same tree, which occurs when the respective tree reaches its so-called division destiny [102, 103, 114]. The publication that most directly addressed the growth of T cell family trees did this by staining T cells with cell proliferation dyes and culturing them either without or in the presence of just very low concentrations of IL-2 (1 U/mL). After a maximum of 72 h, the cells were analyzed via flow cytometry [102]. In line with concordantly growing trees and division cessation, the observations of these experiments were that the cells, originating from the same naïve T cell, were found almost exclusively within the same division peak. Furthermore, the single cell families were often completely consisting of small cells already a few days after priming. Small cell size was used as a surrogate marker for quiescent cells that had reached their division destiny, thus, indicating early division cessation.

However, the results in this thesis show that the T cells continue to proliferate for at least 5 days when IL-2 is not limited and antigen is available (Fig. 11 and Fig. 13). Due to the limited number of epitope specific naïve T cells and because it is important for T cells to strongly proliferate after activation to fight acute infections, it would also be an unexpected mechanism if variability would be generated by quiescence of most T cells after just a few cell divisions. Further on, it is usually not possible to detect all cells from a sample via flow cytometry. Cells that divide slower than the rest within the T-cell family would be present in very low frequencies and could be missed, thus shifting the results in the direction of concordance. But most importantly, concordance regarding ranges and generations until 72 h is in line with the data in this thesis (Fig. 35, Fig. 36 and Fig. 39) but does not exclude the emergence of discordance observed in this thesis at later time points of T cell proliferation.

The results in this thesis show that T cell families seem concordant for the first 72 h and then become surprisingly discordant. This has several causes. The first is, that the time until the first division takes already roughly 36 h (Fig. 14), thus reducing the available time for generation of discordance from 72 h to 36 h. Furthermore, the first three to four cell divisions showed just a very low degree of variability (Fig. 34, Fig. 35 and Fig. 36). (Maybe as a mechanism to guarantee a minimum of single cell-derived proliferation that reduces the number of progenies that completely lack a memory or effector phenotype) The synchronized initial phase reduces the time for the generation of discordance further. In addition, also distinct proliferation rates need a few generations of time until the differences of division speed have accumulated into a complete generation advance that could be detected via cell proliferation dyes.

#### **5.1.1.2 Time point of discordance**

Another publication used also live-cell imaging to directly measure division times of the daughter and granddaughter cells that have been sorted from the 1<sup>st</sup>, 3<sup>rd</sup> or 8<sup>th</sup> generation [115]. These data are also largely in line with the results of this thesis. Namely, they detected a strong correlation between the division times of sister cells that was stronger than the correlation between mother and daughter cells (Fig. 23), and they detected a much stronger variability of division times after the 8<sup>th</sup> generation compared to the early generations (Fig. 35 and Fig. 36). After the 8<sup>th</sup> generation, segregation into slow dividing CD62L high cells and fast dividing CD62L low cells was also detected. However, it was suggested that the 8<sup>th</sup> generation is the time when T cells segregate into fast or slow dividing subsets, without having tracked the generations between four and eight. Being able to measure the division times of whole trees and not just of two subsequent divisions, my results show that segregation already starts after the first approximately three to four cell divisions and can then increase over time, when the putative MPs slow down. (Fig. 34, Fig. 35, Fig. 36, Fig. 37, Fig. 40 and Fig. 46)

### 5.1.2 How division speed is influenced by antigenic and cytokine-based stimuli beyond priming

Availability of antigen and cytokine stimuli are known to modulate the differentiation and proliferation of populations of CD8 T cells. Yet how they impact the fate on the level of individual T cells is not completely understood. Single cell fate mapping could help to show directly whether a certain external stimulus acts on all cells in a similar way or whether only those cells are affected that are particularly susceptible to the signal.

#### 5.1.2.1 Antigenic stimuli

The availability of antigen as well as the intensity of the antigenic stimulus have been observed to result in higher numbers of T cells [111, 116]. Although, it has not always been possible to discriminate between the roles of antigen, costimulation and inflammation, because the pathogens usually lead to all three signals. A way to circumvent this limitation is provided by a system developed by Jung et al. that enabled the control of antigen and inflammation apart from each other via depletion of antigen-presenting dendritic cells *in vivo* [117]. However, only *in vitro* live-cell imaging is, so far, able to show the impact of diverse stimuli on the division times of individual cells.

The comparison between cells that were continuously stimulated with plate-bound  $\alpha$ CD3/ $\alpha$ CD28 and those that received no stimuli via  $\alpha$ CD3 beyond the first 24 h shows that antigen seems to affect proliferation of T cells in at least two ways. Firstly, the inter division times themselves were shorter (Fig. 16, Fig. 26, Fig. 27 and Fig. 32) when  $\alpha$ CD3 was continuously available, and secondly, the just briefly stimulated T cell slowed down after a few divisions. In many trees, cells finally seemed to exit the cell cycle or started to die. Under both conditions, the first few cell divisions were relatively fast and concordant with the variability increasing during the next divisions (Fig. 34, Fig. 35 and Fig. 36). The variability of the inter-division times was high in both settings, although a little lower in the continuously stimulated setting. Thus, it cannot directly be concluded from the inter-division times whether  $\alpha$ CD3 promoted the differentiation of all cells into a fast cycling subset with a slightly narrowed distribution of division times, or whether  $\alpha$ CD3 directly

acted on cell cycle speed and shifted the whole population to shorter inter-division times.

### **5.1.2.2 Cytokine-based stimuli**

Addition of the pro-inflammatory cytokine IL-12 to CD8 T cells had similar effects on the division times as prolonged stimulation via  $\alpha$ CD3 (Fig. 17, Fig. 27, Fig. 28, Fig. 32, Fig. 34 and Fig. 35). However, the effect was weaker: IL-12 did not prevent slow-down and division cessation completely in all family trees, and the overall inter-division times were just slightly reduced. Population-based studies have shown that IL-12 leads to upregulation of IL2R $\alpha$  (CD25) on CD8 T cells [118]. In Fig. 27 and Fig. 32 we could show that this is also true on the level of individual cells. Interestingly,  $\alpha$ CD3 led to an upregulation of CD25 that was even stronger than the IL-12-driven upregulation. Also increasing the concentration of IL-12 could not reach the CD25 levels of  $\alpha$ CD3. Because of increased IL-2 signaling via IL2R $\alpha$ , this could be a part of the mechanism how antigen and inflammation lead to increased division speed.

### **5.1.3 Development and maintenance of division speeds in separate subpopulations of the same clone**

Statistical analysis of the data has shown that the contribution of intra-clonal variability and inter-clonal variability to the total variability of interdivision times was similar (Fig. 24). This immediately raises the question whether the distinct proliferation speeds that develop within the same family tree are randomly distributed or whether the tree separates into distinct branches in which the acquired division speeds are inherited. If there were a segregation into branches, this would be a strong indication for early segregation into slow and fast T cell subsets within the same single cell-derived progeny. These cell fate decisions that result in slow or fast proliferating branches could theoretically occur at any time point. We chose to segregate the trees after the second cell division into four hypothetical subtrees and tested them for distinct proliferation rates. Although later branching events within the same hypothetical subtree would partly average each other out, more than 30 % of the trees showed distinct subtrees emerging after only two cell divisions (Fig. 37). However, this does not mean that all of the detected fate

decisions were made after the second cell division, because distinct distributions of subtrees one generation later could still lead to differences in the superordinate subtree. Nevertheless, without giving the exact time point of cell fate decision, the results show that there is indeed segregation into slow and fast dividing subtrees just a few days after activation of a single T cell *in vitro*. My next task was to investigate whether these slow and fast division activities also correspond to a certain memory or effector phenotype. If this were the case, it could indicate that MPs and SLECs can already segregate from each other during the first days after activation, acquiring distinct proliferation speeds, and that they do not share a common proliferative history until the peak of expansion.

#### **5.1.4 Correlation between SLEC and MP phenotypes and division speed**

##### **5.1.4.1 CD25 correlates with cell-cycle speed**

The first marker I checked for correlation with inter-division time was IL2R $\alpha$  (CD25). Prolonged expression of CD25 has been shown to lead to enhanced differentiation into SLECs [119]. Furthermore, IL-2 is known to drive cell cycle progression [120]. Thus, as the high affinity  $\alpha$ -chain of the trimeric IL-2 receptor, CD25 could be the direct link between differentiation and subset-specific proliferation.

Live-cell imaging in combination with fluorescent antibodies against CD25 has shown that there is indeed a highly significant correlation between CD25 expression levels and division speed within the same single cell-derived progeny (Fig. 29, Fig. 30 and Fig. 31). Although the correlation is low, this is an important finding because only prolonged expression of CD25 is associated with terminal differentiation. A short initial upregulation of CD25 however, is also required for the generation of protective T cell memory [121, 122]. This effect may slightly impair the correlation. In addition to that, the first few cell divisions were mostly quite fast with just a very low degree of variability. Analysis of the correlation between CD25 and division speed segregated into the respective generations revealed that in spite of a broad distribution of CD25 expression levels, already within the first few generations, the CD25 expression seemed to be irrelevant for division

speed. The correlation between CD25 and division speed did not become apparent until generation four, when the first T cells started to slow down (Fig. 33). Although signal 1 itself leads to upregulation of CD25 (Fig. 32), most likely the activation of naïve T cells induces a short program that results in a few fast cell divisions without the involvement of CD25.

#### **5.1.4.2 CD62L inversely correlates with cell-cycle speed**

Initially, CD62L was predicted to be the marker that would segregate slow dividing TCM precursor cells from fast dividing TEM precursors and SLECs [89]. However, CD62L is not an easy marker for early time points because it is shed after activation and TCR signaling [123-125]. Consequently, detection of CD62L could not be measured under continuous stimulation with  $\alpha$ CD3. In the briefly stimulated settings, shedding would be expected to be lower. Nevertheless, during the first days especially, only CD62L high signals were trustworthy, whereas missing signals could either be explained by truly CD62L low cells or by CD62L high cells that had cleaved CD62L. Despite these difficulties that reduced the measured correlation between CD62L expression and inter-division time, the results in this thesis show that the slow-dividing cells were CD62L high (Fig. 12, Fig. 41, Fig. 42, Fig. 43, Fig. 44, Fig. 45 and Fig. 46).

Together, my results reinforce the prediction that MPs segregate from SLECs already early during the immune response after a short phase of fast and synchronized cell divisions. These fate decisions are associated with the acquisition of distinct division speeds. The phenotype-associated division speeds may explain the intra and inter clonal variability that has been observed between and within single cell-derived responses at the peak of expansion *in vivo*.

In the following sections, I will discuss how these findings can contribute to improving our understanding of T cell development.

## 5.2 Implications for our understanding of T cell differentiation

### 5.2.1 Order of differentiation

By now it is well established that the traditional linear differentiation model [66, 86, 87], which proposes the differentiation of effector cells into memory cells, as well as the decreasing potential model [78, 87, 88, 126] that suggests a stepwise progression into a terminal effector phenotype, are, in spite of their dichotomy, both true to some degree. Memory T cells develop from the pool of effector T cells, but nevertheless, the memory precursor cells precede the terminally differentiated effector cells. This contradiction was solved by the discovery that memory precursor cells also exhibit effector functions during the acute immune response [78, 127]. Thus, they were named memory precursor effector cells (MPECs). Measurements of telomere lengths have shown that memory T cells have experienced fewer cell divisions than their effector counterparts [128]. This could be explained by different mechanisms: earlier division cessation, later recruitment, or slower proliferation rates of memory precursor cells. As discussed above, my data strongly indicate that memory precursor T cells divide slower than their effector counterparts, as was predicted by Buchholz et al. [89]. Mathematical analysis revealed that the most probable differentiation pathway would start from naïve T cells to slow dividing central-memory precursors to fast dividing effector-memory precursors and SLECs. A T cell family tree that would fit to this model would start with slow-dividing cells, and at different time points, subtrees would appear that proliferate much faster (Fig. 47A). However, this scheme was not observed. Rather, the distribution of slow and fast subtrees resembled a differentiation into MPs or SLECs out of an early subset of fast and concordant dividing cells (Fig. 29, Fig. 34, Fig. 35, Fig. 36 and Fig. 37). This differentiation pathway (Fig. 47B) would still be in line with fewer cell divisions of memory T cells at the peak of expansion. The early subset could most likely consist of cells in transition to a certain phenotype that has not yet affected cell-cycle speed and is not yet stable – resembling very much the early effector cells (EECs) that were suggested by Lefrancois, Obar and Plumlee [129-131].

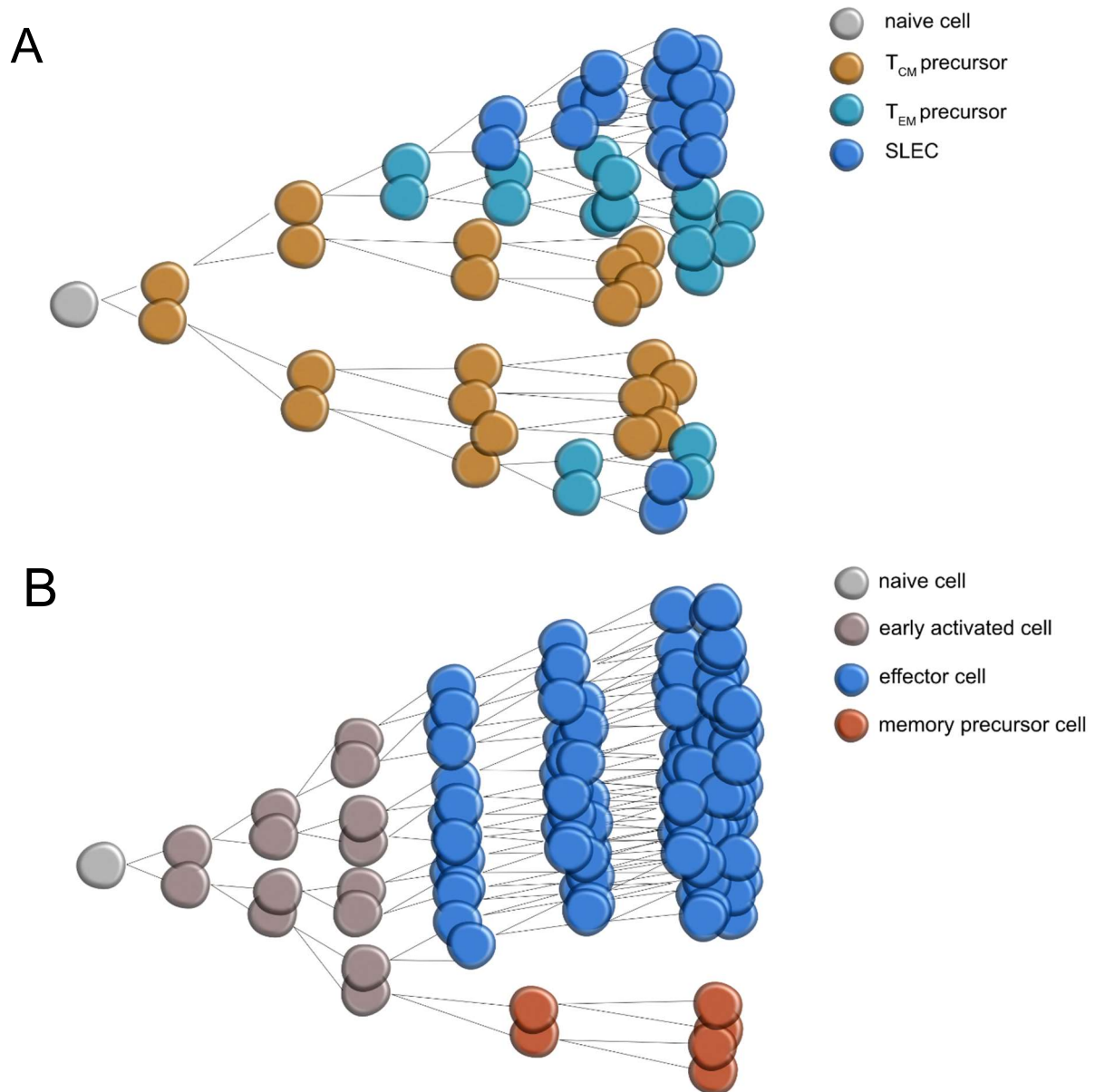


**Fig. 47: Differentiation-linked division. A:** Stochastic model of progressive differentiation. Slow dividing  $T_{CM}$  precursor cells (dark orange) can differentiate further into fast dividing  $T_{EM}$  precursor cells (cyan) and SLECs (blue). The first divisions are predominantly slow until fast dividing subtrees appear. **B:** Inspired by observations from this thesis. After a phase of 3 to 4 fast and homogenous cell divisions (reddish grey), slow and fast dividing branches with a memory (red) and effector (blue) phenotype, respectively, emerge.

### 5.2.2 Signal integration

The huge variability between and within single cell-derived progenies raises the question of how and when the T cells decide to acquire a certain phenotype.

According to the progressive differentiation hypothesis, the fate of a T cell progeny is already determined before or during priming [92, 93]. Variables that could impact the priming quality, thereby activating a developmental program in the cells – comparable to an autopilot – could be provided by the affinity to the pMHC complex, costimulation and cytokines. Indeed, it has been shown that high affinity TCR signals result in larger responses [111]. Similar results were found for costimulation and inflammatory cytokines [58, 95]. Interestingly, T cells that have been activated by peptide pulsed DCs showed very variable levels of the effector cytokine IFN- $\gamma$  even before the first cells division [132]. However, although these factors are likely to impact the fate of a primed T cell, they cannot explain the huge variability that has been observed when single cell-derived progenies were analyzed that harbored exactly the same TCR [89, 133]. Furthermore, the antigen and inflammatory milieu is usually still present after priming. Thus, it is difficult to discern whether the fate was really determined by the signals during priming or whether repetitive signals accumulated to guide the respective cell into a certain phenotype [88]. For the interest of the patient, it would make sense, if the immune system could integrate later signals to react to changes in the antigen load or inflammatory milieu and thus prevent excessive or insufficient immune responses. This would also be in line with observations indicating that the culture conditions during the days after activation have more impact on the cell number and phenotype than the culture conditions during priming. Furthermore, subtrees were developing beyond the first cell division (Fig. 37), indicating that fate-decision making is not complete after the first division.

### **5.2.3 Diversification under homogenous conditions**

The results in this thesis have conclusively shown that single cell-derived responses are very variable – even without the complex environment of an organism. How is diversity established when all T cells harbor the same TCR and the culture conditions are well-defined?

### 5.2.3.1 *Asymmetric cell division*

One mechanism that was suggested to guarantee diversity under homogenous conditions is asymmetric cell division [79, 82, 83]. It was suggested that the part of the naïve cell that is proximal to the DC during priming will acquire an effector phenotype, while the part of the cell that is distal to the DC will acquire a memory phenotype after the first division. Thus, the immune system would not risk generating responses that completely lack memory or effector cells. Also, the reactivation of TCMs has been proposed to start with an initial asymmetric cell division [134]. The operating mode of asymmetric division was proposed to be based on asymmetric distribution of the proteasome, which leads via its degradative function to unequal distributions of transcription factors like T-bet [83]. However, ablation of Scribble, as a part of the asymmetric cell division machinery, does not interfere with functional B cell responses [135], and the variability of single cell-derived responses is not explainable by a single asymmetric cell division [91]. This conflict could possibly be solved if further shaping by asymmetric cell divisions throughout the expansion phase were allowed, but the finding that approximately 20 % of single-cell progenies do not produce functional memory [60] speaks against asymmetric cell divisions that guarantee the maintenance of memory cells [92]. Also, experiments in which the two daughter cells were separated after the first division and cultured apart from each other have shown that only half of the first cell divisions result in two daughter-cell responses that are distinct from each other [136]. Other investigations implicated that only high affinity DC-T cell contacts result in asymmetric cell divisions whereas weak interactions result in symmetric cell divisions [137]. However, the experiment in which the two daughter cells were separated [136] was conducted with OT-I cells and OVA-pulsed DC. Thus, the affinity would be expected to be similar for all activated cells. Although the experiments in this thesis do not facilitate asymmetric cell divisions because real DCs are missing, they show that they are not required to generate diversity (Fig. 12, Fig. 13 Fig. 22, Fig. 24). If, however, one would argue that activation via plate-bound  $\alpha$ CD3/ $\alpha$ CD28 is sufficient to induce asymmetric cell divisions, one would expect that the strong stimulus provided by plate-bound  $\alpha$ CD3/ $\alpha$ CD28 would result in very

distinct fates of the generation 1 daughter cells. This was not the case. Together the publications and results show that asymmetric cell divisions might occur during T cell expansion but their significance for diversification seems very limited – leaving the question open how variability is generated under largely homogenous conditions.

### 5.2.3.2 Stochastic signal integration

Buchholz et al. proposed that the signals that lead to cell fate decisions might be integrated in a stochastic way, meaning that they cannot be predicted before the immune response [89, 92]. In principle, there are two ways for instructive signals to generate diversity. Firstly, only a fraction of cells is exposed to the instructing signal (Fig. 48A) (e.g., because the cells are located in different micro milieus) or secondly, they differ in their responsiveness to the respective signal (Fig. 48B). The results of this thesis show that variability is still very high when the environment is well-controlled (Fig. 12, Fig. 13, Fig. 22, Fig. 24, Fig. 27, Fig. 28 and Fig. 29). Under these conditions, only signals that are produced by the T cells themselves could create a micro milieu. Although it is very likely that different environments stabilize the phenotypes – taking into account the different migration patterns of TCMs, TEMs and SLECs – the remarkably high variability under

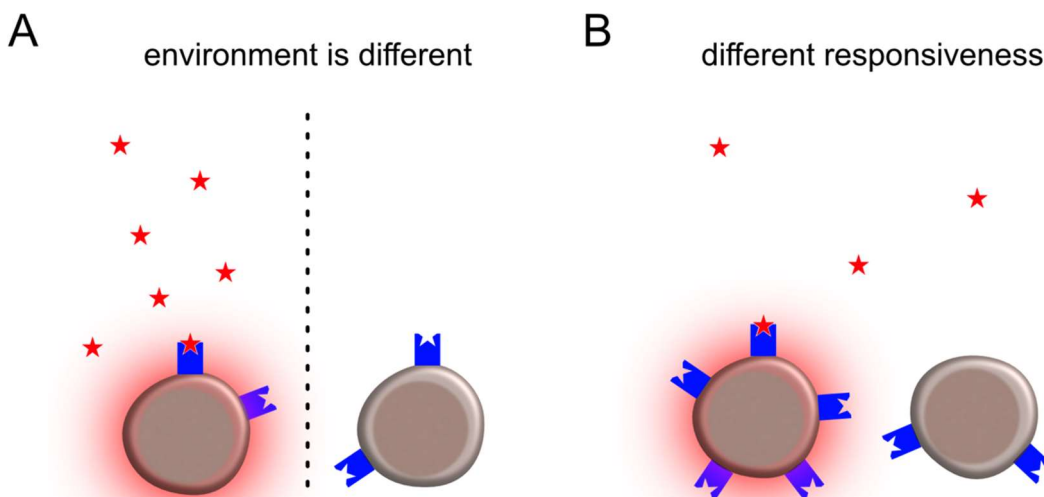


**Fig. 48: Generation of Variability.** **A:** Equal cells are exposed to distinct micro milieus. The cell that is exposed to fate determining factors (red stars) differentiates (red glow). **B:** Minor differences between the cells (e.g., intensity of receptor expression) (receptors: blue structures) can make the difference between receiving a signal (left) and receiving no signal (right).

strictly controlled conditions indicates that the distinct responsiveness of the cells themselves might induce variability. However, this awareness just shifts the problem one level further and raises the question of how distinct responsiveness is achieved.

### **5.2.3.3 Potential role of CD25**

A protein that could be imagined to influence the responsiveness of individual cells to a differentiation signal and to provide at the same time the missing link between phenotype and cell cycle speed is IL2R $\alpha$  (CD25). Interleukin-2 is a cytokine that promotes proliferation and survival of T cells [62]. Expression of CD25 enhances the affinity and sensitivity towards IL-2. Initial upregulation of CD25 after priming is crucial for the generation of functional T cell memory, but subsequent rapid downregulation is equally important, while prolonged expression of CD25 would result in terminal effector differentiation [119]. A potential explanation for this paradox is that IL-2 signaling activates anti-apoptotic, pro-survival and cell cycle pathways that are inevitable for both subsets [62].

Strong IL-2 signaling is thought to operate on T cell differentiation in two ways: by inhibiting memory-differentiation and by promoting terminal effector differentiation. Memory inhibition is most likely achieved by activation of Akt. Akt enables migration into the periphery by downregulating CD62L and CCR7 [138, 139]. Furthermore, it regulates transcription factors of the Foxo family and inhibits the pro-memory transcription factor Bcl-6 [140]. Foxo-1 in turn is known to interfere with cell cycle progression, to upregulate Eomes and downregulate T-bet [141]. The equilibrium between Eomes and T-bet is also thought to be important for memory vs. effector differentiation, with dominance of Eomes favoring memory differentiation and T-bet favoring effector differentiation [69, 142, 143]. Thus, suppression of Foxo-1 drives proliferation further into terminal effector differentiation.

In addition, IL-2 signaling activates the pro-effector transcription factors Blimp-1 and Id-2 via STAT-5 and promotes cell-cycle progression and survival via MAPK and cMYC-mediated upregulation of cyclins, Bcl-2 and inhibition of p21 [62, 144].

A study that cultured primed T cells in different concentrations of IL-2 found that IL-2 signaling also inhibited the expression of IL7R $\alpha$  (CD127) in a graded manner, and the expressions of CD25 and CD127 were mutually exclusive [140]. With CD127 being (together with KLRG1) the earliest surface marker found to enable discrimination between T cells with and without memory potential [69, 145, 146], the mutual exclusiveness underlines the relevance of CD25 in T cell differentiation.

#### **5.2.3.4 How could CD25 expression generate variability?**

Interestingly, it was shown that the sensing of IL-2 via the heterotrimeric IL-2 receptor (including CD25) leads to further upregulation of CD25 [144, 147]. This positive feedback loop could eventually result in fast proliferation and terminal effector differentiation of CD25-expressing cells. Consequently, strong IL-2 signaling may drive the CD25 expression over a certain threshold that is sufficient to sustain the positive feedback loop. Cells that do not reach the requisite threshold would lose CD25 expression, start to downregulate cell cycle proteins and differentiate into memory precursor cells (Fig. 49). As antigen signal also leads to upregulation of CD25 (Fig. 32, Fig. 33 and [148]), the priming event could be responsible for the height of the initial CD25 expression. This would also enable the integration of further variables like costimulation and TCR-pMHC affinity. Stronger or repetitive antigen contacts could enhance the initial upregulation of CD25, thereby explaining the stronger proliferation and effector differentiation in the presence of high loads of antigen, high affinity pMHCs or inflammation.

Together with the present literature, my data strongly indicate that the immune system relies on many mechanisms to guarantee diversification and variability: Differentiation into slow-dividing MPs and fast-dividing SLECs already occurs after a short phase of fast and concordant cell divisions. Small differences in initial CD25 could amplify via a positive feedback loop that lead to fate divergence after the concordant phase. In addition, different antigen loads or affinities, costimulation, inflammation and distinct micromilieus may further shape the immune system during and after priming.

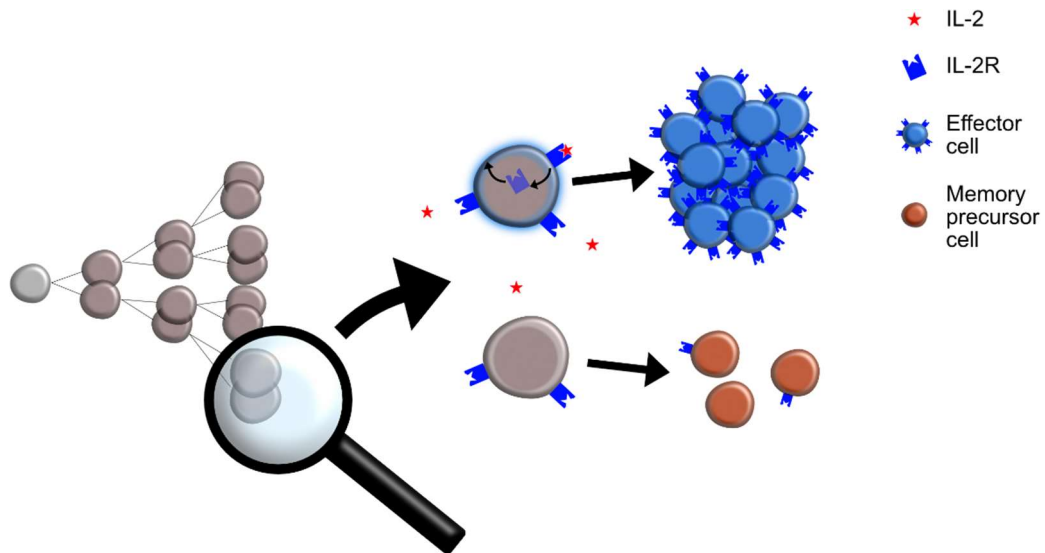


**Fig. 49: Model for CD25-driven diversification.** After the initial phase of fast and homogenous cell divisions, minor differences in the expression of the high affinity version (containing CD25) of the IL-2 receptor (blue structures) have evolved. Binding of IL-2 (red stars) to the receptor leads to further upregulation of the high affinity IL-2 receptor (upper enlarged cell), effector differentiation and fast cell divisions via a positive feedback loop. Cells that do not bind enough IL-2 (lower enlarged cell) lose CD25 again and become slow dividing memory (precursor) cells.

## 6 Summary

Although population-derived responses of CD8 T cells against the same pathogen are predictable and robustly regulated, they are composed of highly individual fates of single cell-derived progenies. These single cell-derived progenies have diverse phenotypes and their size can range over three magnitudes. Because it is very challenging to retrace the fate of a single naïve T cell with all its cell divisions and differentiation steps, the origin of this diversity could not be definitively resolved so far.

During the last few years, studies had indicated that the precursors of memory T cells already segregate from effector cells during the first week of infection. But it was not clear at which time point exactly they segregate and whether they can already be recognized (e.g., by the expression of certain surface antigens) before day four of the expansion phase. Studies that used single-cell transfer and fate-mapping techniques concluded from mathematical analysis that their data fit to a model in which memory-precursor and effector cells are set apart during the very first days of the expansion phase, and that these phenotypes are directly associated with distinct inter-division times. These results were, however, at odds with other studies that claimed homogenous cell divisions (i.e., equal inter-division times) within a single cell-derived progeny until the 8<sup>th</sup> cell division.

In this dissertation *in vitro* live-cell imaging was used to map cell-cycle speed and memory vs. effector fate decisions of individual CD8 T cells and their progeny throughout the first five days after T cell activation *in vitro*.

We found that distinct inter-division times of CD8 T cells were indeed already present during the early expansion phase. This was the case although all T cells were equipped with the same TCR and were cultured under homogenous conditions. The variability in the size of T cell progenies that was generated by distinct proliferation speeds was large enough to explain most of the total size variability. Further on, this variability was not just found between different single cell-derived progenies but also within a

T cell family, speaking against the hypothesis of homogenous cell divisions. However, our results also show that there is an initial phase of homogenous cell divisions, though this phase was completed after 3 to 4 cell divisions.

Investigation of the distribution of inter-division times within individual T cell trees revealed that in more than 30 % of the trees, the slow and fast dividing cells were segregated into distinct subtrees, indicating diversification into slow-dividing memory precursors and fast-dividing effector cells as suggested by Buchholz et al. The combination of the live-cell imaging approach with live-staining of the marker for memory cells CD62L (L-selectin) and the activation and effector-associated marker CD25 (IL2R $\alpha$ ) showed that it was indeed the cells with a memory phenotype (CD62L<sup>high</sup>, CD25<sup>low</sup>) that divided slowly and the cells with an effector phenotype (CD62L<sup>low</sup>, CD25<sup>high</sup>) that divided fast.

The addition of the pro-inflammatory cytokine IL-12 and prolonged stimulation via  $\alpha$ CD3 both led to increased expression of CD25 and shortened inter-division times. The variability of inter-division times stayed, however, intact – indicating that in addition to a base-difference between memory precursor and effector cells, additional signals can further modify division speed. Signaling is also required to sustain proliferation: Without  $\alpha$ CD3 and IL-12, the cell cycles slowed down after a few divisions and finally stopped.

Together, these results indicate that differentiation into slow dividing memory-precursor cells and fast proliferating effector cells already occurs after approximately two to three days and two to three divisions after activation. We suggest the positive feedback loop of CD25 and IL-2 as a potential mechanism that drives diversification into memory and effector cells in the absence of further instructing signals. Sensing of IL-2 via CD25 has been reported to further enhance CD25 expression. Thus, small differences in CD25 expression could amplify over time to distinct T cell subsets.

# Bibliography

1. Murphy, K.M., *Janeway's Immunobiology*. 2011: Taylor & Francis Group.
2. Janeway, C.A., Jr. and R. Medzhitov, *Innate immune recognition*. *Annu Rev Immunol*, 2002. **20**: p. 197-216.
3. Beutler, B., *Microbe sensing, positive feedback loops, and the pathogenesis of inflammatory diseases*. *Immunol Rev*, 2009. **227**(1): p. 248-63.
4. Kawai, T. and S. Akira, *The roles of TLRs, RLRs and NLRs in pathogen recognition*. *International Immunology*, 2009. **21**(4): p. 317-337.
5. Aderem, A. and D.M. Underhill, *Mechanisms of phagocytosis in macrophages*. *Annu Rev Immunol*, 1999. **17**: p. 593-623.
6. Harrison, R.E. and S. Grinstein, *Phagocytosis and the microtubule cytoskeleton*. *Biochemistry and Cell Biology*, 2002. **80**(5): p. 509-515.
7. Bogdan, C., M. Röllinghoff, and A. Diefenbach, *Reactive oxygen and reactive nitrogen intermediates in innate and specific immunity*. *Current Opinion in Immunology*, 2000. **12**(1): p. 64-76.
8. Honda, K. and T. Taniguchi, *IRFs: master regulators of signalling by Toll-like receptors and cytosolic pattern-recognition receptors*. *Nat Rev Immunol*, 2006. **6**(9): p. 644-58.
9. Martinon, F., A. Mayor, and J. Tschopp, *The inflammasomes: guardians of the body*. *Annu Rev Immunol*, 2009. **27**: p. 229-65.
10. Mantovani, A., et al., *The chemokine system in diverse forms of macrophage activation and polarization*. *Trends Immunol*, 2004. **25**(12): p. 677-86.
11. Alon, R. and S. Feigelson, *From rolling to arrest on blood vessels: leukocyte tap dancing on endothelial integrin ligands and chemokines at sub-second contacts*. *Semin Immunol*, 2002. **14**(2): p. 93-104.
12. Johnston, B. and E.C. Butcher, *Chemokines in rapid leukocyte adhesion triggering and migration*. *Semin Immunol*, 2002. **14**(2): p. 83-92.

13. Kleindienst, P. and T. Brocker, *Concerted antigen presentation by dendritic cells and B cells is necessary for optimal CD4 T-cell immunity in vivo*. Immunology, 2005. **115**(4): p. 556-64.
14. Canton, J., *Macropinocytosis: New Insights Into Its Underappreciated Role in Innate Immune Cell Surveillance*. Frontiers in Immunology, 2018. **9**.
15. Dalod, M., et al., *Dendritic cell maturation: functional specialization through signaling specificity and transcriptional programming*. EMBO J, 2014. **33**(10): p. 1104-16.
16. Guermonprez, P., et al., *Antigen presentation and T cell stimulation by dendritic cells*. Annu Rev Immunol, 2002. **20**: p. 621-67.
17. Grommé, M. and J. Neefjes, *Antigen degradation or presentation by MHC class I molecules via classical and non-classical pathways*. Molecular Immunology, 2002. **39**(3-4): p. 181-202.
18. Germain, R.N., *MHC-dependent antigen processing and peptide presentation: Providing ligands for T lymphocyte activation*. Cell, 1994. **76**(2): p. 287-299.
19. Shinkai, Y., *RAG-2-deficient mice lack mature lymphocytes owing to inability to initiate V(D)J rearrangement*. Cell, 1992. **68**(5): p. 855-867.
20. Lieber, M.R., *The polymerases for V(D)J recombination*. Immunity, 2006. **25**(1): p. 7-9.
21. Klein, L., et al., *Positive and negative selection of the T cell repertoire: what thymocytes see (and don't see)*. Nat Rev Immunol, 2014. **14**(6): p. 377-91.
22. Starr, T.K., S.C. Jameson, and K.A. Hogquist, *Positive and negative selection of T cells*. Annu Rev Immunol, 2003. **21**: p. 139-76.
23. Hirahara, K. and T. Nakayama, *CD4+ T-cell subsets in inflammatory diseases: beyond the Th1/Th2 paradigm*. Int Immunol, 2016. **28**(4): p. 163-71.
24. Schatz, D.G., *Antigen receptor genes and the evolution of a recombinase*. Semin Immunol, 2004. **16**(4): p. 245-56.
25. Parker, D.C., *T cell-dependent B cell activation*. Annu Rev Immunol, 1993. **11**: p. 331-60.
26. MacLennan, I.C.M., et al., *The changing preference of T and B cells for partners as T-dependent antibody responses develop*. Immunological Reviews, 1997. **156**(1): p. 53-66.

27. Nimmerjahn, F. and J.V. Ravetch, *Fcγ receptors as regulators of immune responses*. Nat Rev Immunol, 2008. **8**(1): p. 34-47.
28. Goldberg, A.L., et al., *The importance of the proteasome and subsequent proteolytic steps in the generation of antigenic peptides*. Molecular Immunology, 2002. **39**(3-4): p. 147-164.
29. Ashton-Rickardt, P.G., *The Granule Pathway of Programmed Cell Death*. 2005. **25**(3): p. 161-182.
30. Russell, J.H. and T.J. Ley, *Lymphocyte-mediated cytotoxicity*. Annu Rev Immunol, 2002. **20**: p. 323-70.
31. Ackerman, A.L. and P. Cresswell, *Cellular mechanisms governing cross-presentation of exogenous antigens*. Nat Immunol, 2004. **5**(7): p. 678-84.
32. Munoz, M.A., M. Biro, and W. Weninger, *T cell migration in intact lymph nodes in vivo*. Curr Opin Cell Biol, 2014. **30**: p. 17-24.
33. Miller, M.J., et al., *T cell repertoire scanning is promoted by dynamic dendritic cell behavior and random T cell motility in the lymph node*. Proc Natl Acad Sci U S A, 2004. **101**(4): p. 998-1003.
34. Call, M.E., et al., *The Organizing Principle in the Formation of the T Cell Receptor-CD3 Complex*. Cell, 2002. **111**(7): p. 967-979.
35. Birnbaum, M.E., et al., *Molecular architecture of the alphabeta T cell receptor-CD3 complex*. Proc Natl Acad Sci U S A, 2014. **111**(49): p. 17576-81.
36. O'Rourke, A.M. and M.F. Mescher, *The roles of CD8 in cytotoxic T lymphocyte function*. Immunology Today, 1993. **14**(4): p. 177-183.
37. Straus, D., *Genetic evidence for the involvement of the lck tyrosine kinase in signal transduction through the T cell antigen receptor*. Cell, 1992. **70**(4): p. 585-593.
38. van Oers, N.S., N. Killeen, and A. Weiss, *Lck regulates the tyrosine phosphorylation of the T cell receptor subunits and ZAP-70 in murine thymocytes*. J Exp Med, 1996. **183**(3): p. 1053-62.
39. Chan, A.C., et al., *Activation of ZAP-70 kinase activity by phosphorylation of tyrosine 493 is required for lymphocyte antigen receptor function*. The EMBO Journal, 1995. **14**(11): p. 2499-2508.
40. Samelson, L.E., *Signal transduction mediated by the T cell antigen receptor: the role of adapter proteins*. Annu Rev Immunol, 2002. **20**: p. 371-94.

41. Weiss, A., et al., *Functional activation of the T-cell antigen receptor induces tyrosine phosphorylation of phospholipase C-gamma 1*. Proc Natl Acad Sci U S A, 1991. **88**(13): p. 5484-8.
42. Matsumoto, R., et al., *Phosphorylation of CARMA1 plays a critical role in T Cell receptor-mediated NF-kappaB activation*. Immunity, 2005. **23**(6): p. 575-85.
43. Macian, F., C. Lopez-Rodriguez, and A. Rao, *Partners in transcription: NFAT and AP-1*. Oncogene, 2001. **20**(19): p. 2476-89.
44. Hogan, P.G., et al., *Transcriptional regulation by calcium, calcineurin, and NFAT*. Genes Dev, 2003. **17**(18): p. 2205-32.
45. Acuto, O. and F. Michel, *CD28-mediated co-stimulation: a quantitative support for TCR signalling*. Nat Rev Immunol, 2003. **3**(12): p. 939-51.
46. Fayard, E., et al., *Protein kinase B/Akt at a glance*. J Cell Sci, 2005. **118**(Pt 24): p. 5675-8.
47. Goral, S., *The three-signal hypothesis of lymphocyte activation/targets for immunosuppression*. Dialysis & Transplantation, 2011. **40**(1): p. 14-16.
48. Williams, M.A. and M.J. Bevan, *Effector and memory CTL differentiation*. Annu Rev Immunol, 2007. **25**: p. 171-92.
49. Trickett, A. and Y.L. Kwan, *T cell stimulation and expansion using anti-CD3/CD28 beads*. Journal of Immunological Methods, 2003. **275**(1-2): p. 251-255.
50. Black, F.L. and L. Rosen, *Patterns of Measles Antibodies in Residents of Tahiti and Their Stability in the Absence of Re-Exposure*. The Journal of Immunology, 1962. **88**(6): p. 725-731.
51. Hammarlund, E., et al., *Duration of antiviral immunity after smallpox vaccination*. Nat Med, 2003. **9**(9): p. 1131-7.
52. Ku, C.C., et al., *Control of homeostasis of CD8+ memory T cells by opposing cytokines*. Science, 2000. **288**(5466): p. 675-8.
53. Asanuma, H., et al., *Frequencies of memory T cells specific for varicella-zoster virus, herpes simplex virus, and cytomegalovirus by intracellular detection of cytokine expression*. J Infect Dis, 2000. **181**(3): p. 859-66.
54. Schenkel, J.M. and D. Masopust, *Tissue-resident memory T cells*. Immunity, 2014. **41**(6): p. 886-97.

55. Obar, J.J. and L. Lefrancois, *Memory CD8+ T cell differentiation*. Ann N Y Acad Sci, 2010. **1183**: p. 251-66.
56. Rosen, S.D., *Ligands for L-selectin: homing, inflammation, and beyond*. Annu Rev Immunol, 2004. **22**: p. 129-56.
57. Lanzavecchia, A. and F. Sallusto, *Understanding the generation and function of memory T cell subsets*. Curr Opin Immunol, 2005. **17**(3): p. 326-32.
58. Sallusto, F., J. Geginat, and A. Lanzavecchia, *Central memory and effector memory T cell subsets: function, generation, and maintenance*. Annu Rev Immunol, 2004. **22**: p. 745-63.
59. Sallusto, F., et al., *Two subsets of memory T lymphocytes with distinct homing potentials and effector functions*. Nature, 1999. **401**(6754): p. 708-12.
60. Graef, P., et al., *Serial transfer of single-cell-derived immunocompetence reveals stemness of CD8(+) central memory T cells*. Immunity, 2014. **41**(1): p. 116-26.
61. Buchholz, V.R., P. Gräf, and D.H. Busch, *The smallest unit: effector and memory CD8(+) T cell differentiation on the single cell level*. Frontiers in immunology, 2013. **4**: p. 31-31.
62. Kalia, V. and S. Sarkar, *Regulation of Effector and Memory CD8 T Cell Differentiation by IL-2-A Balancing Act*. Front Immunol, 2018. **9**: p. 2987.
63. Gebhardt, T., et al., *Memory T cells in nonlymphoid tissue that provide enhanced local immunity during infection with herpes simplex virus*. Nat Immunol, 2009. **10**(5): p. 524-30.
64. Bradley, L.M., L. Haynes, and S.L. Swain, *IL-7: maintaining T-cell memory and achieving homeostasis*. Trends in Immunology, 2005. **26**(3): p. 172-176.
65. Hendriks, J., Y. Xiao, and J. Borst, *CD27 promotes survival of activated T cells and complements CD28 in generation and establishment of the effector T cell pool*. J Exp Med, 2003. **198**(9): p. 1369-80.
66. Wherry, E.J., et al., *Lineage relationship and protective immunity of memory CD8 T cell subsets*. Nat Immunol, 2003. **4**(3): p. 225-34.
67. Gerlach, C., et al., *The Chemokine Receptor CX3CR1 Defines Three Antigen-Experienced CD8 T Cell Subsets with Distinct Roles in Immune Surveillance and Homeostasis*. Immunity, 2016. **45**(6): p. 1270-1284.

68. Hansen, S.G., et al., *Profound early control of highly pathogenic SIV by an effector memory T-cell vaccine*. *Nature*, 2011. **473**(7348): p. 523-527.
69. Joshi, N.S., et al., *Inflammation directs memory precursor and short-lived effector CD8(+) T cell fates via the graded expression of T-bet transcription factor*. *Immunity*, 2007. **27**(2): p. 281-95.
70. Badovinac, V.P. and J.T. Harty, *CD8+ T-cell homeostasis after infection: setting the 'curve'*. *Microbes and Infection*, 2002. **4**(4): p. 441-447.
71. Dowling, M.R., et al., *Stretched cell cycle model for proliferating lymphocytes*. *Proc Natl Acad Sci U S A*, 2014. **111**(17): p. 6377-82.
72. Homann, D., L. Teyton, and M.B. Oldstone, *Differential regulation of antiviral T-cell immunity results in stable CD8+ but declining CD4+ T-cell memory*. *Nat Med*, 2001. **7**(8): p. 913-9.
73. Yoon, H., T.S. Kim, and T.J. Braciale, *The cell cycle time of CD8+ T cells responding in vivo is controlled by the type of antigenic stimulus*. *PloS one*, 2010. **5**(11): p. e15423-e15423.
74. Kretschmer, L., et al., *Differential expansion of T central memory precursor and effector subsets is regulated by division speed*. *Nature Communications*, 2020. **11**(1): p. 113.
75. Murali-Krishna, K., et al., *Counting Antigen-Specific CD8 T Cells: A Reevaluation of Bystander Activation during Viral Infection*. *Immunity*, 1998. **8**(2): p. 177-187.
76. Choo, D.K., et al., *Homeostatic turnover of virus-specific memory CD8 T cells occurs stochastically and is independent of CD4 T cell help*. *J Immunol*, 2010. **185**(6): p. 3436-44.
77. Akondy, R.S., et al., *Origin and differentiation of human memory CD8 T cells after vaccination*. *Nature*, 2017. **552**(7685): p. 362-367.
78. Sarkar, S., et al., *Functional and genomic profiling of effector CD8 T cell subsets with distinct memory fates*. *J Exp Med*, 2008. **205**(3): p. 625-40.
79. Arsenio, J., et al., *Early specification of CD8+ T lymphocyte fates during adaptive immunity revealed by single-cell gene-expression analyses*. *Nat Immunol*, 2014. **15**(4): p. 365-372.
80. Kakaradov, B., et al., *Early transcriptional and epigenetic regulation of CD8+ T cell differentiation revealed by single-cell RNA sequencing*. *Nature Immunology*, 2017. **18**(4): p. 422-432.

81. Reiner, S.L., F. Sallusto, and A. Lanzavecchia, *Division of labor with a workforce of one: challenges in specifying effector and memory T cell fate*. *Science*, 2007. **317**(5838): p. 622-5.
82. Chang, J.T., et al., *Asymmetric T lymphocyte division in the initiation of adaptive immune responses*. *Science*, 2007. **315**(5819): p. 1687-91.
83. Chang, J.T., et al., *Asymmetric proteasome segregation as a mechanism for unequal partitioning of the transcription factor T-bet during T lymphocyte division*. *Immunity*, 2011. **34**(4): p. 492-504.
84. Knoblich, J.A., *Mechanisms of asymmetric stem cell division*. *Cell*, 2008. **132**(4): p. 583-97.
85. Beckmann, J., et al., *Asymmetric cell division within the human hematopoietic stem and progenitor cell compartment: identification of asymmetrically segregating proteins*. *Blood*, 2007. **109**(12): p. 5494-501.
86. Opferman, J.T., B.T. Ober, and P.G. Ashton-Rickardt, *Linear differentiation of cytotoxic effectors into memory T lymphocytes*. *Science*, 1999. **283**(5408): p. 1745-8.
87. Ahmed, R. and D. Gray, *Immunological memory and protective immunity: understanding their relation*. *Science*, 1996. **272**(5258): p. 54-60.
88. Celli, S., Z. Garcia, and P. Bousso, *CD4 T cells integrate signals delivered during successive DC encounters in vivo*. *J Exp Med*, 2005. **202**(9): p. 1271-8.
89. Buchholz, V.R., et al., *Disparate Individual Fates Compose Robust CD8+ T Cell Immunity*. *Science*, 2013. **340**(6132): p. 630-635.
90. Alt, F., *Advances in Immunology*. 2018: Elsevier Science.
91. Flossdorf, M., et al., *CD8(+) T cell diversification by asymmetric cell division*. *Nat Immunol*, 2015. **16**(9): p. 891-3.
92. Buchholz, V.R., T.N. Schumacher, and D.H. Busch, *T Cell Fate at the Single-Cell Level*. *Annu Rev Immunol*, 2016. **34**: p. 65-92.
93. Bevan, M.J. and P.J. Fink, *The CD8 response on autopilot*. *Nat Immunol*, 2001. **2**(5): p. 381-2.
94. van Stipdonk, M.J., et al., *Dynamic programming of CD8+ T lymphocyte responses*. *Nat Immunol*, 2003. **4**(4): p. 361-5.
95. Gett, A.V., et al., *T cell fitness determined by signal strength*. *Nat Immunol*, 2003. **4**(4): p. 355-60.

96. Schlub, T.E., et al., *Division-linked differentiation can account for CD8+ T-cell phenotype in vivo*. Eur J Immunol, 2009. **39**(1): p. 67-77.
97. Schlub, T.E., et al., *Predicting CD62L expression during the CD8+ T-cell response in vivo*. Immunol Cell Biol, 2010. **88**(2): p. 157-64.
98. Cossarizza, A., et al., *Guidelines for the use of flow cytometry and cell sorting in immunological studies*. Eur J Immunol, 2017. **47**(10): p. 1584-1797.
99. Eilken, H.M., S. Nishikawa, and T. Schroeder, *Continuous single-cell imaging of blood generation from haemogenic endothelium*. Nature, 2009. **457**(7231): p. 896-900.
100. Hilsenbeck, O., et al., *Software tools for single-cell tracking and quantification of cellular and molecular properties*. Nat Biotechnol, 2016. **34**(7): p. 703-6.
101. Hilsenbeck, O., et al., *fastER: a user-friendly tool for ultrafast and robust cell segmentation in large-scale microscopy*. Bioinformatics, 2017. **33**(13): p. 2020-2028.
102. Marchingo, J.M., et al., *T-cell stimuli independently sum to regulate an inherited clonal division fate*. Nat Commun, 2016. **7**: p. 13540.
103. Heinzl, S., et al., *A Myc-dependent division timer complements a cell-death timer to regulate T cell and B cell responses*. Nature Immunology, 2016. **18**(1): p. 96-103.
104. Sopper, S., et al., *Reduced Expression of CD62L Is Associated with Increased ADAM17 Activity and Predicts Molecular Response to Nilotinib Therapy in Patients with Early Chronic Phase Chronic Myelogenous Leukemia (CML-CP)*. Blood, 2014. **124**(21): p. 4522-4522.
105. Gall, S.M.L., et al., *ADAMs 10 and 17 Represent Differentially Regulated Components of a General Shedding Machinery for Membrane Proteins Such as Transforming Growth Factor  $\alpha$ , L-Selectin, and Tumor Necrosis Factor  $\alpha$* . Molecular Biology of the Cell, 2009. **20**(6): p. 1785-1794.
106. Chao, C.C., R. Jensen, and M.O. Dailey, *Mechanisms of L-selectin regulation by activated T cells*. The Journal of Immunology, 1997. **159**(4): p. 1686-1694.
107. Mohammed, R.N., et al., *ADAM17-dependent proteolysis of L-selectin promotes early clonal expansion of cytotoxic T cells*. Scientific Reports, 2019. **9**(1): p. 5487.

108. Arribas, J., et al., *Diverse cell surface protein ectodomains are shed by a system sensitive to metalloprotease inhibitors*. J Biol Chem, 1996. **271**(19): p. 11376-82.
109. Schroeder, T., et al., *Continuous long-term detection of live cell surface markers by 'in culture' antibody staining*. Protocol Exchange, 2011.
110. Semberger, C., et al., *A single naive CD8+ T cell precursor can develop into diverse effector and memory subsets*. Immunity, 2007. **27**(6): p. 985-997.
111. Zehn, D., S.Y. Lee, and M.J. Bevan, *Complete but curtailed T-cell response to very low-affinity antigen*. Nature, 2009. **458**(7235): p. 211-4.
112. Moreau, H.D., et al., *Dynamic in situ cytometry uncovers T cell receptor signaling during immunological synapses and kinapses in vivo*. Immunity, 2012. **37**(2): p. 351-63.
113. Fazilleau, N., et al., *The function of follicular helper T cells is regulated by the strength of T cell antigen receptor binding*. Nat Immunol, 2009. **10**(4): p. 375-84.
114. Marchingo, J.M., et al., *T cell signaling. Antigen affinity, costimulation, and cytokine inputs sum linearly to amplify T cell expansion*. Science, 2014. **346**(6213): p. 1123-7.
115. Kinjyo, I., et al., *Real-time tracking of cell cycle progression during CD8+ effector and memory T-cell differentiation*. Nat Commun, 2015. **6**: p. 6301.
116. Henrickson, S.E., et al., *T cell sensing of antigen dose governs interactive behavior with dendritic cells and sets a threshold for T cell activation*. Nat Immunol, 2008. **9**(3): p. 282-91.
117. Jung, S., et al., *In vivo depletion of CD11c+ dendritic cells abrogates priming of CD8+ T cells by exogenous cell-associated antigens*. Immunity, 2002. **17**(2): p. 211-20.
118. Nguyen, T., R. Wang, and J.H. Russell, *IL-12 enhances IL-2 function by inducing CD25 expression through a p38 mitogen-activated protein kinase pathway*. European Journal of Immunology, 2000. **30**(5): p. 1445-1452.
119. Kalia, V., et al., *Prolonged interleukin-2Ralpha expression on virus-specific CD8+ T cells favors terminal-effector differentiation in vivo*. Immunity, 2010. **32**(1): p. 91-103.
120. Smith, K.A., *Interleukin-2: inception, impact, and implications*. Science, 1988. **240**(4856): p. 1169-76.

121. Williams, M.A., A.J. Tzgnik, and M.J. Bevan, *Interleukin-2 signals during priming are required for secondary expansion of CD8+ memory T cells*. Nature, 2006. **441**(7095): p. 890-893.
122. Mitchell, D.M., E.V. Ravkov, and M.A. Williams, *Distinct roles for IL-2 and IL-15 in the differentiation and survival of CD8+ effector and memory T cells*. J Immunol, 2010. **184**(12): p. 6719-30.
123. Kishimoto, T.K., M.A. Jutila, and E.C. Butcher, *Identification of a human peripheral lymph node homing receptor: a rapidly down-regulated adhesion molecule*. Proc Natl Acad Sci U S A, 1990. **87**(6): p. 2244-8.
124. Jung, T.M. and M.O. Dailey, *Rapid modulation of homing receptors (gp90MEL-14) induced by activators of protein kinase C. Receptor shedding due to accelerated proteolytic cleavage at the cell surface*. The Journal of Immunology, 1990. **144**(8): p. 3130-3136.
125. Jung, T.M., et al., *Down-regulation of homing receptors after T cell activation*. The Journal of Immunology, 1988. **141**(12): p. 4110-4117.
126. Newell, E.W., et al., *Cytometry by time-of-flight shows combinatorial cytokine expression and virus-specific cell niches within a continuum of CD8+ T cell phenotypes*. Immunity, 2012. **36**(1): p. 142-52.
127. Bannard, O., M. Kraman, and D.T. Fearon, *Secondary Replicative Function of CD8<sup>+</sup> T Cells That Had Developed an Effector Phenotype*. Science, 2009. **323**(5913): p. 505-509.
128. Plunkett, F.J., et al., *The loss of telomerase activity in highly differentiated CD8<sup>+</sup>CD28<sup>-</sup>CD27<sup>-</sup> T cells is associated with decreased Akt (Ser473) phosphorylation*. J Immunol, 2007. **178**(12): p. 7710-9.
129. Lefrancois, L. and J.J. Obar, *Once a killer, always a killer: from cytotoxic T cell to memory cell*. Immunol Rev, 2010. **235**(1): p. 206-18.
130. Obar, J.J., et al., *Pathogen-induced inflammatory environment controls effector and memory CD8+ T cell differentiation*. J Immunol, 2011. **187**(10): p. 4967-78.
131. Plumlee, C.R., et al., *Early Effector CD8 T Cells Display Plasticity in Populating the Short-Lived Effector and Memory-Precursor Pools Following Bacterial or Viral Infection*. Sci Rep, 2015. **5**: p. 12264.
132. Beuneu, H., et al., *Visualizing the functional diversification of CD8+ T cell responses in lymph nodes*. Immunity, 2010. **33**(3): p. 412-23.
133. Gerlach, C., et al., *Heterogeneous differentiation patterns of individual CD8+ T cells*. Science, 2013. **340**(6132): p. 635-9.

134. Ciocca, M.L., et al., *Cutting edge: Asymmetric memory T cell division in response to rechallenge*. J Immunol, 2012. **188**(9): p. 4145-8.
135. Hawkins, E.D., et al., *Regulation of asymmetric cell division and polarity by Scribble is not required for humoral immunity*. Nat Commun, 2013. **4**: p. 1801.
136. Lemaitre, F., et al., *Phenotypic CD8+ T cell diversification occurs before, during, and after the first T cell division*. J Immunol, 2013. **191**(4): p. 1578-85.
137. King, C.G., et al., *T cell affinity regulates asymmetric division, effector cell differentiation, and tissue pathology*. Immunity, 2012. **37**(4): p. 709-20.
138. Finlay, D. and D.A. Cantrell, *Metabolism, migration and memory in cytotoxic T cells*. Nat Rev Immunol, 2011. **11**(2): p. 109-17.
139. Waugh, C., et al., *Phosphoinositide (3,4,5)-triphosphate binding to phosphoinositide-dependent kinase 1 regulates a protein kinase B/Akt signaling threshold that dictates T-cell migration, not proliferation*. Mol Cell Biol, 2009. **29**(21): p. 5952-62.
140. Pipkin, M.E., et al., *Interleukin-2 and inflammation induce distinct transcriptional programs that promote the differentiation of effector cytolytic T cells*. Immunity, 2010. **32**(1): p. 79-90.
141. Hedrick, S.M., et al., *FOXO transcription factors throughout T cell biology*. Nat Rev Immunol, 2012. **12**(9): p. 649-61.
142. Paley, M.A., et al., *Progenitor and terminal subsets of CD8+ T cells cooperate to contain chronic viral infection*. Science, 2012. **338**(6111): p. 1220-5.
143. Banerjee, A., et al., *Cutting edge: The transcription factor eomesodermin enables CD8+ T cells to compete for the memory cell niche*. J Immunol, 2010. **185**(9): p. 4988-92.
144. Malek, T.R., *The biology of interleukin-2*. Annu Rev Immunol, 2008. **26**: p. 453-79.
145. Kaech, S.M., et al., *Selective expression of the interleukin 7 receptor identifies effector CD8 T cells that give rise to long-lived memory cells*. Nat Immunol, 2003. **4**(12): p. 1191-8.
146. Huster, K.M., et al., *Selective expression of IL-7 receptor on memory T cells identifies early CD40L-dependent generation of distinct CD8+ memory T cell subsets*. Proc Natl Acad Sci U S A, 2004. **101**(15): p. 5610-5.

147. Nakajima, H., et al., *An indirect effect of Stat5a in IL-2-induced proliferation: a critical role for Stat5a in IL-2-mediated IL-2 receptor alpha chain induction*. *Immunity*, 1997. **7**(5): p. 691-701.
148. Shatrova, A.N., et al., *Time-Dependent Regulation of IL-2R alpha-Chain (CD25) Expression by TCR Signal Strength and IL-2-Induced STAT5 Signaling in Activated Human Blood T Lymphocytes*. *PLoS One*, 2016. **11**(12): p. e0167215.

# Acknowledgement

An dieser Stelle möchte ich mich gerne bei den vielen Menschen bedanken, die zum Gelingen dieser Arbeit beigetragen haben. Denn niemand kann ein wissenschaftliches Projekt tatsächlich alleine stemmen.

Zunächst möchte ich mich bei Dirk Busch bedanken. Seine Vorlesung hat mich erst auf die Immunologie aufmerksam gemacht und als Instituts- und Arbeitsgruppenleiter lag es in seiner Verantwortung, mir ein Projekt anzuvertrauen und zusammen mit Frau Bäuerle die nötigen finanziellen Mittel dafür aufzutreiben. Auch, wenn ich aufgrund der Thematik meines Projektes nicht Teil der Montag-Morgen-Couch war, erhielt ich von Dirk in den Lab-Meetings immer wieder konstruktive und motivierende Anregungen. Seine ehrliche Begeisterung für neue Daten vermochte mich stets anzustecken und ich konnte mich immer auf seine Unterstützung verlassen.

Die direkte Aufsicht über meine Arbeit und damit wohl den aufwendigsten Teil meiner Betreuung, hat Veit Buchholz übernommen. Sehr beeindruckt hat mich, wie Veit es geschafft hat, ein Meister der wissenschaftlichen Literatur zu werden, aber dennoch so nah am Labor zu bleiben, dass er stets den Überblick über meinen Fortschritt behielt und die Machbarkeit, sowie den Zeitaufwand der Experimente realistisch einzuschätzen vermochte. Mit seinen Ideen hätten wir auch noch viele Jahre weiterforschen können, aber ich denke, dass wir den richtigen Zeitpunkt für den Abschluss des Projekts gefunden haben.

Im praktischen Bereich möchte ich mich gerne für die Unterstützung durch unsere TAs bedanken. Insbesondere Katherine Molter und Inge Hensel haben meine Experimente durch Übernahme der Mauszucht und der zahlreichen Antikörperbestellungen erst möglich gemacht. Und auch wenn ich nicht direkt mit ihr zusammen an einem Projekt gearbeitet habe, möchte ich auch noch Monika Hammel hervorheben, die durch ihre pragmatische

und zweckorientierte Herangehensweise den Laden am Laufen gehalten hat, ohne sich dabei in den Vordergrund zu spielen.

Unersetzlich für meine Experimente war auch die Sortfacility unter der Leitung von Matthias Schiemann. Fast jedes Experiment führte mich irgendwann in den Sortraum zu Lynette Henkel, Immanuel Andrä oder Corinne Angerpointner.

Ferner möchte ich mich noch bei Simon Grassmann und Lorenz Kretschmer für gute fachliche Diskussionen und bei Michael Floßdorf und Atefeh Kazeroonian für die weitergehende mathematische Analyse meiner Daten bedanken.

So... es könnte sein, dass es ab hier etwas ausschweifend wird, aber ich werde einfach trotzdem weiterschreiben. Denn im Gegensatz zu einer Dankesrede, bei der das Publikum mehr oder weniger gefangen ist, obliegt es hier dem Leser einfach aufzuhören, wenn er oder sie nicht mehr mag.

Hmmm... fünfeinhalb Jahre Doktorarbeit (bis sie eingereicht ist sicherlich 7)... Wieso tut man so etwas? Die Fragen aus der Verwandtschaft, wann ich denn eigentlich fertig sein werde, haben schon ein halbes Jahr nach Beginn der Promotion angefangen – vor ca. 2 -3 Jahren dann aber auch wieder aufgehört. Die ehemaligen Kommilitonen, die nicht promoviert haben, haben schon längst einen richtigen Job mit Festanstellung, Planungssicherheit und einem Gehalt, das dann auch nicht unbedingt niedriger ist, als das, was man dann irgendwann mal mit Promotion verdient. Zu diesem Zweck hat man es also offenbar nicht gemacht. Dafür wissen potenzielle Arbeitgeber: Du bist frustrationserprobt. Hat diese Auszeichnung ein angemessenes Kosten-Nutzenverhältnis?

Ich finde schon. Denn es war eine einzigartige Zeit, die man nirgends so hätte erleben können. Woanders findet man kaum ein Kollegium das überwiegend aus Leuten besteht, die in einem ähnlichen Alter sind und ähnliche Interessen haben. Das geht natürlich Hand in Hand mit einem hohen Durchsatz an Leuten. Fängt man mit einem Praktikum oder der

Masterarbeit am Institut an, kann man es innerhalb weniger Jahre schaffen, vom Institutsküken zum alten Hasen zu werden – quasi schon einmal das spätere Berufsleben im Zeitraffer – und eine Trennung zwischen Privat- und Berufsleben war im Prinzip nicht einmal im Ansatz vorhanden.

Dass ich nicht nach drei Jahren einfach aufgehört und zusammengeschrieben habe, hat im Wesentlichen zwei Gründe: Zum einen hatte ich schon so viel Zeit und Arbeit in eine Fragestellung investiert, dass ich es nicht eingesehen hatte, einfach aufzugeben. Die Indizien hatten klar gezeigt, dass es eigentlich funktionieren müsste, wenn einfach mal alle Komponenten (inkl. Mikroskop) gleichzeitig funktionieren würden. Diese haben sich aber auf fast schon unfaire Weise mit Händen und Füßen gewehrt. So habe ich also stur immer wieder wiederholt und mit dem technischen Kundendienst an der Optimierung des Geräts gearbeitet, bis dann am Ende tatsächlich mal alles störungsfrei durchgelaufen ist.

Noch wichtiger waren aber meine Freunde und Kollegen, die die einfachen Zeiten noch besser und die schwierigen Zeiten erträglich gemacht haben.

Wichtig war hier natürlich insbesondere die Mensa-Crew und das Tischkicker-Team. Diese Gruppen waren neuen Mitgliedern immer sehr aufgeschlossen und daher stetigem Wandel unterworfen. Auf Wichtl, Andy, und Simon (Fräßle) konnte man aber an jedem Tag bei jedem Wetter zählen. Unvergessen ist auch die sogenannte Sportler-Gruppe. Angefangen hat es im Prinzip mit der spontanen Idee von Manuel und mir, eine Fahrradtour nach Neuschwanstein zu machen (er auf seinem Rennrad, ich auf meinem 20 kg Trekkingbike). Leider war die Tour zu heftig für mein altes Fahrrad und es hat einen Totalschaden erlitten (wir sind aber trotzdem noch irgendwie angekommen). So habe ich mich dann dazu überreden lassen, auch ein Rennrad zu kaufen. In den folgenden Jahren haben wir mit Thomas und Fabian sehr viele schöne und immer absolut ambitionierte Rennradtouren und -Urlaube an entlegenste und wunderschöne Orte unternommen. Leider war es körperlich meist so anstrengend, dass man die Natur nur in begrenztem Ausmaß genießen konnte. Daher war es sehr schön, mit Kat zum Ausgleich viele Ausflüge ins Gebirge (ebenfalls ziemlich

anspruchsvoll, aber immerhin mit großzügiger Pause am Gipfel) zu unternehmen.

Auch feucht-fröhliche Abende waren im Institut reichlich gesät. Neben den Küchen- und Dachterrassenpartys trug hierzu besonders die DnD-Gruppe bei. Simon (Grassmann) gibt dabei einen absolut genialen Spielleiter ab und koordiniert einen mittlerweile großen Haufen sehr individueller Charaktere durch eine seiner Phantasie entsprungene Welt. Dazu haben wir (die beiden Simons, Wichtl, Andy, Steven, Ludwig, Fabian, Justin, Vicky) auch gelegentlich Kurzurlaube unternommen, die immer in sehr ungewöhnlichen Unterkünften stattgefunden haben (z.B. Waldhütte im Schwarzwald, Schloss in Franken, ehem. Kirche in der Toskana, ...) – also immer so weit abgelegen, dass man ungestört etwas Pause von zivilisiertem Verhalten machen konnte... Es hat folglich auf jeden Fall unheimlich viel Spaß gemacht.

Natürlich gab es auch mal schwierigere Zeiten und so bin ich sehr dankbar, dass insbesondere Andy, Wichtl, Simon und Vicky zur richtigen Zeit da waren und mich auch dann wieder aufgebaut haben, wenn ich gerade vielleicht mal nicht die beste Laune hatte.

Zuletzt möchte ich mich noch bei meiner Familie bedanken. Meine Eltern haben mir immer meine Freiräume gelassen und nicht versucht, mir vorzuschreiben, was ich aus meinem Leben machen soll. Da sie auf der anderen Seite des Landes leben, mussten sie leider sehr viel auf mich verzichten und wir konnten uns nur wenige Male im Jahr sehen. Leider musste auch das letzte geplante Treffen wegen des Corona-Virus verschoben werden. Ich freue mich aber darauf, sie alle bald wieder zu sehen.